

---

# **Wearable Biometric Monitoring for Collegiate Soccer Athletes**

## **Project Professors:**

**Mehul Bhatia, Department of Mechanical Engineering**

**Taimoor Afzal, Department of Biomedical Engineering**

**Bashima Islam, Department of Electrical & Computer Engineering**

**Walter Towner, WPI Business School**

## **Submitted By:**

**Evan Brady**

**James Carmody**

**Krish Patel**

**Jennifer Russo**

## **Date:**

**25th of April 2024**



**WPI**

---

*This report represents the work of one or more WPI undergraduate students submitted to the faculty as evidence of completion of a degree requirement. WPI routinely publishes these reports on the web without editorial or peer review.*

## **Abstract**

In collegiate soccer, athletes' health and performance are affected by overexertion and fatigue throughout the season. Current methods rely on subjective evaluations and inconsistent tests, making it difficult for coaches to effectively manage their team for optimizing performance. Smart wearable devices offer a promising solution to this problem. This project aims to develop a non-invasive body sensor network to quantitatively measure fatigue. The project monitors key biometrics such as body temperature, respiration rate, heart rate, and muscle exertion, alongside performance metrics and enables coaches to make data-driven decisions to prevent overexertion. The team used a variety of data analysis techniques, filtering techniques, and exercises to compare real-time performance and after workout reports. Not only does this initiative enhance performance, but it provides individualized insights into their physiological responses during exercise.

## **Authorship**

<b>Section</b>	<b>Primary Author(s)</b>	<b>Primary Editor(s)</b>
Abstract	All	James, Jennifer
Introduction	All	James, Jennifer
Background	All	All
Project Strategy	All	James, Jennifer, Evan
Design Process	All	All
Testing and Procedures	All	James, Jennifer, Evan
Design Verification	All	All
Final Design Validation	All	James, Jennifer, Evan
Discussion and Recommendations	James, Evan	James, Jennifer, Evan
Conclusion	James	Jennifer
References	All	Evan
Appendices	Jennifer, Krish	Evan

### **Contacts:**

Evan Brady: evanbrady.2020@gmail.com

James Carmody: carmodyj03@optonline.net

Jennifer Russo: jennifer.russo4@gmail.com

Krish Patel: krishpatel1077@outlook.com

<b>Abstract</b>	<b>2</b>
<b>Authorship</b>	<b>3</b>
<b>List of Figures</b>	<b>7</b>
<b>1.0 Introduction</b>	<b>10</b>
<b>2.0 Background</b>	<b>12</b>
2.1 Fatigue in Athletes	12
2.1.1 Current ways athletes measure performance and monitor exhaustion	13
2.1.2 Current Performance monitoring devices on the market	17
2.2 Important Performance Metrics and Biometrics	20
2.2.1: Biometrics	20
2.2.1.1: Heart Rate	20
2.2.1.3: Respiration Rate	21
2.2.1.4: Body temperature	22
2.2.1.5: Electromyography	23
2.3.2: Performance Metrics	24
2.3.2.1: Location	24
2.3.2.2: Pace	25
2.4 Measuring Biometrics	26
2.4.1: Measuring Heart Rate	26
2.4.3: Measuring Respiration Rate	30
2.4.4: Measuring Body Temperature	34
2.4.5: Measuring EMG signal	35
2.5 Measuring Performance Metrics	36
2.5.1: Measuring Location:	36
2.5.4: Measuring Pace	38
<b>3.0 Project Strategy</b>	<b>39</b>
3.1 Initial Client Statement	39
3.2 Objectives and Constraints	39
3.3 Revised Client Statement	43
3.4 Project Approach	44
<b>4.0 Design Process</b>	<b>46</b>
4.1 Needs Analysis	46
4.1.1: Design Decomposition	47
4.2 Important Industry Standards	48
4.3 Conceptual Designs	49
4.3.1: Sensor Development	49

4.3.1.1: EMG	49
4.3.1.2: ECG	51
4.3.1.3: LM35	52
4.3.1.4: GPS	53
4.3.1.5: Power Source	54
4.3.2: Software Development	55
4.3.2.1: Internet Based Data Transmission	55
4.3.2.2: ESP 8266	57
4.3.2.3: Data Analysis via Local Webpage Application	61
4.3.3: Manufacturing Procedure	62
4.3.4: Developing a Fatigue Index	63
4.3.4.1: Ranking of Metrics	63
4.3.4.2: Calculations of Score	64
4.3.4.1.1 Heart Rate and Respiration Rate	64
4.3.4.1.2 Muscle Activation	65
4.3.4.1.3 Body Temperature	67
4.4 Feasibility Study/Experiments	68
4.5 Alternative Designs	69
4.6 Modeling	72
4.7 Preliminary Data	73
4.8 Final Design	76
<b>5.0 Testing and Procedures</b>	<b>80</b>
<b>6.0 Design Verification</b>	<b>83</b>
6.1 ECG Results	83
6.2 EMG Results	94
6.3 Temperature Results	106
6.4 GPS Results	108
6.5 Fatigue Index	110
<b>7.0 Final Design Validation</b>	<b>114</b>
7.1 Economics	114
7.1.1 Net Present Value	114
7.1.2 Estimated Costs	114
7.2 Environmental Impact and Sustainability	117
7.3 Societal Influence	118
7.4 Political Ramifications	119
7.5 Ethical Concerns	119
7.6 Health and Safety Issues	121
7.7 Manufacturability	121

<b>8.0 Discussion and Recommendations</b>	<b>124</b>
<b>9.0 Conclusion</b>	<b>128</b>
<b>References</b>	<b>129</b>
<b>Appendices</b>	<b>137</b>
Appendix A	137
Appendix B	141
Appendix C	143
Appendix D	144
Appendix E	145

## List of Figures

Figure 2.1: Current Fatigue Tests by Sport, (Taylor et al., 2012)	14
Figure 2.2: Graph showing relationship between light, moderate, and heavy exercise time with pulmonary ventilation rate (PT Direct, 2010)	22
Figure 2.3: Graphs of muscle fatigue detection with mean frequency linearly decreasing (Yousif et al., 2019)	23
Figure 2.4: Photoplethysmography (PPG) waveform compared to an electrocardiogram (ECG) waveform (P. Välisuo, 2015)	27
Figure 2.5: Sample electrocardiogram (ECG) showing the wave segments and RR interval (Vinzio Maggio et al., 2012)	29
Figure 2.6: Process for piezoresistive sensor prediction of respiratory rate, $f_R$ , using strain ( $\epsilon$ ), resistance change from strain ( $R(\epsilon)$ ), voltage change from strain ( $V(\epsilon)$ ). (Massaroni et al., 2019).	31
Figure 2.7: Overall GPS Tracking system components (Archevapanich et al., 2021)	37
Figure 2.8: Example 10-minute heatmap output (Archevapanich et al., 2021)	38
Figure 3.1: Gantt Chart from A term 2023 through D term 2024	44
Figure 4.1: Diagram of ECG and EMG electrode placement, with the ECG electrodes (Hakami et al, 2018) being placed on the right shoulder (negative), left shoulder (ground),	52
Figure 4.2: GPS Arduino Code	54
Figure 4.3: Software Communication Diagram	56
Figure 4.4: Digitalwrite Mux Arduino Code	57
Figure 4.5: ESP 8266 code to read serial data from Arduino Uno	59
Figure 4.6: ESP 8266 code to append data to csv files	59
Figure 4.7: ESP 8266 Website Display	59
Figure 4.8: ESP 8266 code for web service routes	60
Figure 4.9: ESP 8266 code that updates csv files on the website	60

Figure 4.10: Python code to calculate RMS and MDF from raw signal csv file	66
Figure 4.11: Python code to calculate a line of fit for the RMS feature	66
Figure 4.12: Seeed Grove EMG signal on quadricep, squat, 9 repetitions	74
Figure 4.13: Myoware EMG Signal on quadriceps, squat, 8 repetitions	75
Figure 4.14: Final Product	77
Figure 4.15: Electrical Schematic of the ESP 8266 Circuit	78
Figure 4.16: Live Data Display Website Screenshot	79
Figure 6.1: Subject 1 heart rate for “Baseline” testing procedure	85
Figure 6.2: Subject 1 heart rate for “Dribble” testing procedure	86
Figure 6.3: Subject 2 heart rate for “Baseline” testing procedure	87
Figure 6.4: Subject 2 heart rate for “Dribble” testing procedure	87
Figure 6.5: Subject 3 heart rate for “Shuttle Run” testing procedure	88
Figure 6.6: Subject 3 heart rate for “Dribble” testing procedure	89
Figure 6.7: Subject 4 heart rate for “Baseline” testing procedure	90
Figure 6.8: Subject 4 heart rate for “Dribble” testing procedure	91
Figure 6.9: Subject 5 heart rate for “Baseline” testing procedure	92
Figure 6.10: Subject 5 heart rate for “Shuttle Runs” testing procedure	92
Figure 6.11: Subject 6 heart rate for “Baseline” testing procedure	93
Figure 6.12: Subject 1 “Baseline” raw, analyzed, and linear fit graphs	95
Figure 6.13: Subject 1 “Dribble” raw, analyzed, and linear fit graphs	96
Figure 6.14: Subject 2 “Shuttle Sprint” raw, analyzed, and linear fit graph	98
Figure 6.15: Subject 2 “Baseline” sprint raw, analyzed, and linear fit graph	99
Figure 6.16: Subject 3 “Baseline” data	100

Figure 6.17: Subject 3 fatigue (left) vs non fatigued (right) calf muscle	<b>101</b>
Figure 6.18: Subject 4 “Dribbling” data	<b>102</b>
Figure 6.19: Subject 5 “Baseline” data	<b>104</b>
Figure 6.20: Subject 5 “Shuttle Run” Data	<b>105</b>
Figure 6.21: Maximum increase in recorded body temperature of subjects during different activities	<b>107</b>
Figure 6.22: example GPS data from a workout	<b>109</b>
Figure 6.23: Total workout heatmap over Rooftop Field	<b>109</b>
Figure 7.1: Part cost list for each component in the final prototype	<b>115</b>
Figure 7.2: Cash Flow of one soccer team over 5 years	<b>117</b>
Figure A.1: National sprint test scores for 16 to 19 year olds (Davis, 2005)	<b>138</b>
Figure A.2: Beep test levels and associating measurements (SoccerWire, 2023)	<b>139</b>

## 1.0 Introduction

In the dynamic world of collegiate soccer, athletes constantly strive to push their physical boundaries and enhance their performance during practice and in games. However, the consistent strive towards excellence can increase their potential of injury from fatigue, leading to disrupted soccer seasons. Today, soccer athletes rely on sprint and jump tests to measure readiness and subjective surveys to monitor fatigue and exhaustion (Lourenço, J., Gouveia et al., 2023). However, these methods are inconsistent and subjective, resulting in uncertainty when evaluating athlete training, performance, and fatigue. This uncertainty increases the risk of injury and could prevent athletes from achieving their maximum performance.

Smart wearable devices are revolutionizing sports analysis with advanced sensors and data analysis techniques that provide crucial insight for coaches to make practice and game decisions. Commercially available wearable devices include fitness trackers, smart watches, chest straps, and more that provide real time data on metrics including steps taken, heart rate, distance covered and blood oxygen monitoring. However, these devices can suffer from poor accuracy when recording biometrics due to their positioning on the body (Dreckett, 2022). Devices capable of measuring biometrics are emerging as a transformative form of athlete monitoring and there is potential to improve the accuracy of measurements by placing sensors at ideal locations on the body.

Smart wearable devices have also shown promise in monitoring exercise fatigue. They are capable of real time monitoring of critical biometrics, which can be used to evaluate an athlete's risk of fatigue. One study compared the effectiveness of a sensor network health monitoring system relative to traditional medical methods and determined that such a sensor network is 85% as accurate (Ke & Xing, 2023). They evaluated the sensor network based on its

speed of measurement, accuracy, and impact on an athlete's recovery rate and treatment satisfaction.

This project aimed to develop a non-invasive body sensor network to monitor key biometrics in soccer athletes such as body temperature, respiration rate, heart rate, and muscle activation in addition to performance metrics. Biometric data was collected and wirelessly transmitted to a website, where it was analyzed to determine athlete performance. The resulting data can advise a coach's training regimen to help prevent overexertion in players and help these players learn about their body.

## **2.0 Background**

### **2.1 Fatigue in Athletes**

Athletes need to take care of their bodies to enable them to perform at a competitive level. However, athletes also need to continuously push their bodies in practice and competitions. More detail regarding athlete health and the risks they face from overexertion can be found in Appendix A. This introduces the risk of exercise fatigue in athletes. Exercise fatigue is controversial to define, with many experts having different definitions of the concept. One study refers to exercise fatigue as “the inability of the human body to continue to maintain the original amount of exercise after a certain period of continuous exercise” (Wang, 2022). Another source defines fatigue as a “reduced capacity for maximal performance” (Taylor et al., 2012). However, all definitions agree that fatigue reduces an athlete’s performance and can lead to injury.

Fatigue is often classified into two broad categories, physical fatigue and psychological fatigue (Lock et al, 2018). These categories can be further divided, with physical fatigue encompassing central fatigue, nerve muscle junction fatigue, and peripheral fatigue and psychological fatigue mainly including mental fatigue (Wang, 2022). Central fatigue is defined as “a deficient drive of motor cortical output attenuating performance” (Toreno-Aguilera et al., 2022) and peripheral fatigue results from “processes at the neuromuscular junction that lead to a reduction in force at a given neural input (Weavil & Amann, 2019).” Essentially, central fatigue is reduction in performance stemming from the central nervous system while peripheral fatigue originates at the muscles themselves. Mental fatigue in athletes is defined as “a psychobiological state caused by prolonged periods of demanding cognitive activity shown to negatively influence physical performance” and it often develops cumulatively in elite athletes (Russell et al., 2019).

While definitions of the different types of fatigue exist, in real world scenarios it can be difficult to separate them in athletes. This is because different types of fatigue can compound on each other and further reduce the athlete's ability to perform. For instance, if an athlete undergoes high intensity, high volume training for long periods of time muscle fatigue can compound with psychological fatigue to produce acute fatigue. If this condition is not addressed it can lead to chronic fatigue, which poses significant risks to the health and safety of the athlete (Wang, 2022). Despite its complexity, the risks associated with fatigue make it essential for coaches and athletes to monitor for warning signs.

While significant research into fatigue monitoring exists, often coaches monitor fatigue on a subjective basis. First, the current methods commonly used by athletes and coaches were investigated and their effectiveness discussed. Second, devices and services that currently exist were investigated.

### **2.1.1 Current ways athletes measure performance and monitor exhaustion**

Currently, athletes and their coaches monitor fatigue in a myriad of ways. These methods can include subjective measures, athlete surveys, performance metrics and more. While there are some specific metrics that are more important to soccer athletes, there are still common methods of fatigue tracking that are used across many aerobic sports. Studies have indicated that the primary motivations for monitoring fatigue in athletes are to prevent overtraining, reduce injuries, monitor the effectiveness of training programs, and to maintain athlete performance.

One study reached out to coaches and individuals in sport science support roles across a variety of 23 sports including soccer, swimming, track and field, basketball and more to determine current practices for assessing fatigue. The study indicates that self-report questionnaires are the most common method of evaluating fatigue, with 84% of respondents

utilizing them. The next most popular fatigue measuring method was performance tests at 61% of respondents. Tracking performance in sporting activities was also popular, with 43% of respondents using this method. Occasionally coaches monitored athlete's active heart rates, but heart rate variability was seldom monitored. Coaches rarely relied on musculoskeletal screenings, resting heart rate, and hormonal profiling (Taylor et al., 2012).

The commonly used questionnaire forms were often custom designed by the coaches, who said that the comprehensive studies found in scientific literature were too time consuming to complete and analyze. These forms often included questions on perceived muscle soreness, perceptions on wellness and fatigue, and sleep duration and quality. The frequency of data collection varied from coach to coach, with 22% collecting data daily, 24% multiple times a week, 18% once a week, and 2% monthly (Taylor et al., 2012).

A mixture of performance tests were used to evaluate athlete performance. Examples of tests included maximal jump tests, maximal strength tests, overground sprints, submaximal cycling or running tests, and sport specific running tests.

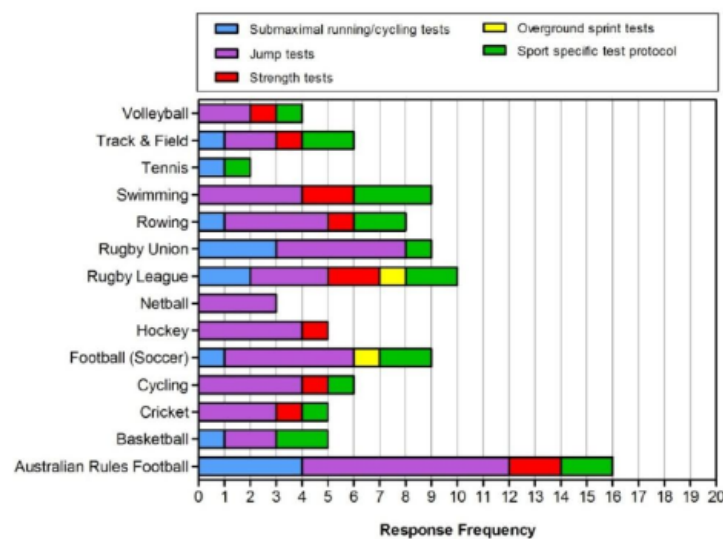


**Figure 2.1: Current Fatigue Tests by Sport, (Taylor et al., 2012)**

For soccer, jump tests were the most common performance test followed by a soccer specific performance test. Jump tests were also popular among other sports, with the majority of respondents using them. Jump tests often used equipment such as linear position transducers, force plates, contact mats, and a vertical jumping apparatus. It was common for athletes to use a counter movement jump, with half of the respondents indicating they did so in an unloaded condition and the other half using a 45 lb Olympic bar (Taylor et al., 2012).

Soccer was also a sport that commonly relied on tracking performance within the sporting activity. This was often done through GPS that “measured work rate (meters per minute), time spent in high intensity work ranges, and total distance (Taylor et al., 2012).” Occasionally additional data collection tools such as accelerometers were utilized.

Coaches also divide fatigue into 3 levels of fatigue and monitor athletes based on that. They look at an athlete’s self-described feeling, complexion, perspiration level, breathing, and ease of movement. Mild fatigued athletes have no discomfort, slightly red complexion, slight perspiration, moderately brisk breathing, and steady footsteps. Moderately fatigued athletes have leg pain, red complexion, more perspiration, heavy breathing, and unsteady swaying. Severely fatigued athletes have pain that does not improve with rest, very red complexion, very heavy perspiration, chaotic breathing, and uncoordinated limbs (Wang, 2022).

Soccer athletes and coaches rely on many of the same metrics as participants in other aerobic sports, but they also prioritize certain metrics applicable to soccer. These metrics include player’s VO<sub>2</sub>MAX, relative strength, speed and agility, and flexibility. VO<sub>2</sub>MAX is the volume of oxygen an athlete can consume relative to their body weight, and it is measured in milliliters of oxygen per minute per kilogram of body weight (ml/kg/min). It represents the maximal aerobic power of an athlete and can be accurately measured in a lab, approximated through

physical endurance tests, or determined using other biometrics. Soccer coaches also prioritize the relative strength of their athletes. For upper body muscles, relative strength is determined by the athlete's one repetition maximum of bench press divided by their body weight and the leg press is used for the lower body. A good relative strength for the upper body is anything greater than 1 while a score greater than 2 is great for the lower body. Additionally, it is important for soccer players to have properly distributed strength in their muscles to prevent imbalances that lead to injury. Specifically, soccer athletes should aim to have quadriceps that are twice as strong as their hamstrings (Anderson, 2023).

Speed, agility, and flexibility are also essential in soccer to prevent injury and improve performance. Speed and agility are often measured through a 30-yard sprint test. Often the average of three to four sprints is taken as the athlete's final score, with anything under five seconds considered good. Flexibility can be measured through sit and reach tests, groin flexibility tests, trunk rotation tests, or by using a goniometer to measure a specific joint's flexibility (Anderson, 2023). These metrics and tests can be done throughout the season and compared with previous results to determine if an athlete is improving or not. If the scores decline it can be a sign of overtraining and demonstrates a risk of injury.

Coaches currently rely on a wide range of metrics to determine an athlete's fatigue levels and the effectiveness of their training. They use objective methods such as jump and sprint tests as well as subjective tests like surveys and observations. A lot of their methods have been developed through the coach's personal experiences and are not necessarily backed by scientific research. This creates a market for companies to design performance monitoring equipment that can assist athletes and coaches when developing their training schedules.

### **2.1.2 Current Performance monitoring devices on the market**

Smart fitness is a large and rapidly growing industry, estimated to be worth \$16.90 billion in 2022 (“Smart Fitness Market Size”, 2023). Companies prevalent in this market include Fitbit, Apple Inc., Garmin Ltd, Samsung Electronics Co. and more. Many of these companies make smart fitness devices such as watches that have mass market appeal while still being useful to dedicated athletes. For example, the Apple Watch Series 9 includes sensors capable of measuring heart rate, heart rhythm, oxygen saturation, location, speed, and sleep tracking (Apple, 2023). Apple’s competitors offer similar products, with some Samsung products offering the ability to calculate body composition as well.

While these products can be valuable resources to athletes, they have several limitations. The first is the accuracy of some of their measurements. One study investigated the accuracy of the pulse oximeter sensor on four industry leading products when compared to a clinical grade pulse oximeter. It found that accuracy varied between the devices, but even the most accurate device was only within the acceptable error range of the clinical device 58% of the time. The least accurate device was only within the acceptable error range 17% of the time. Additionally, the devices failed to give any measurement at all between 11% and 31% of the time (Jiang et al., 2023). Additionally, smartwatches can only collect health data from one node, the wrist, and this can limit the amount of biometrics they record. This means that valuable biometrics such as respiratory rate, temperature, blood pressure, and more cannot be recorded through current smart watches.

Studies have indicated that a solution to this problem lies in the idea of a body sensor network (BSN). BSNs are networks of sensors applied to the human body through skin electrodes, elastic straps, and more to enable continuous monitoring of valuable health metrics.

BSNs have a variety of health applications, including activity recognition, activity level estimation, caloric expenditure, medication adherence assessment, sports training and more. They can include accelerometers, gyroscopes, pressure sensors, electrocardiograms (ECGs), electromyograms (EMG), galvanic skin response (GSR), electrical impedance plethysmography (EIP), microphones, electroencephalogram (EEG), and more (Gravina et al., 2017).

The optimal way to design a BSN is through multi-sensor data fusion as opposed to relying on a single sensor or multiple sensors considered individually. This is because relying on single sensors can reduce the coverage area, give imprecise data, introduce uncertainty, and pose a risk of sensory deprivation due to sensor failure. A BSN can solve this problem by using multiple sensors and data fusion techniques to yield an improved signal to noise ratio, reduce uncertainty, increase confidence in measurements, improve precision of data, and gain more coverage over the body. For data fusion within activity recognition, the study recommends that data features are extracted from sensors and transmitted to be analyzed elsewhere for activity recognition. This provides power consumption benefits and reduces the communication burden (Gravina et al., 2017).

A common method of data processing for BSNs is to combine data from multiple sensor inputs through analyzing features such as mean, standard deviation, entropy, spectral energy, root mean squares, discrete cosine transform coefficients, cumulative histogram, and more. These features can be processed through a variety of machine learning models, but the most common were Naive Bayes, Support Vector Machine, Decision Trees, and k-Nearest Neighbor (Gravina et al., 2017). Through those features and processing models, researchers were able to identify activities such as walking, running, climbing stairs, riding a bike, and more from biometric data.

When building a BSN it is also important to note the hardware, software, and communications standards for such a device. BSNs can be successful with a variety of hardware architectures, but the most common are TelosB and Shimmer, with many also electing to design their own custom hardware (Gravina et al., 2017). For communications standards, IEEE 802.15.4, Bluetooth Low Energy, and ANT+ are the most common. For software, lightweight operating systems such as TinyOS and Contiki are often used. Many developers also use programming middleware such as CodeBlue, a middleware tailored for BSNs, or Titan, a more general-purpose middleware that can be successfully applied to BSNs (Gravina et al., 2017).

There are commercially available BSNs that monitor a range of biometrics for user health. One example is Hexoskin, a company that offers machine washable, bluetooth enabled, rechargeable, smart clothing. This company offers two products, the Hexoskin Smart Clothing Monitor and the Astroskin Smart Clothing Monitor. Their first product, Hexoskin, offers continuous cardiac, pulmonary, activity, and sleep data and retails for around \$650. It also provides in-depth heart rate reporting through an ECG that monitors resting heart rate, heart rate variability, heart rate recovery, and heart rate zones. Through its chest and abdominal respiratory inductance plethysmography sensors it also records breathing rate, minute ventilation, and VO2MAX. Finally, it also offers information about activity intensity, acceleration, cadence, and positioning through a 3-axis accelerometer. The company's second product, Astroskin, offers additional health metrics such as blood pressure, skin temperature, and blood oxygen levels and retails for around \$6000 (Hexoskin, 2023).

Another company, Restwise, offers a way to evaluate athlete training to predict fatigue. The company offers a proprietary algorithm that takes specific biometrics as an input and returns a daily score with an explanation as an output. The biometrics this company monitors are resting

heart rate, body mass, sleep, oxygen saturation, hydration, appetite, muscle soreness, energy level, mood state, and the previous day's performance ("Restwise: What We Do", 2017).

However, the limitation of this solution is that it does not collect the data, only processes it. This means that athletes still need to monitor their own biometrics to make use of this tool.

## **2.2 Important Performance Metrics and Biometrics**

In pursuit of ensuring the health of collegiate soccer athletes, measuring performance metrics and biometrics have become valuable tools. These metrics can provide insight about an athlete's current abilities and trends in their performance over time. This information can be essential to determining an athlete's health.

### **2.2.1: Biometrics**

Biometrics can measure a wide range of psychological data that can offer real-time, useful information about the athlete's physical condition. Some crucial biometrics include heart rate, respiratory rate, body temperature, and muscle activation with electromyography (EMG) to monitor and reduce overexertion (see Appendix A for more information on athlete health and risks of overexertion).

#### **2.2.1.1: Heart Rate**

Heart rate is a fundamental biometric that can assess the physical demand of an athlete while playing soccer. As a person is exercising, the heart is contracting faster to increase blood circulation to the rest of the body because of excess demand for oxygen and energy. The average collegiate soccer player has a resting heart rate of about 50 beats per minute (bpm) with a maximum heart rate of 188 bpm (Raven, P. B., 1976). Maximum heart rate is the highest a

person's heart rate can go while under stress before risk of overexertion. While playing soccer, the average heart rate among collegiate soccer athletes is about  $172 \pm 12$  bpm (Ali et al., 1991). However, studies have shown that rapid and significant increases in heart rate during exercise can mean overexertion. "Heart Rate-Based Training Intensity and Its Impact on Injury Incidence Among Elite-Level Professional Soccer Players" by Owen Adam, L. et al claims that "an increased proportion of time spent at  $85\text{--}90\%$  HRmax significantly increased the odds of sustaining a match injury" (Owen et al., 2015). Musculoskeletal injuries are soft tissue injuries that can affect a wide range of structures including bones, tendons, muscles, and ligaments. Frequent musculoskeletal injuries are sprains, strains, fractures, and tendonitis. In response to overexertion, a variety of musculoskeletal injuries are common which is why measuring and monitoring heart rate can be a crucial biometric.

#### **2.2.1.3: Respiration Rate**

Respiration causes blood volume variations on both the arterial and venous sides, as the deoxygenated blood enters the lungs to become oxygenated before traveling to the rest of the body. Respiration rate is another valuable tool for measuring exertion in soccer players as it measures the number of breaths taken in a minute. As the athlete engages in physical activity, muscles require more oxygen, so respiration rate increases to meet this need (Figure 2.4). Pulmonary ventilation, or breathing, is directly proportional to the increase in metabolic activity, so this biometric can be used to analyze potential overexertion in players who have spikes or really high respiration rates (PT Direct, 2010).

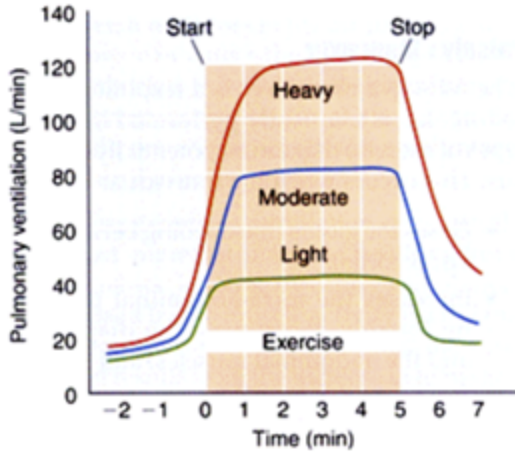


**Figure 2.2: Graph showing relationship between light, moderate, and heavy exercise time with pulmonary ventilation rate (PT Direct, 2010)**

#### 2.2.1.4: Body temperature

Some specific assessments that body temperature can help determine are heat stress, dehydration, fatigue, and risk of muscle cramps and injuries. However, body temperature is not the sole determining factor. Soccer athletes often play in extensive heat waves and humidity which can cause heat stress as the body has a difficult time getting rid of excess heat. When this occurs, body temperature rises from normal body temperature ranging from 97.7 to 99.5 degrees Fahrenheit while exercising. During heat exhaustion, the body can rise to temperatures around 101 to 104 degrees Fahrenheit. Monitoring body temperature can help determine when players should sit out to prevent heat exhaustion and heat strokes. Additionally, the high body temperatures that can indicate dehydration also range from about 101 to 104 degrees Fahrenheit. Both heat exhaustion and dehydration are often connected and lead to fatigue in the player. Finally, studies show that high body temperature can increase the likelihood of muscle cramps and injuries due to reduced muscle flexibility. When body temperature is above normal, muscle stiffness increases which makes muscles more susceptible to strains, sprains and tears (González-Alonso et al., 1999).

### 2.2.1.5: Electromyography

Electromyography (EMG) measures changes in muscle activation and intensity of a muscle contraction. Muscle fatigue is the decline in the ability to create force for muscle contraction and takes place in the muscle fiber cells. These cells produce high frequency signals during contraction, but cannot maintain the high frequency for long periods of time which reduces effective contraction and leads to decreased muscle forces. Studies found that muscle fatigue is correlated to musculoskeletal injuries during sports (Yousif et al., 2019). Therefore, surface EMGs can measure and detect muscle fatigue by analyzing the amplitude and frequency received by the sensor. A reduced amplitude and frequency over exercising time indicates that there is less muscle force production (Figure 2.3).

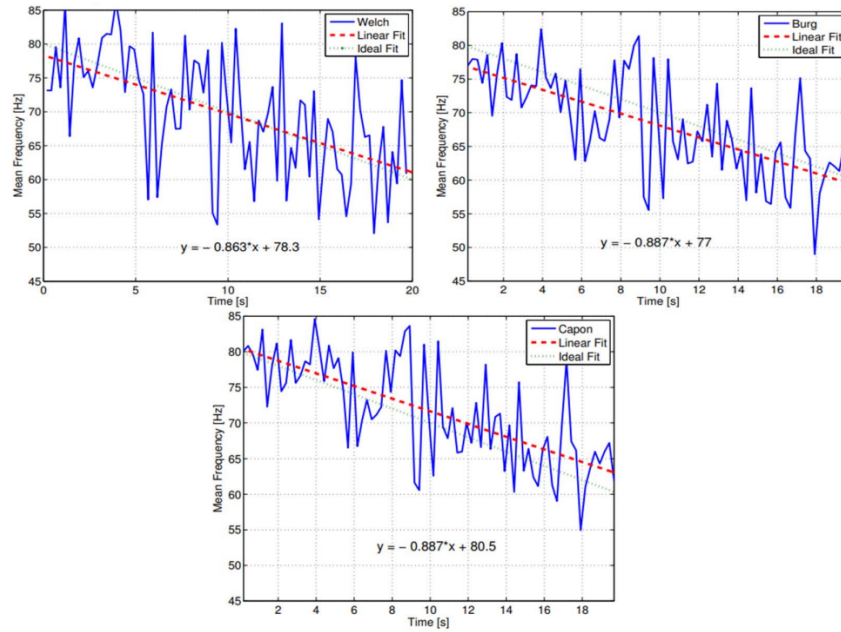


**Figure 2.3: Graphs of muscle fatigue detection with mean frequency linearly decreasing (Yousif et al., 2019)**

The study also suggested that for increased accuracy in EMG muscle fatigue detection, time domain features should be analyzed in addition to frequency domain features to ascertain

fatigue (Yousif et al, 2019). Examples of time domain features that were analyzed include the root mean square (RMS) and mean absolute value (MAV). Frequency domain features were calculated through a fast fourier transform and the change in mean and median power frequencies were monitored. The study suggests that fatigue can be recognized when the frequency domain feature decreases as there is an increment present in the time domain feature (Yousif et al, 2019).

### **2.3.2: Performance Metrics**

Performance metrics can measure a wide range of data that can offer real-time, useful information about the athlete's effectiveness in the sport. Some crucial metrics include location, pace, and velocity. These metrics can be used by the individual player and help coaches analyze game aspects and make informed decisions based on the provided data.

#### **2.3.2.1: Location**

Tracking the location of each player can provide insight to player performance to evaluate technique and make decisions. Tracking an athlete's location provides information on their positioning, movement patterns, and interactions between teammates and opponents. This helps designing game strategies to improve performance and can also help identify potential injuries by analyzing asymmetrical moving patterns. Recording location throughout a game also enables coaches to track the distance a player has covered throughout the game. A decline in distance from the first half to the second half of the game could indicate they were more fatigued in the second half.

### **2.3.2.2: Pace**

Pace is a person's speed and endurance in minutes per mile and is an important metric used for performance and personal health. Pace is typically a consistent speed kept over a period of time so there are no sudden movements; however, a person's average pace compared to their real time pace can demonstrate muscle and endurance fatigue. As stated before, muscle and endurance fatigue positively correlates with risk of injury, so it is important to make sure there are no sudden spikes or dips in an athlete's pace. According to "How Fast Should a Soccer Player Run a Mile?" by Sean Tinney, an average college soccer athlete should run a mile in 5.5 minutes indicating healthy endurance (Tinney, 2023). Some common injuries that can happen because of pace include shin splints, tendonitis, and stress fractures which occur over time. To reduce these number of injuries, measuring pace and making sure the athlete does not overexert themselves in this way is key.

External load is physical movement of work being done on the body with acceleration and deceleration measurements being considered key indicators. One study tested and explained how "intense accelerations and decelerations could be particularly vulnerable to neuromuscular fatigue and consequently to an exacerbated risk of incurring injury" (Harper et al., 2019). This is because constant acceleration and deceleration typically involves sudden movements that puts stress on muscles, tendons, and joints leading to sudden and explosive injuries like ACL tears, tendinopathies, and hip flexor injuries. The muscle damage is caused by strain to the muscle fibers during eccentric or lengthening contractions which interferes with the muscle cells (Guilhem et al., 2016). Therefore, measuring acceleration and deceleration provides data and insight on how to reduce these explosive movements and further improve performance and reduce injuries.

## **2.4 Measuring Biometrics**

### **2.4.1: Measuring Heart Rate**

Heart rate can be measured through multiple methods that utilize different techniques and body parts, producing measurements with various levels of accuracy. Photoplethysmography (PPG) is one of the most common methods used, focusing on obtaining heart rate by measuring the light absorption (Alian & Shelley, 2014) from an infrared light-emitting diode and photodetector through the skin to find the volumetric change in blood flow (Koshy et al., 2018). Essential frequencies to obtain accurate measurements of heart rate through the PPG waveform include a 600 to 700 nm frequency for the light-emitting diode and 0.01 to 15 Hz for the photodetector (Subasi, 2019). This absorption is measured over time and amplified and analyzed for the cyclic reemergence of light intensity due to blood flow that occurs with the ejection of blood from the left ventricle of the heart. This waveform is flipped across the y-axis to properly display the amplitude of blood flowing through the blood vessels as the amplitude of light flowing through the blood vessels is recorded by the photodetector. The PPG waveform is also heavily filtered through bandpass filters to eliminate erroneous noise due to movement while additionally centered through autogain to prevent drift of the waveform data (Alian & Shelley, 2014). The resulting waveform displays the amplitude of the volume of blood against time, creating a graph that can be analyzed for heart rate and compared against other important biometrics, as seen in Figure 2.4.

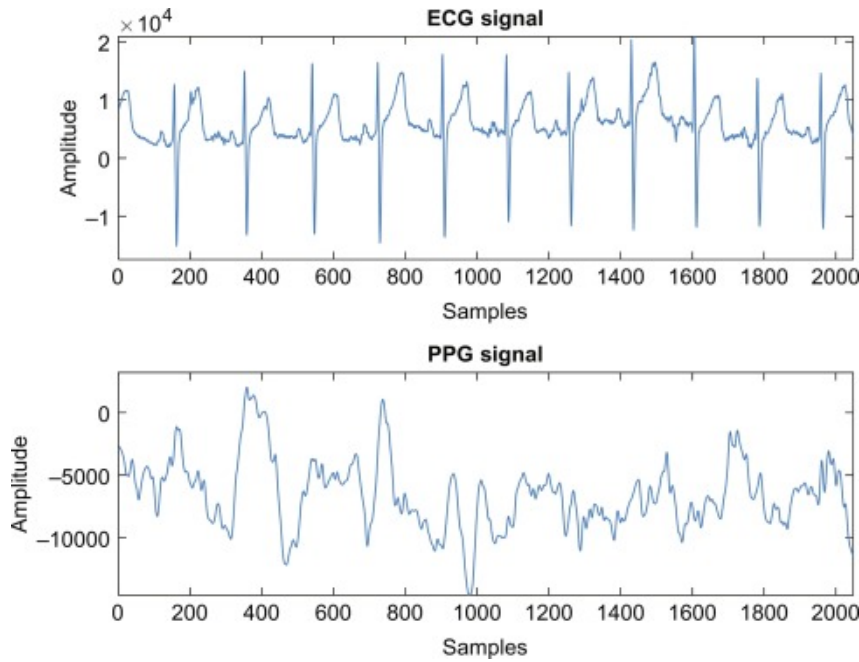


**Figure 2.4: Photoplethysmography (PPG) waveform compared to an electrocardiogram (ECG) waveform (P. Välisuo, 2015)**

Due to the high sensitivity of the infrared waveform towards the change in blood flow, the heart rate variability, which is the change in the time between peaks in the heartbeat waveform, as well as any irregularities in heart rate can be observed through irregularities in the waveform (Alian & Shelley, 2014), which is essential to quickly determine signs of compensated shock before deterioration into decompensated shock (AAOS, 2016). The amplitude of the pulse in the PPG waveform is often filtered out but indicates changes in blood vessels, such as increased stroke volume or the narrowing of the blood vessels with the increased amplitude. PPG waveforms can also be analyzed for the pulse transit time, the amount of time required for the waveform to arrive at the distal end of a body part, which has been associated with increased vascular resistance and reduced elasticity of the blood vessels, often accompanied with hypertension, diabetes, and aging. Viable locations in which the PPG waveform are regions of the skin in which the tissue below the epidermis contains capillaries and arterioles in the tissue

below, such as the forehead, fingertips, earlobe, and nose. Benefits of PPG include the noninvasive measuring of the pulse while also having the ability to obtain potential sources of poor oxygen saturation through observations in the hemoglobin (Alian & Shelley, 2014). Optical measurements of heart rate can have accuracy and reliability significantly reduced due to a multitude of factors, including the source of vein pulsation, vasoconstriction, thickness of skin, skin tone, tissue composition, changing tissue blood fraction, exposure of the photodetector to ambient light, and more, making PPG unreliable when comparing results of different users (Mannheimer, 2007).

Another practical method of heart rate monitoring that is frequently used is electrocardiography, a noninvasive method using electrodes to obtain, measure, and display electrical signals from the heart in an electrocardiogram (ECG). This noninvasive technique measures the electrical difference between pairs of electrodes with a variety of lead placement techniques available. Electrical signals in the heart originate through the depolarization of the sinoatrial node (Galli et al., 2022), a group of muscle tissue that sets and controls the rhythm of heart rate, signals for the atria to contract. This electrical signal then transmits to the group of muscle tissue called the atrioventricular node that distributes the signals through the bundle of His and Purkinje fibers, causing the ventricles to contract and pump blood to the lungs to be reoxygenated and throughout the body through capillaries to distribute oxygen, becoming deoxygenated (AAOS, 2016). Depolarization and repolarization of muscle tissue in the heart create low-intensity electric fields on the surface of the human body, which are measured through the various electrodes placed on the skin, delivering an ECG showing changes in voltage over time with the identifiable P wave, T wave, and QRS complex in the waveform (Figure 2.5). The RR interval, the length between the two consecutive R peaks, can be used to obtain the heart

rate by measuring and dividing the RR interval time by sixty, giving the number of times the heart beats a minute. It should be noted that it is more accurate to obtain heart rate from an ECG by obtaining the number of R peaks over a period of at least fifteen seconds to indicate if there is any noticeable abnormal heart rate with significantly varying HRV, such as atrial or ventricular fibrillation. Although other methods of obtaining heart rate from the ECG are available, the QRS complex is easiest to identify and use in the waveform, still used 70 years after being proposed (Galli et al., 2022).

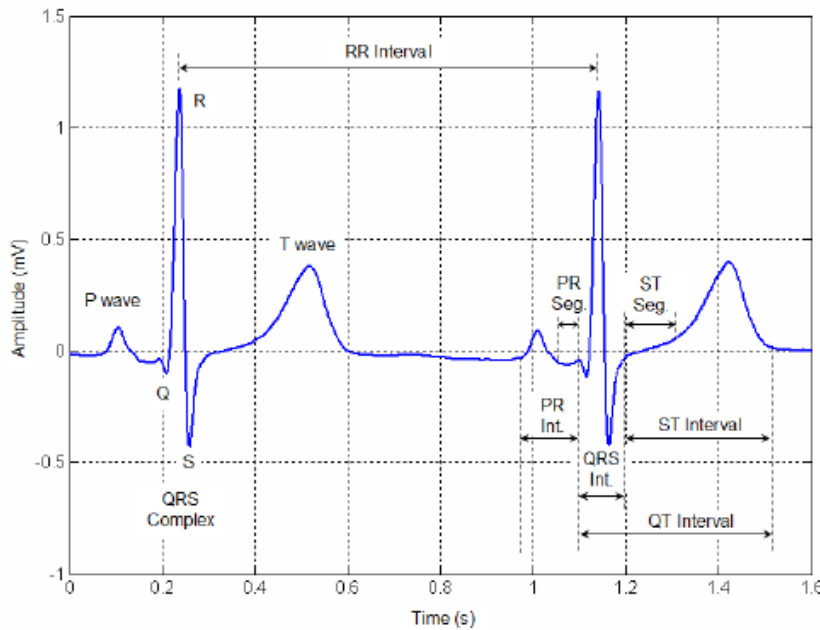


**Figure 2.5: Sample electrocardiogram (ECG) showing the wave segments and RR interval**  
**(Vinzio Maggio et al., 2012)**

Lead quantity determines the quality of the ECG obtained, with the simplest ECG lead method involving the usage of 3 leads, comparing the difference in electrical signals between each lead. This involves the placement of an electrode under both clavicles in the region of the upper rib cage with a third electrode placed in the left upper quadrant of the abdomen on the ribcage. It is essential to achieve good skin contact and placement to help reduce artifacts in the

resulting ECG, as this can result in incorrect or indecipherable biometric data. One such way to maintain correct lead placement is by shaving the hair on the lead site before placement to prevent the lead from rising off the skin, which is preferably done with an electric razor to prevent skin irritation or laceration from a manual razor. The lead site should also be swabbed with an alcohol wipe after shaving to rid of any oil or dead tissue that may remain (AAOS, 2016). A multitude of electrode types are available based on user preference, such as wet and dry electrodes, each having their own advantages. Wet electrodes provide good signal transmission and are the simplest to apply, but the signal may worsen as the gel adhesive begins to wear and may have issues with biocompatibility from the type of adhesive used. Dry electrodes have been seen to be more comfortable and durable, being able to withstand usage during intensive movements and exercise while being able to maintain good signal collection. However, dry electrodes suffer from impedance in the electrical signal due to low contact during measurement due to having no adhesive, as well as potential signal reduction after repeated washing (Galli et al., 2022).

#### **2.4.3: Measuring Respiration Rate**

Respiratory rate (RR) has a multitude of collection methods, with most techniques being invasive and often being limited to clinical and occupational settings. The most widely available non-invasive methods for measuring respiratory rate for exercise involve measuring the movement of the abdomen or chest wall during breathing. Obtaining RR through strain sensors focuses on the indirect movement of the body, primarily in the diaphragm and intercostal muscles, due to breathing to find the pattern of respiration. Piezoresistive strain sensors are used to detect strain applied across the resistor, which produces a variation in the electric charge concentration, which can be used to detect the respiratory frequency (Figure 2.6). This change in

electric charge concentration, represented as the voltage output, when compared to time shows the frequency of breathing rate when observing the peaks in voltage, which denote periods in which breathing occurs and strain increases due to stretching of the piezoresistive from skin stretching with the expansion of the lungs during breathing (Massaroni et al., 2019).

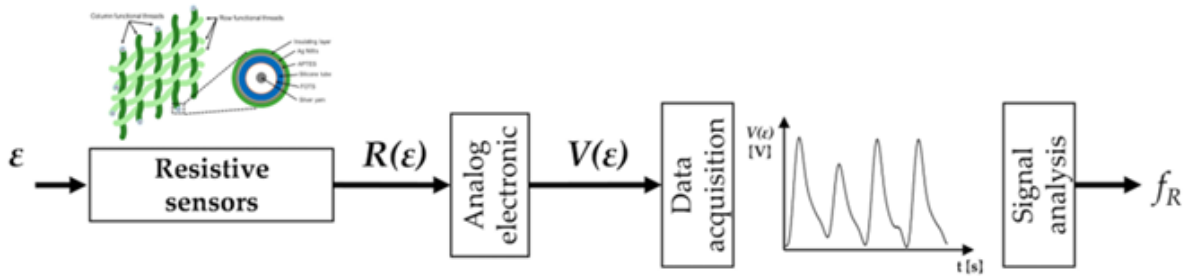


**Figure 2.6: Process for piezoresistive sensor prediction of respiratory rate,  $f_R$ , using strain ( $\epsilon$ ), resistance change from strain ( $R(\epsilon)$ ), voltage change from strain ( $V(\epsilon)$ ). (Massaroni et al., 2019).**

The ideal mechanical properties of the strain sensor can be found by using the following equation:

$$\frac{\Delta R}{R_0} = k_G \cdot \frac{\Delta L}{L_0} \quad (1)$$

which states that the change in resistance due to strain  $\Delta R$  divided by the original resistance  $R_0$  is equal to the gauge factor  $k_G$  multiplied by the change in length due to strain  $\Delta L$  divided by the original length  $L_0$  (Massaroni et al., 2019). Piezoresistive strain sensors, while compact, affordable, and having the ability to measure respiration volume during inhalation and exhalation, have decreased performance due to repeated folding and artifact motion during exercise and motion, but it has been observed that placement of the sensor on the upper thorax when compared to the abdomen was exposed less to erroneous motion (Chu et al., 2019). Similar

methods of measuring differences in electric charge have been accomplished through the usage of capacitors, inductors, and fiber-optic sensors, but have been found to produce similar results (Massaroni et al., 2019). Another similar method to the usage of strain sensors is that of pressure sensors to analyze the force of the chest wall expanding is also a common technique used in the measurement of respiration rate. This technique also offers similar advantages to that of strain sensors, such as limited artificial noise when applied tight around the upper chest (Nicolò et al., 2020).

Calculating respiration rate with movement sensors is also viable with the usage of either acceleration or angular velocity sensors on the chest wall to detect motion during lung expansion. An acceleration sensor can transform mechanical acceleration across all 3 axes forces into an electrical signal by exerting compressional or tensile force onto a transduction element, such as a capacitor, piezoresistive, or piezoelectric sensor, in response to inertial motion. Various breathing patterns have been analyzed and verified with the usage of acceleration sensors, but activities with excessive movements, such as walking or running, have been seen to cause errors of up to 7.45 breathes per minute, significantly reducing the accuracy of the accelerometer, with similar results found between the use of accelerometers on both one axis and three axes (Massaroni et al., 2019). Angular velocity sensors, with the mechanical and micro-electromechanical system gyroscope being the most commonly used sensor, have calculated the change in the thorax angle during respiration by recording the angular velocity of the frame it is attached to. Sensor units measuring inertial motion, such as the angular velocity sensor, are extremely prone to drift errors, which would make the use of such a sensor unfit for long-duration data collection (Singh et al., 2021) without the additional use of an accelerometer. Strenuous activities also increased the percentage of error when calculating breathing frequency,

having an average error upwards of 3.0 breaths per minute. Both the acceleration and angular velocity sensors output their biometric data as velocity across time, giving a plot of chest motion with each peak being measured as a singular breath (Massaroni et al., 2019). Similar to clinical measurements of breathing rate, a minimum interval of fifteen seconds should be used to gather biometric data on chest movement (AAOS, 2016).

Another method that has been suggested for determining respiratory rate is that it can be calculated from ECG or PPG data. Several studies have developed algorithms to derive respiratory rate from ECG and PPG data, and a python library called Neurokit exists that enables the use of these. One study used matlab to analyze a variety of algorithms meant to determine respiratory rate from ECG and PPG signals, and it determined that it is a viable technique (Charlton et al, 2018). This study was done to determine which algorithms are the most effective for determining respiratory rate from heart rate signals. It found that most algorithms relied on either ECG or PPG signals, and some considered both (Charlton et al, 2018). Software libraries have also been developed that can calculate breathing rates from ECG or PPG signals. An example of this is the python library NeuroKit2 (Makowski et al, 2021). This is a comprehensive library capable of analyzing ECG, PPG, and EMG signals and calculating respiratory rate from ECG or PPG signals. Four methods are packaged in the library; they were developed by Van Gent et al, Charlton et al, Soni et al, and Sarkar et al (Makowski et al, 2021). ECG derived respiration rate is a cost-effective technique that can give a valuable estimate of breathing rate without invasive sensors.

#### **2.4.4: Measuring Body Temperature**

Body temperature is important to measure as it can help athletes mitigate heat stress, determine dehydration, serve as a rudimentary illness detection, and provide warning for cramps or fatigue related injuries. There are multiple methods of measuring a person's body temperature, including infrared sensors, thermometers, thermistors, or other temperature sensors. These different sensors have different locations on the body they must be placed for an effective measurement.

The sensor's placement can vary from invasive to unintrusive. For example, infrared thermometers are frequently used on a person's forehead and they require a distance from the skin to achieve an accurate measurement. For other temperature sensors, various locations of measurement include oral, rectal, or axillary (MedlinePlus, 2018). The first two of those methods are very invasive and impractical for use during exercise. Therefore, an infrared sensor or an axillary mounted temperature sensor would be ideal for use on athletes.

According to a manufacturer of IR human temperature sensors, the ideal distance for their product is between 5 to 15 centimeters from the human skin being measured (Non-contact Temperature Measurement FAQs, n.d.). This distance could present a challenge for use on a soccer athlete, as it would add considerable bulk to the equipment they are using and could be cumbersome to their movements. While these sensors are accurate, they would be impractical to implement on a wearable device due to that constraint.

Axillary temperature has the benefit of being easy to integrate on a wearable device because clothes are already worn in that area and it would not disrupt a player's movement. However there are some drawbacks to this method. Axillary temperature has been shown to be less accurate than rectal or oral temperature readings, with a lower temperature reading overall

and a larger temperature range compared to other methods. The range was observed by one study to be between 2.5 and 3 degrees Celsius (Falzon et al., 2003). While using axillary temperature to determine illness could be ineffective, it can work for the purpose of identifying heat stroke and fatigue. During intense exercise the body temperature increases (D'amato et al., 2019). If the change in temperature between the start of the workout and the end is measured, axillary readings could be used to partially evaluate fatigue.

#### **2.4.5: Measuring EMG signal**

Significant research has been conducted on the signals collected by EMG sensors and their effect on muscle performance. One study explores the relationship between electromyography (EMG) or surface myoelectric (SMG) features with respect to muscle strength level, particularly focusing on the tibialis anterior muscles during plantar-flexion among hemiplegia patients (Li et. al, 2014). This study makes the point that muscle rehabilitation plans depend on muscle strength, and how the current disability muscle strength measurement systems - such as the Barthel Index (BI) or the motor component of Functional Independent Measure (M-FIM) - tend to have limitations and can lead to subjective/biased data. By focusing more on EMG/SMG techniques, more finely grained quantitative data would be collected, leading to better rehab plans for injured athletes. The study noted that there was a linear relationship between EMG signals and isometric (single muscle contraction) / isotonic (external constraints) muscle exertions. It also noted that a key limitation of EMG sensors is that they only work on the surface level and wouldn't be optimal for deeper rooted muscles. Hence the placement and security of the EMG electrodes is extremely important for signal measurement. Below is an example of an interval based workout for an EMG signal, after the root mean square (RMS) of the data has been taken:

## **2.5 Measuring Performance Metrics**

For soccer athletes, measuring performance metrics can be just as important as measuring biometrics. Performance metrics such as velocity, acceleration, location, and more can give insight to an athlete's performance throughout the game, and trends in the data can be analyzed to look for signs of fatigue or injury in a player. Having access to performance metrics can also enable coaches to make better informed decisions about positioning their players because they would better understand their abilities.

### **2.5.1: Measuring Location:**

A key metric for understanding athlete performance is player tracking. A common method of player tracking and visualization is GPS tracking systems and heat maps, which are commonly implemented in sports, most recently as a small chip within the 2022 World Cup game ball from Adidas (Adidas, 2022). Research from Tuanjai Archevapanich and their team looked into athlete movement tracking via GPS and a NodeMCU (Archevapanich et al., 2021). Their overall structure of the system operated like so:

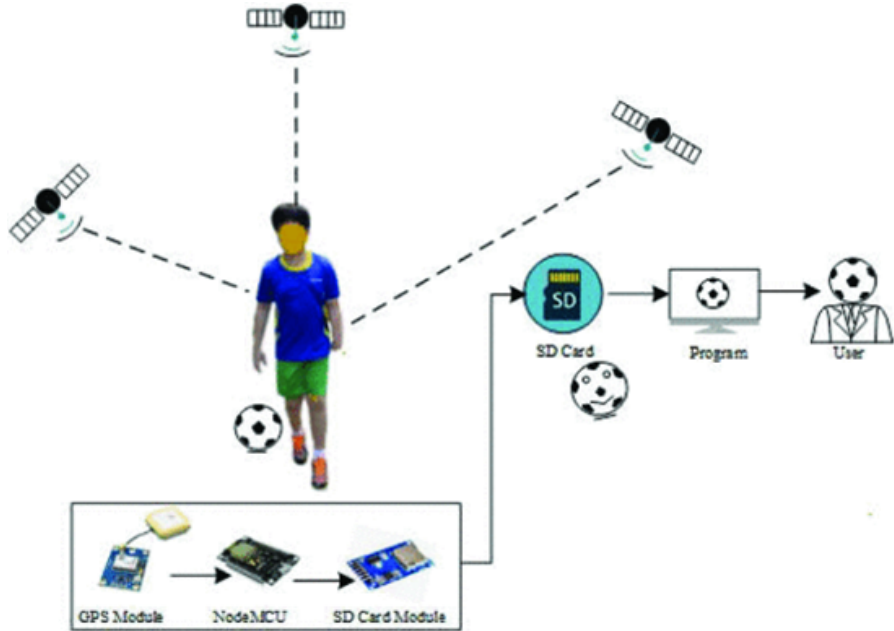


**Figure 2.7: Overall GPS Tracking system components (Archevapanich et al., 2021)**

The essential system contains 3 major components: The GPS Module (which links to a tri-satellite system), the NodeMCU (central microcontroller), and the SD Card Module (compression/visualization of the data). After setting up their central power unit and their microcontroller, their next step was to create the heatmap. In order to do this, the software has to initialize the Latitude/Longitude coordinates of the four corners of the soccer pitch, and then track the movement of the central chip (which is mounted to the player) relative to the corners. Measuring the data in ten minute intervals before compressing it to the SD card, the data turned out in the following format.

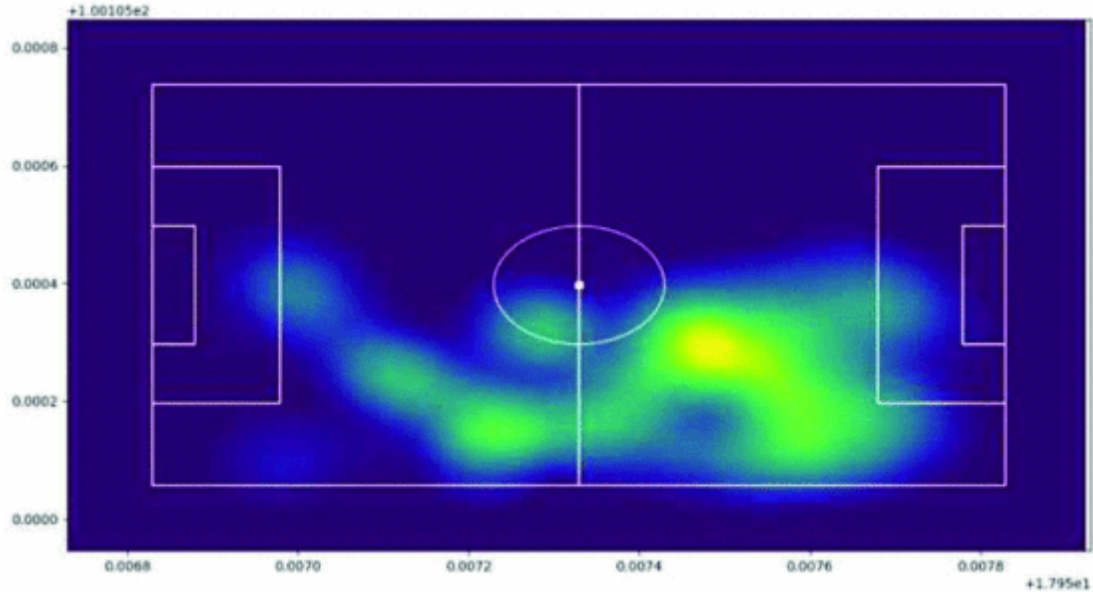


**Figure 2.8: Example 10-minute heatmap output (Archevapanich et al., 2021)**

#### 2.5.4: Measuring Pace

The formula for calculating pace requires the distance traveled over the period of time. Using the previous method for finding distance, dividing this by the total time the athlete has moved gives pace, which should be an accurate representation of the effort the player is giving. As mentioned previously, it is essential that a higher frequency is used with GPS-based tracking of distance as the increased intensity of movement, such as in soccer or basketball, decreases the reliability of results as non-linear movements can not be as effectively tracked and recorded, which in turn lowers the accuracy of pace (Gray et al., 2010).

Additionally, some GPS units include the ability to record velocity. These values could be stored with the locations and analyzed for features such as average velocity, maximum velocity, and more. It would also show velocity trends over time, which is essential to understanding an athlete's fatigue level.

## **3.0 Project Strategy**

An effective project strategy is essential to the success of the development of a new product. Several approaches were used to define the scope, requirements, design parameters, and final design of this project. First the functional requirements of a device to determine fatigue and their corresponding design parameters were determined based on the needs of the users of this product. Once the design parameters were segmented, the team developed and verified different sensors and software concurrently to save time and ensure that all parts could work in conjunction with one another. This enabled the team to create an effective design capable of achieving the goals set for it.

### **3.1 Initial Client Statement**

Currently, there are limited options to quantitatively measure athlete readiness in the buildup to official matches. This results in coaches relying on observations and subjective analysis for evaluating athlete training, performance, and fatigue, which increases the risk of injury and potentially decreases athlete performance. This project's objective is to create a smart wearable device that allows for the real-time indication of an athlete's level of fatigue using both performance and biometric data during operation. This device should record accurate data regardless of user actions or mobility as well as not inhibit the user's performance in any ability.

### **3.2 Objectives and Constraints**

The goal of this project is to develop a non-invasive body sensor network to monitor key biometrics in soccer athletes. The team intends to monitor an athlete's body temperature, respiration rate, heart rate, and muscle exertion through a combination of wearable devices.

Biometric data was collected and wirelessly transmitted to a website, where it was displayed and then analyzed to determine athlete performance. The team determined four objectives to achieve this goal:

1. Select most important biometrics to accurately measure fatigue in a person
2. Develop sensor integration via wearable body network device
3. Implement data analysis and scoring system to accurately display biometric and performance metrics to user
4. Ensure effective and user friendly interface

Constraints that were analyzed include battery life, sensor accuracy during excessive movements/activities, network availability and accessibility, GPS location precision, and budget and part availability. Due to the large volume and variety of sensors utilized in both the athlete vest and leg sleeve, battery life and output is a major concern. Each sensor requires a specific power input to function, and the battery of choice must be able to power at least five different sensors simultaneously. More information on the sensor VI characteristics can be seen in Appendix D. Collegiate soccer practices, scrimmages, and games are projected to require an extended battery life capable of up to a three hour duration (Mackey E., 2023). Bulkiness and cost of larger batteries causes restrictions on both the mobility of users and project budget, which limits battery selection to that of a smaller capacity. This could reduce the time that the device can be powered to less than the length of traditional collegiate soccer activities mentioned above. However, the battery life would still be long enough for proper validation and verification testing of the fatigue measuring device.

Another constraint found through testing and research includes the accuracy of data due to excessive movements and actions of users during testing. Erroneous noise can be present due

to the placement of sensors and electrodes, secureness of data cables, and the sensor modules used. Wires used for the transferring of data of analog sensors were found to produce major variations in voltage, caused by movement or compression during testing. Limited internal views of the human body from the positioning of analog sensors also caused unintended increases in voltage output. The usage of analog sensors additionally led to the accuracy of data being significantly reduced due to the previously mentioned issues. Although major actions were taken and procedures were put in place to prevent excessive noise in the form of voltage in analog sensors, noise could not be eliminated from the extracted data sets.

Accuracy and connectivity with positioning of the athlete on the soccer pitch was found to be a major limitation as the GPS module was found to be consistently inaccurate, as finding the position of an athlete on a field within 2.5 meters would be acceptable for larger applications but not for sports. After multiple tests and verification trials with the module, the GPS was found to be sufficient for a concept of how such a device would be used in fatigue measurement but should not be regarded as entirely accurate. While the connection of the GPS module was sometimes difficult to achieve due to weather or satellite availability, the tall buildings on the WPI campus were found to cause brief interruptions in data collection and possibly even a complete sever of connection. This was kept in mind during the actual tests and trials of fatigue measurement, as the soccer field utilized for testing were next to tall buildings that could obstruct the view of the module to the satellite, creating an incomplete dataset in relation to other metrics. Availability of the testing area also caused issues, as the rooftop field was changed to be the primary testing location due to its increased availability and access. Although the same field was used for each trial, the location on the field varied for each test subject, allowing for inconsistency and possibly inaccurate results.

Network availability is another major constraint due to the distance of the testing field, the H.Carr Field at Alumni Stadium, from any access to the WPI network. As the testing application requires a connection to a network to properly operate and communicate data between the testing vest and the website, the limited to non-existent connection prevents due to distance the proper relationship needed for the analysis of datasets. In addition to the limited accessibility of the WPI network, another source of constraint involves the network protocols of the WPI network. If a connection to the WPI network was possible, the private network does not allow for the transfer of information due to security protocols. A solution to the networking issues involved the utilization of a mobile hotspot connection hosted from a smartphone to allow for continuous and uninterrupted internet access for the transfer of data.

Part availability and budget heavily constrained the outcome of the fatigue-measuring vest, as only a proof of concept was able to be produced with the resources given. The parts and modules that would have best suited the needs of data collection were too expensive for the allocated budget. Moreover, the availability of parts also severely limited the sensors that could be used, as long lead times and even parts being completely unavailable for purchase led to alternatives needing to be sought. This can be seen in the limited computing power provided by the economically viable microcontroller that was used for this project. This resulted in a decreased sampling rate and a cap to the number of data points in each collection of data. The limited power of the microcontroller meant that the sampling rate for certain sensors were artificially lowered to enable data transmission. This affects the accuracy and viability of data collected. An increased budget would have enabled the trial and error testing to be significantly decreased in duration and budget spent, as the lower budget modules that were purchased were

often more unpredictable and difficult to work with as there were limited documentation for these parts.

Specific functions were defined as essential to the operation of the project. The team determined the following functions to achieve the objectives:

1. Accurately measure and record a baseline dataset of biometric and performance metric data for usage in the fatigue scoring system
2. Accurately transfer and analyze datasets from biometric and performance metric sensors in real-time from the microcontroller unit to the website.
3. Run executable commands to filter the gathered data for display on the website.
4. Show trends of biometric and performance patterns in graphical format to show changes of metrics across the entire data collection period.
5. Accurate scoring system to indicate possible increases or decreases in levels of fatigue.

Specifications were also created to define certain ranges and accuracies that data should follow in order to exclude possible inaccurate results from the recorded data, which is included in section 4.1 Needs Analysis (pg. 45-47).

### **3.3 Revised Client Statement**

In the fast-paced realm of collegiate soccer, where athletes continuously strive for excellence, there is a pressing need to balance performance enhancement with injury prevention. Relying on conventional tests and subjective evaluations to gauge player readiness and fatigue introduces significant challenges such as jeopardizing the athletes' well-being and the team's success. Recognizing these challenges, this team's project relies on the power of smart wearable devices to detect and monitor fatigue in soccer through a harnessed sensor network placed on the body. This product aims to provide real-time, accurate data on key biometrics including body

temperature, respiration rate, heart rate, and muscle exertion, as well as performance metrics including location and pace. The collected data was wirelessly transmitted to a centralized platform for in-depth analysis, empowering coaches to adjust training and mitigate the risk of overexertion.

### 3.4 Project Approach

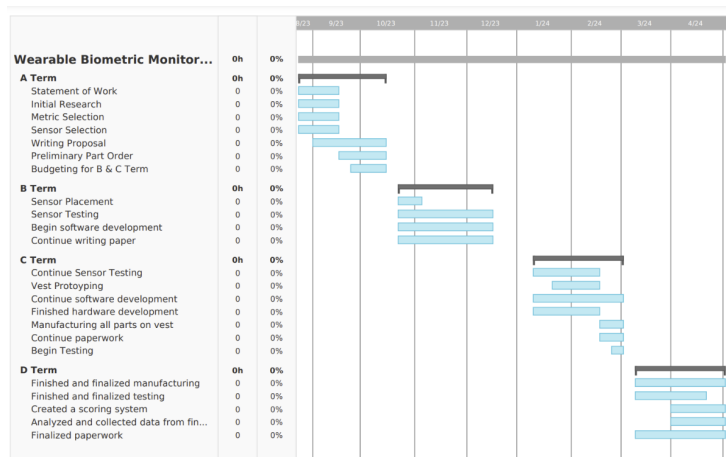


**Figure 3.1: Gantt Chart from A term 2023 through D term 2024**

This project began with researching generalized soccer athlete health and understanding the factors that make a healthy athlete. With this information, the team decided to evaluate the risk of overexertion in athletes to help reduce injuries and improve performance. Further research was conducted regarding current fatigue tests and how fatigue could be detected through heart rate, muscle activation, body temperature, and respiratory rate while also investigating current monitoring devices on the market. To ensure this product resulted in a comprehensive fatigue monitoring device, a software component was designed and added. This software system allows the user to easily view and analyze their live data. Continuing with this design, the team conducted further research to find robust and effective sensors to build and manufacture the product. After this research, the team resulted in sensors for measuring body temperature with an

LM35, respiratory rate and heart rate with a sen023 ECG, and muscle activation with a Myoware EMG.

Over the course of two terms, the team tested each sensor to ensure accurate data. The team came across a multitude of issues ranging from time management to technical issues, but with the help of Professor Bhatia and Professor Afzal, those issues were resolved. After finalizing accurate data collection, the team began manufacturing the product as one system for wearable use.

## **4.0 Design Process**

To develop the design for the smart wearable device, first the requirements of the design had to be determined. Using an axiomatic approach to define the functional requirements and design parameters, the team developed requirements for the system. Next the relevant industry standards for biometrics were investigated to ensure the system was of good quality. Finally, the hardware and software was developed concurrently with one another. Hardware was developed with a piecemeal approach that involved ensuring every sensor worked properly before slowly integrating all of them in the final design. Software was developed similarly, where after each sensor was verified the appropriate code was developed for it. Data transmission software was developed simultaneously with hardware verification. Finally, the wearable device was manufactured and tested on volunteer participants. Data collected from these trials was used to develop and verify a fatigue index scoring system to quantify fatigue.

### **4.1 Needs Analysis**

The top-level functional requirement (FR0) is to monitor biometrics in collegiate soccer athletes with a wearable device to predict and prevent injuries and health conditions caused by overuse or exhaustion (Appendix A). There are multiple requirements for this product to work as intended. First, a safe battery system that prevents electric shock, has proper temperature management, and contains safe wires is required. The battery life must run for at least 1 hour per person, allowing the athlete to warm up, complete their exercise, and cool down while the device is connected.

Another requirement is that the sensors must be within an acceptable range of accuracy. The temperature sensor must be accurate within +/- 2°C. The heart rate data must be within 5%

of the user's accurate beats per minute (BPM). The GPS must measure within +/- 5 meters in all directions of the location of the user.

Other requirements address data transmission and power concerns. The ECG and EMG data must send real time data within 17 milliseconds along with the electrodes being placed within 1 inch of the given diagram and skintight. The WiFi microcontroller must have a static IP address so data can be consistently read from it. The buck converter must deliver at least 5 Volts (V) and 2 Amps (A) as an output supply. All wires must be secure with enough flexibility for varying heights and sizes with the Arduino securely fastened to the user's body. Other nonfunctional requirements include comfortability, low cost, and ease of use.

#### **4.1.1: Design Decomposition**

Design decomposition is crucial in the development of complex systems as it brings several significant benefits to the engineering and design process. This process involves breaking down the complex system into manageable and interconnected components, each serving a specific function. In the context of a monitoring device for soccer athletes, this approach ensures a comprehensive understanding of the intricate requirements, enabling a more efficient and targeted development process. By decomposing the design, developers can focus on optimizing individual components such as heart rate monitoring, GPS tracking, and biomechanical analysis. This meticulous breakdown facilitates the creation of a device that not only seamlessly integrates into the athletes' training regimen but also delivers accurate and actionable data. Ultimately, design decomposition is instrumental in achieving a sophisticated and cohesive wearable biometric monitoring device for athletes (Appendix A). The Functional analysis decomposition simplifies the complexity of the system ensuring that all functional requirements do not restrict

another functional requirement from working. As seen in Appendix A, each requirement functions independently from the rest, assuring that the product was as effective as possible.

## **4.2 Important Industry Standards**

This project is multidisciplinary and must consider a variety of industry standards. These include standards for data transmission, measuring the biometrics, soccer regulations, and more. These standards provide valuable reference points and targets for the vest to adhere to. The industry standards were created for their effectiveness so they can be suitable goals for the vest.

For the biometrics chosen, there are standards for each type of sensor. For the ECG sensor, the ISO/IEC Joint Work Group 22 created the standard 80601, part 2-86: Particular requirements for the basic safety and essential performance of electrocardiographs, including diagnostic equipment, monitoring equipment, ambulatory equipment, electrodes, cables, and leadwire. This is a standard that applies to many aspects of ECG sensors, including their lead wires, electrodes, and ECG sensors (International Organization for Standardization, 2024). For clinical thermometers the industry standard is ISO 80601-2-56:2017 and it gives standards for the safety and performance of thermometers (International Organization for Standardization, 2017). For EMG sensors, there is no relevant ISO standard, but most medical equipment aims for a sampling rate of 1000 Hz and electrode placement parallel to the muscle groups of interest.

For the standards of soccer gameplay, the team referred to the Laws of the Game, which are the regulation rules that are internationally accepted and in use by FIFA. They do not allow the use of wireless communication devices during games. However such devices can be used during practice to assess athletes' performance and monitor them for fatigue (International Association Football Federation, 2023).

## **4.3 Conceptual Designs**

Conceptual designs are essential to ensure the effectiveness of the final design. For certain biometrics, such as the EMG sensors, the team went through multiple types of hardware to test how they would integrate with the final product. The software aspect of the project also went through multiple iterations. Different conceptual designs included having an app, storing user data in the cloud, a web-based interface and more. Weighing the pros and cons of different conceptual designs allowed the team to ensure the final design was as strong as possible.

### **4.3.1: Sensor Development**

The sensors of this project were tested individually before being integrated onto the final design. This enabled the team to verify each sensor worked without any interference from other sensors, and allowed for more effective troubleshooting if issues did arise during integration. Additionally, if sensors did not work properly, were overly sensitive to noise, or it was impossible to transmit data with them then it is better to learn that before attempting to place it on the final product. This was an effective strategy that enabled the team to save money and time when developing this project.

#### **4.3.1.1: EMG**

EMGs are crucial sensors for measuring an athlete's muscle fatigue. To ensure the EMG collects accurate data several considerations are necessary. The first is the placement of the three EMG electrodes. The electrodes contain two sensing electrodes and one ground electrode. The ground electrode must be placed on a bony surface of the body such as the ankle, shin, or elbow while the two sensing electrodes should be placed in parallel with the muscle fibers of the muscle being measured, approximately 2 centimeters apart. Additionally, hair interferes with electrode

readings so the skin should be shaved before the electrode is applied. The second main consideration is that the electrode wires should be properly secured to limit noise and disconnections. The third consideration is that external pressure should not be applied to the electrodes because that would create erroneous data.

The project tested two different types of EMG sensors to evaluate their performance and select the best one. The first was a Grove EMG v1.1 detector from Seeed and the second was a Myoware 2.0 muscle sensor. The two sensors were evaluated for their accuracy in recording muscle activation, ability to limit noise, and their durability and ease of use. The different EMG sensors had different shapes. The Grove EMG had a three-lead wire that connects to two sensing electrodes and one ground electrode on one end and the sensor unit on the other. The Myoware EMG had three electrodes attached directly to the sensing unit without a wire between. It is triangular and requires additional attachments to transfer data to the Arduino and receive power. The two sensors both required electrodes, but the Myoware required modifications to the electrode shape to ensure a proper fit.

The Grove EMG v1.1 was significantly less successful than the Myoware Muscle Sensor. The Grove was easily susceptible to noise, and this noise overpowered what signals it could detect. The primary cause of the noise was from the three-lead wire that connected the electrodes on the skin to the sensor. Whenever the wire was slightly moved, this movement would cause a significant voltage spike on the sensor's output, obscuring any real data that was collected. Numerous attempts at reducing the noise were made, such as limiting wire movement, securing wire to the skin using tape, and relying on different three-lead wires. Unfortunately, these measures were ineffective, and the Grove EMG was unable to provide a working solution.

Therefore, the final EMG sensor chosen for this project is the Myoware 2.0 Muscle Sensor. It has three electrode leads directly attached to the sensor, which reduces the impact of noise on sensor measurements. The Myoware sensor relies on a link shield that connects directly to it. The link shield uses an auxiliary cable to connect to a power shield on the arduino. The auxiliary cable can transfer data and power between the sensor and the arduino, and the power shield can connect to five sensors at the same time. The noise was significantly reduced because there was no length of wire that could move and introduce noise, and the muscle activation detection was improved.

#### **4.3.1.2: ECG**

To obtain accurate and robust data from the electrocardiography sensors, proper electrode placement was seen as crucial to reduce erroneous noise while also ensuring electrical impulses from the heart were recorded. Multiple electrode placements were trialed and evaluated for their ability to collect ECG data and limit noise. The first placement involved an electrode placed to the right of the heart, another to the left, and a ground electrode placed below the rib cage. This placement was able to collect ECG data correctly when sitting still but it was susceptible to noise when the test subject was moving around. To improve the noise reduction another placement was attempted. The second placement had one electrode on the right shoulder, one on the left shoulder, and a third on the hip. Moving the electrodes away from the heart reduced the effect of noise. This placement that produced the most reliable results is seen in the figure below. Wires were also secured to the user's chest in order to ensure no erroneous noise from wire movement could interfere with the sensor's voltage output.

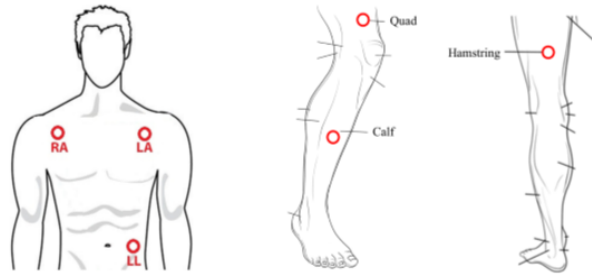


**Figure 4.1: Diagram of ECG and EMG electrode placement, with the ECG electrodes (Hakami et al, 2018) being placed on the right shoulder (negative), left shoulder (ground), and lower left abdomen (positive) and the EMG electrodes being placed on the hamstring, quadricep, and calf muscles.**

The ECG sensor chosen was the SEN-0213. It is capable of being powered off of a 5V or 3.3V pin and it can send signal information to an arduino's analog input pin. It is a 3 lead sensor that relies on three electrodes; one for a ground signal, one to be placed to the right of the heart, and one to be placed to the left of the heart. From there the code to read the ECG signal on the arduino is a simple analog read.

#### 4.3.1.3: LM35

The LM35 sensor outputs a signal that is proportional to temperature in celsius. Formulas can be used to acquire temperature in celsius and fahrenheit from the LM35 sensor output. First the raw LM35 signal must be converted into a voltage signal by multiplying the reading by  $(5.3/1024)$ , where 5.3 is the voltage input into the sensor. 0.1 volts recorded by the LM35 is equivalent to 1 degree Celsius. From there the temperature can be converted into fahrenheit using standard unit conversions.

First the LM35 sensor was tested with ambient room temperature and compared the recorded data to both a mercury and digital thermometer to ensure accuracy. If inaccuracies are recorded, then it is possible that the input voltage used in the formula is inaccurate. This can be

because the 5V power supply on the arduino is not exactly 5V. Therefore the voltage conversion formula would need to be adjusted accordingly.

When testing the LM35, it is important that the sensor does not have contact with the skin, as this was found to result in the shorting of the sensor and erroneous data collection. To ensure accurate readings, it should be placed on top of the individual's shirt between their upper arm and their torso with an armband on the outside of the sensor to keep it tight to the limb.

#### **4.3.1.4: GPS**

For measuring the GPS location of athletes on the field, the NEO-6M module was chosen for its simple setup and ease of accessibility. In order to retrieve longitude and latitude outputs, the Arduino IDE was used to create a code to record and calculate performance values. The code starts with identifying the pins used and setting a baud rate for serial monitor viewing. The digital pins D7 and D8 were chosen and the baud rate was chosen to be 9600. The NEO-6M is powered by a 3.3V pin and ground connection to an Arduino.

The connection from the Arduino to the NEO-6M is checked by sending and receiving a signal to ensure accurate readings are recorded. If a correct voltage return is given, the code records and displays the longitude and latitude values. The NEO-6M is also capable of returning velocity measurements along with the coordinates. The Arduino code for reading the latitude, longitude, and velocity from the GPS is shown below.

```

//GPS
while (SerialGPS.available() > 0)
    if (gps.encode(SerialGPS.read()))
{
    if (gps.location.isValid())
    {
        Latitude = gps.location.lat();
        LatitudeString = String(Latitude , 6);
        Longitude = gps.location.lng();
        LongitudeString = String(Longitude , 6);
        velocity = gps.speed.kmph();
    }
}

```

**Figure 4.2: GPS Arduino Code**

The code first ensures that the GPS is connected to a satellite, then ensures that the location is a valid coordinate location. Then it records the latitude, longitude and velocity collected with the GPS. Velocity is recorded in kilometers per hour.

#### 4.3.1.5: Power Source

The team wanted the various sensors and microcontrollers contained within the vest to be powered by a single power source. The electronics cumulatively require a lot of power, so a battery was selected with enough capacity to power the two microcontrollers and their associated sensors. The battery chosen for the vest has a potential of 12 volts and a current of 3 amps. It can output power through a 12V 3-amp barrel jack and a 5V 0.5-amp usb port.

The usb port was connected to the ESP 8266, powering the microcontroller, the LM35 and the NEO-6M. The 12V barrel jack was too strong to power the sensors or the Arduino Uno without damaging them, so a step-down converter was needed to enable the barrel jack to be used. A buck converter was chosen that has a 9V to 36V input and two outputs. The two outputs are a usb port and a separate 5V port. The usb is connected to the Arduino Uno which also powers the three Myoware EMG sensors and the 5V port powers the ECG sensor.

The requirements of the vest necessitated a 60-minute battery life, so the power source chosen must be able to meet or exceed this requirement. To test the longevity of the battery, all of the microcontrollers and associated sensors were plugged in when the battery was at full charge. The battery was considered dead when it could no longer provide enough power for all of the sensors to provide accurate measurements. During testing the battery exceeded the sixty minute requirement, lasting at least two to three hours.

### **4.3.2: Software Development**

#### **4.3.2.1: Internet Based Data Transmission**

An important facet of the overall software package is the transmission of sensor data over the internet. As touched on in previous sections, the initial plans for the data transmission involved a bluetooth connection to a companion app that would request and receive data in five-minute intervals. However, after further deliberation, the decision was made to swap bluetooth for WiFi direct transmission. While bluetooth transmission has the capabilities to run offline, most bluetooth modules don't have the range to handle a FIFA approved soccer pitch (9085 sq yards, 1.87 Acres), and those that did were extremely bulky and not optimal for design purposes. WiFi-Direct based transmission is more costly (through the usage of a dedicated WiFi hotspot, most commonly applied via phone tethering), but it can handle the FIFA approved dimensions comfortably, and at faster write speeds than bluetooth. The team also believed making a strong commitment to real-time data transmission (constrained within 5 seconds) would provide greater benefit to the athlete as opposed to offline capability. With that in mind, it was decided that an internet-based approach was better for the scope of the research. After deliberation, the device of choice for WiFi direct transmission was confirmed as an ESP8266, a

microcontroller with WiFi Capabilities and a hidden private server (on a user provided WiFi Hotspot). When the sensors were applied, the overall software diagram looked as such:

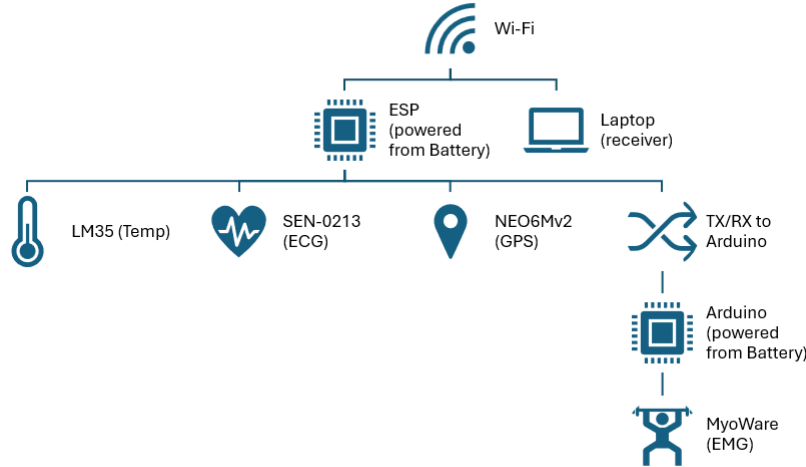


**Figure 4.3: Software Communication Diagram**

Sensor data from the LM35, ECG sensor, and GPS is fed directly into the ESP-8266 and EMG data - read from the MyoWare - is taken from an Arduino Uno and sent through the TX/RX connection ports to the ESP-8266. From there, the ESP8266 creates its own private IP address on the WiFi hotspot of choice, which any device on the network is able to access. This IP address contains CSV files of data from all of the sensors that are time stamped, generally in the format of “[“{ip\_address}/{output\_prefix}.csv”] where the output prefix is either *temperature*, *heart\_rate*,

Then a device on the same network as the ESP-8266 can retrieve the CSV files from the ESP’s website and perform analysis on the data and display it to the user.

It is important to note that this system is highly insecure, and for the safety of the electronics and the metadata, one should never consider sending data through a private IP address on a public, insecure, network. The team does not condone the theft of PII or any kind of

network reverse engineering. This system is purely for development purposes only and everyone who has used this has consented to their data being funneled through a potentially insecure platform. The team has also been vigilant on informing users of the risk of sending PII related to health and well being over the internet, and their choice is deliberated off their own means.

#### 4.3.2.2: ESP 8266

The prioritization of data transmission resulted in the selection of the ESP-8266 as the WiFi microcontroller. It is an extremely versatile piece of technology, primarily serving as an WiFi-based transmitter, but also with the potential to double as a pure arduino-based microcontroller. It is capable of connecting to an external WiFi connection and hosting a website on it that all devices connected to the same network are able to access. Since it is also a microcontroller, it is capable of reading sensor input to put on its website.

However a large limitation of the ESP 8266 is there is only one analog input on the board. The project had two sensors, the LM35 temperature sensor and the SeEN-0123 ECG sensor that needed an analog input pin. To solve this issue a CD4051 multiplexor was introduced into the circuit. The multiplexor is wired directly to the ESP 8266 and it increases the potential analog input pins from one to seven. The multiplexor is controlled by three digital pins on the ESP 8266 that can send different combinations of high and low signals to switch the inputs on the multiplexor. The multiplexor output is then wired to the A0 analog input pin on the ESP 8266 so the signals can be read. To control the multiplexor in the code, a changeMux function was created and it is shown below.

```
void changeMux(int c, int b, int a) {  
    digitalWrite(MUX_A, a);  
    digitalWrite(MUX_B, b);  
    digitalWrite(MUX_C, c);  
}
```

#### **Figure 4.4: Digitalwrite Mux Arduino Code**

Mux A, B, and C are defined as the digital pins on the ESP8266 that are connected to the multiplexor to control its input switching. The inputs on the function (a, b, and c) are set to either LOW or HIGH when the function is called to allow the multiplexor to switch inputs. The temperature sensor was connected to pin X0 on the multiplexor (LOW, LOW, LOW) and the heart rate sensor to pin X1 (LOW, LOW, HIGH). This allows the ESP 8266 to switch between reading inputs from both sensors and collect data from both.

The GPS module needs a 3.3 V power pin, a ground pin, and two digital pins to connect to the ESP 8266. Pins D7 and D8 of the ESP 8266 were used to connect to the GPS's Rx and Tx pins. Once the GPS was wired, the GPS code required no modifications to enable it to work with the ESP 8266.

The Arduino Uno mounted on the leg for collecting EMG data also needed to communicate with the ESP 8266 on the chest. The microcontrollers relied on the Rx and Tx pins on the Uno and the ESP 8266 to transmit the data. The Rx of the Uno was connected to the Tx of the ESP, the Tx of the Uno was connected to the Rx of the ESP, and their grounds were connected together to enable communication. From there code was developed that had the Uno collect EMG data from three sensors, and print those values to its serial monitor. The code running on the Arduino Uno can be found in the project github repository found in Appendix C. The ESP could then read that data by relying on the Serial.read function. The ESP is able to parse the data from the Uno because the Uno sends all data from the same timestamp on the same line, then starts a new line with each time stamp. The ESP code then reads the string sent to it until it sees a new line and can then manipulate it as necessary.

```

if (Serial.available() > 0) {
| emgValue = Serial.readStringUntil('\n');
}

```

**Figure 4.5: ESP 8266 code to read serial data from Arduino Uno**

Once the ESP 8266 was able to get input from all of the sensors it needed to be able to upload this data to its website. To do this the ESP code creates four strings, GPS\_DATA, heartRateData, temperatureData, and emgData. As the EMG reads data from the sensors, it appends the data to the corresponding strings in CSV format. It records the time in milliseconds, then the data. An example of this procedure can be found below for heart rate.

```

changeMux(LOW, LOW, HIGH);
heartRateValue = analogRead(ANALOG_INPUT);
heartRateData += String(millis()) + "," + String(heartRateValue) + "\n";

```

**Figure 4.6: ESP 8266 code to append data to csv files**

On the website itself, the ESP displays four links that each have a unique address. These links contain the csv files for their respective sensor. The home screen of the website is shown below:

## ESP8266 Data Recording

[Heart Rate Data](#)

[Temperature Data](#)

[GPS Data](#)

[EMG Data](#)

**Figure 4.7: ESP 8266 Website Display**

The website and CSV files can be accessed by all devices on the same network as the ESP 8266. The ESP is able to know when a client accesses the website and can execute code when it is visited. The ESP code defines five web server routes, one for the basic website, and one for each of the links to CSV files. The code that defines the web server routes is shown below.

```
// Define web server routes
server.on("/", HTTP_GET, handleRoot);
server.on("/heart_rate", HTTP_GET, handleHeartRate);
server.on("/temperature", HTTP_GET, handleTemperature);
server.on("/gps_data", HTTP_GET, handleGPSData);
server.on("/emg_data", HTTP_GET, handleEMGData);
```

**Figure 4.8: ESP 8266 code for web service routes**

The handleRoot function simply sends html code to the website to display the appropriate text in the proper locations so the website can be navigated. All four of the sensor routes operate similarly to one another. Once clicked, the ESP creates a CSV file with the corresponding name and puts the string variable containing all of the data inside of the file. After the file is downloaded, the ESP clears the data string so the next time data is accessed it is all fresh data. The code for handleHeartRate is shown below, and the other three functions all operate similarly.

```
void handleHeartRate() {
    // Send response to client
    server.sendHeader("Content-Disposition", "attachment; filename=heart_rate.csv");
    server.send(200, "text/csv", heartRateData);
    heartRateData = "";
}
```

**Figure 4.9: ESP 8266 code that updates csv files on the website**

To summarize the ESP 8266 code in its entirety, its primary two functions are to collect data and store it in CSV format and to send data to the website so it can be accessed. It collects

data from four different types of sensors through various means, including a CD 4051 multiplexor for heart rate and temperature, two digital pins for GPS, and the Rx and Tx pins for the EMG sensors. It stores this data in CSV files on a website it creates, and users can download these files by clicking on the links on the website. The data then resets after each click. The code in its entirety can be found in Appendix C.

#### **4.3.2.3: Data Analysis via Local Webpage Application**

As touched on in the software diagram for data collection, the data transmitter is the Node MCU ESP 8266 and the receiver is the laptop. Since the ESP8266 has its own private web server which holds its own generated csv files (touched on in 4.3.2.2), there was consensus to use a local webpage application (LWA) which fetches and analyzes data from the server with minimal delay. The LWA was created using a combination of python and html coding techniques, split into four general sections, all run on a constant refresh rate of 2 seconds:

1. Data fetching
2. Data storage
3. Data plotting
4. HTML generation

To achieve this, the file *website\_total.py* was created, and it generates a live website that has a constant refresh rate, allowing the user to constantly view changes to their data with minimal delay. The text from *website\_total.py* can be found in Appendix C. The code begins with defining IP addresses and URLs for fetching various types of data including EMG, heart rate, temperature, and GPS data. A function named *fetch\_csv\_data* is defined to handle the fetching of CSV data from the specified URLs. This function utilizes the requests library to make

HTTP requests and fetch the data. It then writes the fetched data into CSV files locally. Error handling is implemented to manage cases such as connection errors or unsuccessful requests.

After fetching the data, the code proceeds to store the fetched CSV data into local files. Each type of data, including EMG, heart rate, temperature, and GPS data, is fetched and stored separately using the *fetch\_csv\_data* function. These stored files serve as a source for further processing and analysis. The naming conventions for these files are consistent in nature, following the format of *[USERNAME]\_[METRIC]\_[EXERCISE].csv*.

The next section of the code focuses on plotting the fetched data. Two main plotting functions are defined: *plot\_emg\_data* and *plot\_heart\_rate\_data*. These functions read the respective CSV files, extract the necessary data, and generate plots using Matplotlib. For EMG data, multiple plots are created for different channels if available. Similarly, for heart rate data, a single plot displaying the heart rate over time is generated. The plots are saved as PNG images and embedded into HTML files for visualization.

Finally, the code generates an HTML report incorporating the plotted data and additional information. The *generate\_html* function constructs an HTML page with sections for EMG signals, heart rate, biometrics (including average velocity, temperature, and BPM), and respiratory rate graphs. The function dynamically inserts the paths of the generated plot images into the HTML code. This HTML report provides a comprehensive overview of the fetched data along with visualizations and analysis results. Screenshots of the live webpage can be found in Section 4.8.

#### **4.3.3: Manufacturing Procedure**

The manufacturing procedure for the vest was relatively straightforward. An athletic vest was purchased with two shoulder pockets and a larger pocket on the back. A waist bag was also

purchased to hold the Arduino Uno and the Myoware hardware. The ESP8266 microcontroller was connected to the other sensors and Arduino Uno using a breadboard, and then the connections were secured using hot melt adhesive. The same adhesive was then used to affix the ESP8266 breadboard to the battery. Below the breadboard the buck converter was secured, which enabled effective cable management that limited the size of the device. The battery and ESP device was then placed into the back pocket on the vest to be secured while worn. Additional fabric was also sewn onto the back pocket of the vest to ensure that the battery is secure.

#### **4.3.4: Developing a Fatigue Index**

For the smart wearable device to be capable of quantifying fatigue, it must be capable of synthesizing biometric data into a single number that can be compared to a baseline throughout the workout. However, quantifying fatigue is a complex topic that has varying definitions depending on the individual, activity, and accuracy of biometric sensors. To overcome this hurdle the team first defined individual scores for the most essential biometrics. To determine the weights of each biometric in the final fatigue index the team first made a hypothesis on the importance of each metric before verifying it using the data collected. Adjustments were made as necessary to the weights depending on the data collected to create the final index formula.

##### **4.3.4.1: Ranking of Metrics**

To develop the first iteration of the fatigue index, the team ranked each biometric on their relevance to determining fatigue based on background research. The ranking is as follows:

1. ECG Signals
2. EMG Signals

### 3. LM35 Temperature Sensor

Background research has suggested the data that can be determined from an ECG signal, including heart rate, respiratory rate, and others, are essential to understanding a person's level of fatigue. There is previous research that has developed markers of fatigue for the ECG signal and features such as BPM are easily understandable by users. Therefore ECG was placed with the highest importance. EMG signals are essential to understanding the fatigue in individual muscles, but they are less easy to quantifiably analyze and can have issues with noise during data collection. Therefore they were placed with lower importance. Finally temperature readings have relatively low bearing on fatigue, and are mainly useful for detecting signs of heat stroke in athletes. Therefore temperature was placed as the lowest importance.

#### **4.3.4.2: Calculations of Score**

An exhaustive score was created to provide an easy way to understand the user's biometrics and performance metrics from a perspective of fatigue. Before calculating the exhaustive score, individual scoring systems were created for each biometric.

#### **4.3.4.1.1 Heart Rate and Respiration Rate**

The user can estimate their maximum heart rate based on age using the equation:

$$\text{Maximum Heart Rate} = 220 - \text{Age} \quad (2)$$

According to the CDC, a person's heart rate during moderate-intensity physical activity should be between 64% and 76% of their maximum heart rate. During vigorous-intensity physical activity, a person's heart rate should be between 77% and 93% of their maximum heart rate (CDC, 2020). To determine the user's possible point of fatigue, this equation can determine whether the user's heart rate exceeds vigorous-intensity range for physical workout:

$$\text{Heart Rate Score} = \frac{\text{Current Heart Rate}}{\text{Maximum Heart Rate}} \cdot 100 \quad (3)$$

The range of vigorous-intensity physical activity starts at 77%, so if the heart rate score exceeds 77, then the user is at a potential point of fatigue. In order to test, the user's initial heart rate is taken and compared to current heart rate using the above equation throughout the workout. A heart rate score below 0.64 indicates not fatigued, between 0.64 and 0.77 indicates physical workout but not fatigued, and a score above 0.77 indicates fatigued with a higher score meaning the athlete is increasingly fatigued.

#### **4.3.4.1.2 Muscle Activation**

Previous research conducted by Hayder A., et al suggested that fatigue would be signaled by an increment of the signal's Root Mean Square (RMS) and a decline in the signal's median frequency (MDF). To determine if the muscles were fatigued, this project relied on the same method. The raw muscle activation signals collected by the Myoware sensors had the RMS and MDF features calculated for them. The calculations were done using a python script that ran at the conclusion of the workout and calculated the features for each muscle group individually. The features were calculated using a rolling window size of 300 data points and a graph of the features for each muscle group was displayed. After the RMS and MDF features for the quads, hamstring, and calves were calculated, a linear fit was created for each feature to determine if it increased or decreased throughout the workout. If the slope of the fit line was positive for the RMS feature and the slope was negative for the MDF feature, then the muscle group was fatigued throughout the workout. Samples of the code used to calculate the features for the muscle groups are shown below:

```

import pandas as pd
import numpy as np
import matplotlib.pyplot as plt

# Read the CSV file into a DataFrame with the correct delimiter
df = pd.read_csv('test.csv', sep=',')

# Compute point-by-point RMS for Quads, Calves, and Hamstrings
window_size = 300
rms_quads = np.sqrt(df.iloc[:, 1].rolling(window=window_size).mean() ** 2)
rms_calves = np.sqrt(df.iloc[:, 2].rolling(window=window_size).mean() ** 2)
rms_hamstrings = np.sqrt(df.iloc[:, 3].rolling(window=window_size).mean() ** 2)

# Compute point-by-point MDF for Quads, Calves, and Hamstrings
mdf_quads = df.iloc[:, 1].rolling(window=window_size).apply(lambda x: np.mean(np.abs(x - np.mean(x))))
mdf_calves = df.iloc[:, 2].rolling(window=window_size).apply(lambda x: np.mean(np.abs(x - np.mean(x))))
mdf_hamstrings = df.iloc[:, 3].rolling(window=window_size).apply(lambda x: np.mean(np.abs(x - np.mean(x))))

```

**Figure 4.10: Python code to calculate RMS and MDF from raw signal csv file**

After the features were calculated, they plotted on separate graphs for easy visualization and the line of fit was determined. The line of fit was determined through an average of the first and last 750 points in each feature to ascertain a general trend within the data. The code for calculating the RMS fit line is shown below, and the MDF code is identical except with MDF substituted for RMS.

```

# Calculate average of first 750 points in Quads, Calves, and Hamstrings RMS
avg_first_quads_rms = np.mean(rms_quads[:750])
avg_first_calves_rms = np.mean(rms_calves[:750])
avg_first_hamstrings_rms = np.mean(rms_hamstrings[:750])
print("Average of first 750 points in Quads RMS:", avg_first_quads_rms)
print("Average of first 750 points in Calves RMS:", avg_first_calves_rms)
print("Average of first 750 points in Hamstrings RMS:", avg_first_hamstrings_rms)

# Calculate average of last 750 points in Quads, Calves, and Hamstrings RMS
avg_last_quads_rms = np.mean(rms_quads[-750:])
avg_last_calves_rms = np.mean(rms_calves[-750:])
avg_last_hamstrings_rms = np.mean(rms_hamstrings[-750:])
print("Average of last 750 points in Quads RMS:", avg_last_quads_rms)
print("Average of last 750 points in Calves RMS:", avg_last_calves_rms)
print("Average of last 750 points in Hamstrings RMS:", avg_last_hamstrings_rms)

```

**Figure 4.11: Python code to calculate a line of fit for the RMS feature**

Fatigue was then quantified depending on the trend of the lines of fit for the RMS and MDF. If the RMS trend line had a positive slope while the MDF trend line possessed a negative one, the subject was said to be fatigued. If both trends are not present then it is not possible to determine that a subject is fatigued. Research has not suggested that it is possible to determine the level of fatigue from this method, and it is unknown if the analysis can be that granular. To compensate for this the data was classified as either fatigued or not able to determine depending on what trends are present in the lines of fit.

#### **4.3.4.1.3 Body Temperature**

According to Johns Hopkins Medicine, body temperature including and between 38 degrees Celsius and 40 degrees Celsius indicates heat exhaustion with a fever starting at 38 degrees Celsius or higher (Exercise-Related Heat Exhaustion, 2021). The user can use this scoring system to determine potential point of fatigue due to body temperature:

$$\text{Body Temperature Score} = \frac{(38 + \text{Max } \Delta \text{Temp}) - 38}{43 - 38} \cdot 100 = \frac{\text{Max } \Delta \text{Temp}}{5} \cdot 100 \quad (4)$$

Since 38 degrees Celsius is the indicated point of a fever, when the body temperature score reaches this score, this would indicate a point of potential fatigue. In order to test, the user's maximum change in temperature is calculated after filtering and plugged into the formula above.

#### **4.3.4.1.4 Fatigue Index**

The hypothesis for the fatigue index score is shown below. It was developed based on the accuracy of sensors, the relevance of the biometric data they collect, and how granular their individual scores are capable of being.

$$\begin{aligned} \text{Exhaustive Score} = & 0.6 \cdot \text{Heart Rate Score} + 0.3 \cdot \text{Muscle Activation Score} \\ & + 0.1 \cdot \text{Body Temperature Score} \end{aligned} \quad (5)$$

The fatigue index is a weighted scoring system out of 100 with heart rate weighing the highest at 0.6, muscle activation weighed at 0.3, and body temperature weighted the lowest at 0.1. Since this scoring system is subjective and difficult to prove, the teams' reasoning behind these weights is solely based on this project and the findings from the team's data, but they were verified from data collected from testing subjects. The team's ECG data is the most accurate and consistent when detecting fatigue which is why it is scored the highest. As heart rate increases, fatigue increases as seen in the equation above. The ECG data is also able to capture multiple stages of fatigue depending on the current heart rate. Muscle activation follows body temperature because of the inconsistency with the collected EMG data and the binary output of the analysis. While a coupled force sensor with an EMG sensor would be ideal to measure fatigue, due to limited budget and resources the team could not integrate such a design. To make up for the lack of force sensor, the team used alternative ways to visualize fatigue with the raw EMG data which is less consistent and with lower quality, which resulted in a lower weight for the EMGs in the fatigue index. Additionally, the current method of determining EMG fatigue is binary, returning either fatigued or not fatigued. If a method could be developed for a more precise EMG fatigue score that would increase its weight. Finally, body temperature is weighted the lowest at 0.1 since this biometric is used to detect heat exhaustion and does not change significantly during exercise.

#### **4.4 Feasibility Study/Experiments**

Excel data streamer is a tool in Microsoft 365 that allows users to stream data in real time with visualization and analysis features. It can be used for various data, and the team utilized this

tool for EMG, ECG, and temperature data collection, analysis and verification. For example, the data streamer was used to display the EMG signal that is acquired from the electrodes placed on the user's skin which are then amplified to extract features including amplitude, frequency, time, identifying muscle patterns, and comparing data across multiple subjects. This tool easily allowed the team to conduct further analysis and detect fatigue through muscle activation patterns.

The data streamer allowed for data to be graphed live across longer time scales than the Arduino IDE allows. It also allows for the data to be saved in csv files for post processing and to preserve data. For the EMG sensors, the tool allowed the team to try different muscle placements and exercises while saving the results and ensuring they were acceptable. For the ECG sensor it assisted in determining proper electrode placements and experiments to isolate and reduce causes of noise. It also allowed the temperature readings of the LM35 to be easily viewed and verified against thermometers in the same room as the LM35.

This excel add-on was essential to verifying the function of the sensors, conducting experiments to improve their measurement quality, and understanding how the biometrics react to different external stimuli.

#### **4.5 Alternative Designs**

The first design of the smart wearable vest involved a vest attached to a multilayered shirt which would allow for proper and organized placements of sensors and wiring. The base layer of the shirt would have the sensors incorporated into the fabric through pockets or holes so that the sensors would have snug skin-to-skin contact, ensuring that consistently accurate data would be collected throughout testing regardless of excessive movement or activity. The second layer of the shirt would prevent exposure of the wires and sensors to the operational environment and

user, protecting the components from any snagging, sweat, debris, or other damaging actions or materials that may be encountered during operation. The outer layer of the shirt would be stitched to the base layer to fully seal the wiring and sensors for full coverage of the electrical components. The vest with pockets would be the outside of the outer shirt, and it would house the non-skin-contact sensors and the battery to ensure external access to these components. The vest would be stitched to the second layer of the shirt so that the whole shirt-vest would be one article of clothing, making the device easier to maintain as well as repair, install, and/or house components.

The first design was also composed of a different selection of sensors for a majority of the recorded metrics. Initial research indicated a multitude of methods for measuring the breathing rate of athletes, with an inertial movement unit and strain gauge placed on the chest or abdomen simultaneously being used for the measurement of this biometric. Velocity and acceleration would both be measured through a separate inertial movement unit placed on a non-flexing surface of the body, such as the hip or shoulder, to ensure that no movement of the body would be collected when measuring the performance metrics. The EMG sensors would be attached to the main vest towards the bottom to allow for all components to be housed on the vest, allowing for a less complicated system while also allowing for enough room for movement of the user. Other biometrics were also considered to be measured, such as blood pressure, due to correlations found related to fatigue. Communication would also be completed through a bluetooth module with a Sparkfun OpenLog Artemis, which would act as the microcontroller for all sensors. OpenLog Artemis would connect and transfer data over bluetooth to the laptop of the user, which would also act as a base station for mapping the coordinates of the field.

The second design involved splitting the smart wearable device into two different subsystems: a vest and a leg sleeve, each collecting biometric and performance data from the two separate locations. This was also incorporated with the reselection of sensors used for the collection of data, both with sensor type and types of data. The smart vest would incorporate all sensors placed on the upper body, including the ECG, GPS, and LM35, but no longer utilize the blood pressure sensor due to availability issues or the multiple breathing rate sensors due to their complexity and sensitivity. In place of the breathing rate sensors, a biometric algorithm would be used to estimate the breathing rate based on the ECG waveform. The OpenLog Artemis microcontroller was replaced with an ESP8266 in order to host a website straight from the vest itself, allowing for each user to see their individual stats on this website. The base layer of the vest would be shed in order to allow for increased comfortability, only being used for the securing of wires against the body to ensure reduced noise from unnecessary movement of the wires.

The leg sleeve would be composed of only the Myoware 2.0 EMG sensors with a separate ESP8266 to transmit data to the website, allowing for the complete, wireless transmission of data and for free movement without any snagging of wires due to connections between the vest and leg sleeve. The leg sleeve would also introduce a base layer which held the EMG sensors and wires tight to the body, preventing the wires from any pulling or ripping during operation as well as ensuring a proper connection between the electrodes and skin is achieved. The ESP8266 would be connected to an Arduino Uno and Myoware 2.0 Arduino Shield, which would connect to each EMG sensor using 3.5mm auxiliary cables instead of jumper wires to limit the noise during data transfer and simplify the connection between microcontroller and sensor. This leg sleeve would also contain its own power source allowing for

a completely separate subsystem from the vest, permitting users to more free and natural movements in their operating environments. The ESP, Arduino Uno, and Arduino Shield would be housed in an additively manufactured case, which would be secured by velcro around the upper thigh of the user on their dominant leg.

The final design incorporated all of the sensors in the previously mentioned design, but switched to be more comfortable and fitting for a variety of user types. This included removing the usage of any shirt to keep the sensors and wires snug to the users body, as it was found to not be flexible for larger users. Instead, all wiring was routed through the vest through straps that held loose components tight to the fabric while allowing room for movement and pulling of the wires due to body movement. The vest was also reinforced with fabric in order to allow for heavier loads and stress to be placed upon it during intense exercise. A separate armband was added to keep the temperature sensor close and secure to the body during all types of movement while not being uncomfortable to the user. The positioning of the Arduino UNO used for the transfer of EMG data was transitioned from the thigh to the hip, being enclosed in a waist bag to allow for easy rotation and a more pleasant experience when worn. Instead of having two separate ESP8266 microcontrollers communicate to each other, a hard wired connection between the Arduino UNO and the ESP8266 attached to the vest would allow for easier and more reliable communication as well as a singular power source for all sensors.

#### **4.6 Modeling**

Modeling in this project was primarily used to verify the analysis software, provide a proof of concept for the algorithms, and test portions of the website. ECG, EMG, and GPS data was all synthetically generated using a variety of methods for this purpose. The primary methods

used to create data was the python software library Nuerokit 2.0 and generative artificial intelligence.

ECG data was synthetically generated using the Neurokit 2.0 library. Neurokit allows users to define the sampling rate, heart rate, length of data it generates, and the simulated data collection method. These data sets were used to verify that the code to determine beats per minute from an ECG signal was accurate and usable. It was also used to verify the algorithm to determine respiratory rate from an ECG signal. The modeling was useful because it enabled software to be developed concurrently with sensor development. The ECG sensor originally gave noisy data, but those issues did not hinder the software development due to modeling.

A similar strategy was used for EMG analysis. Neurokit can generate synthetic EMG data, and the number of bursts, sampling rate, and duration of data can be defined within it. In addition to Neurokit, generative AI was also used to create a consistent EMG burst that should show fatigue. The synthetic data was used to troubleshoot and verify the RMS and MDF analysis code. This modeling was essential to the development of the code because the synthetic data was free of noise and more compatible with analysis code than the Myoware EMG sensors originally were.

Finally, GPS coordinates were synthetically generated using generative AI to test heat map features on the website. The heat map software was developed before the GPS sensor was chosen, so the modeling was essential to developing the software concurrently with hardware development.

#### **4.7 Preliminary Data**

Collecting preliminary data was essential to verifying the functionality of the sensors and the validity of the data they collected. Before the wireless data transmission method was chosen

and developed, preliminary data was collected using the excel data streamer tool. This tool allows for live viewing of data collected from an Arduino on an excel sheet, which can be modified, saved, and graphed with ease. To collect preliminary data, fitness machines such as a leg press, treadmill, and smith machine were used.

To collect preliminary EMG data, the leg press and smith machine were used to record muscle activation. An EMG sensor was attached to one muscle group at a time and an exercise was done to isolate that muscle. For example, a squat would be done with a sensor attached to the quadricep or a calf raise with a sensor attached to the calf. This method isolated muscle groups and allowed a controlled load to be applied to the muscles through the weight. This testing was essential to evaluating the first EMG sensor that was used, the Seeed Grove EMG.

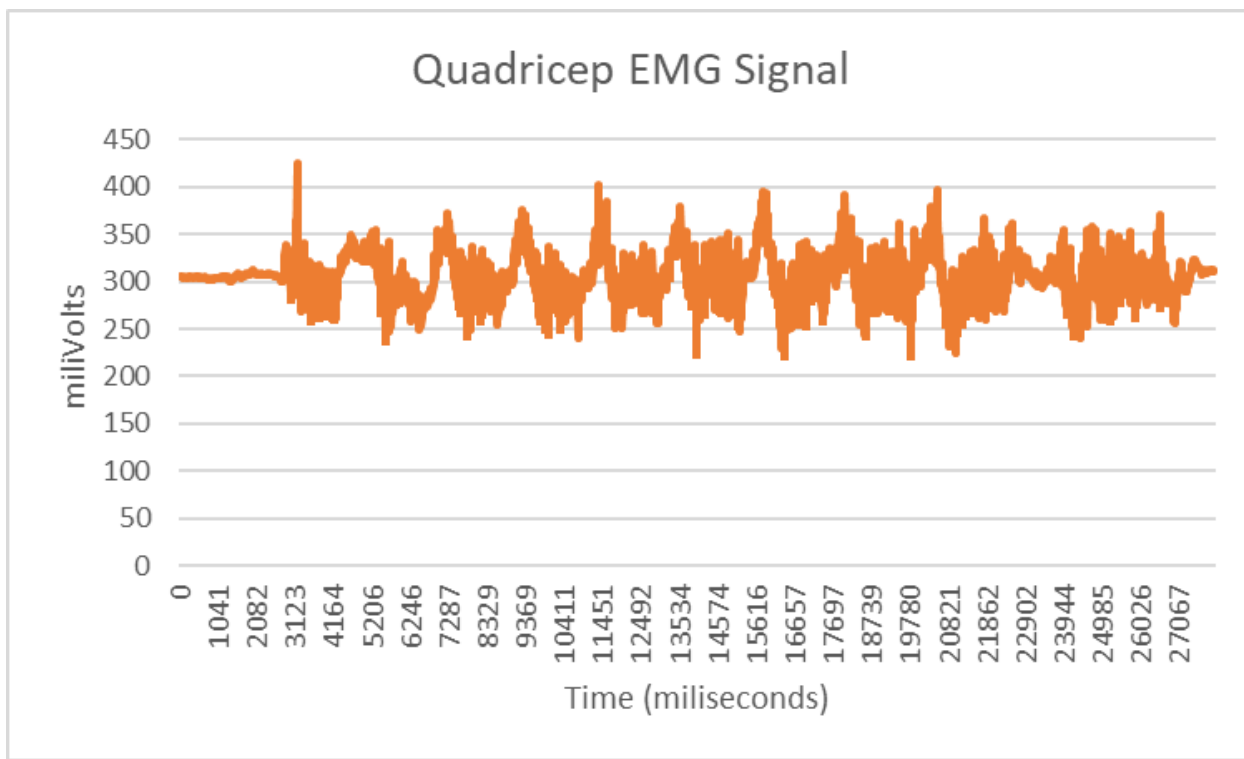


**Figure 4.12: Seeed Grove EMG signal on quadricep, squat, 9 repetitions**

Shown above is data collected from the Grove EMG sensor on the quadriceps while squatting. The beginning period of the data, until approximately 3 seconds is the resting period, so the signal is flat. From 3 seconds to 5 seconds is likely some muscle activation, but it is difficult to ascertain due to the noise present afterwards. The large spikes in the data set are due to the movement of the data transmission wires during the exercise. This is noise in the system and it makes it very challenging to find muscle activation within the data.

After understanding the impact that wire movement can have on EMG data collection, a Myoware EMG sensor was purchased to evaluate its noise and data collection. Shown below is the Myoware EMG signal from the same subject on the same quadricep conducting the same exercise.

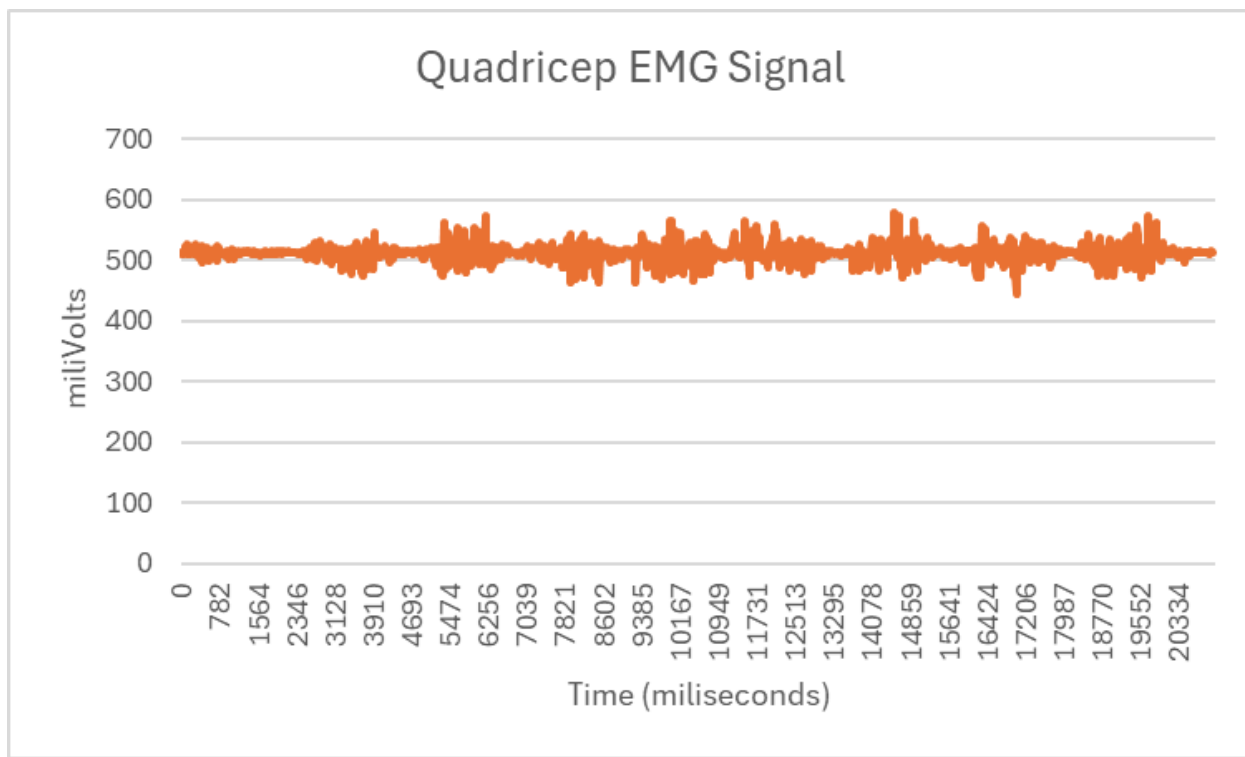


**Figure 4.13: Myoware EMG Signal on quadriceps, squat, 8 repetitions**

The data from the Myoware sensor is significantly improved compared to the Grove. The large spikes from wire movement are non-existent and periods of rest and muscle activation can clearly be seen on the graph. The preliminary test yielded the result that the Myoware EMG sensor was superior to the Grove EMG.

The preliminary testing for other sensors was mainly concerned with verification of sensor data. ECG data was verified using the excel data streamer and a graph to see if the R peaks and QRS complex of the signal could be found. The result was that the ECG sensor was reliable and accurate when a subject was sitting still, but noise could be introduced from movement. To reduce the effect of movement, the wires were taped to the subject's skin and data was taken while they were on a treadmill. The results from this were positive, as taping significantly reduced the noise present in data collection.

#### **4.8 Final Design**

The final design consisted of two main components: a vest containing the battery unit, ESP8266, and the majority of the circuit and a waist bag that contained the Arduino Uno and Myoware hardware. The entire product is shown below, represented on a mannequin to demonstrate its wearability.

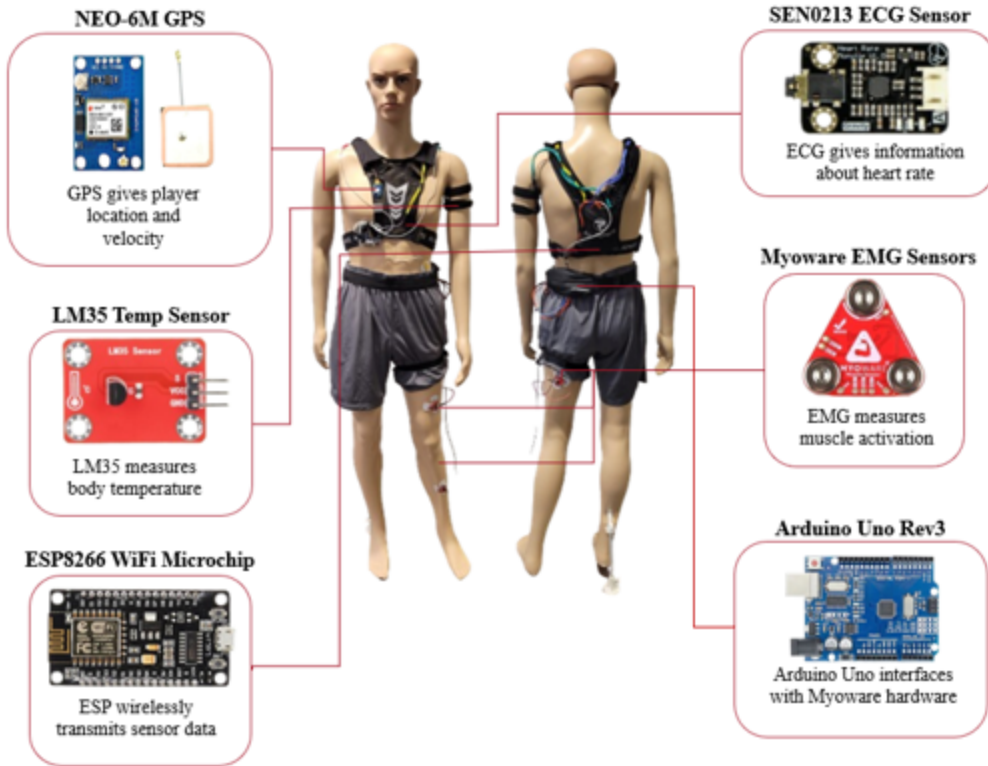


**Figure 4.14: Final Product**

In the final product, the wires for each sensor were color coded for ease of repair, maintenance, and manufacture. Yellow was used for the ECG sensor, green for the temperature sensor, blue for the GPS, and red to connect the Arduino Uno to the ESP8266. Additionally, different colored wires were used to differentiate the Myoware EMG sensors on the legs, with a blue and red wire going to the quadricep, a silver cable going to the calf, and a white and red wire connecting to the hamstring. Electrodes were used to secure the ECG sensor and the three EMG sensors, two arm bands were used to secure the LM35 temperature sensor to the arm, and the GPS was secured in a shoulder pocket on the right shoulder.

The ESP circuit and battery were well secured inside the back pocket on the vest. An additional piece of fabric was attached to the back to further secure it and guard against tearing.

The ESP circuit was complex, and the protections built into the vest protected it from damage.

The final circuit diagram for the ESP can be seen below:

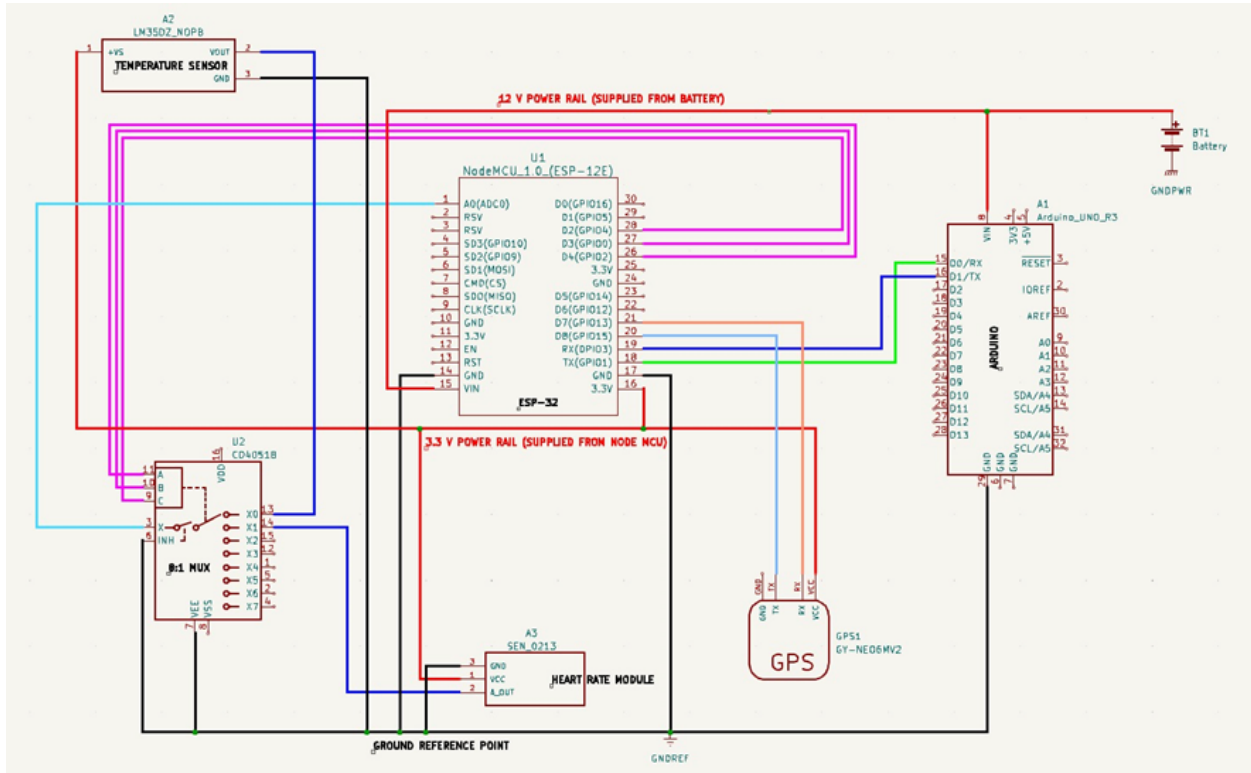


**Figure 4.15: Electrical Schematic of the ESP 8266 Circuit**

Additionally, data from the ESP 8266 was transmitted to the ESP's IP address, where it could be retrieved from an additional website to display live biometric data. The website was capable of displaying live signals from all three EMG sensors, a live ECG graph, running BPM calculations on the ECG signal, calculating respiratory rate live from the ECG graph, displaying velocity from the GPS unit, and showing the user's body temperature as well. The code for respiratory rate derivation was developed using the Neurokit 2 library and the BPM calculation was also done by relying on NeuroKit2 Library. A screenshot of this website is presented below:

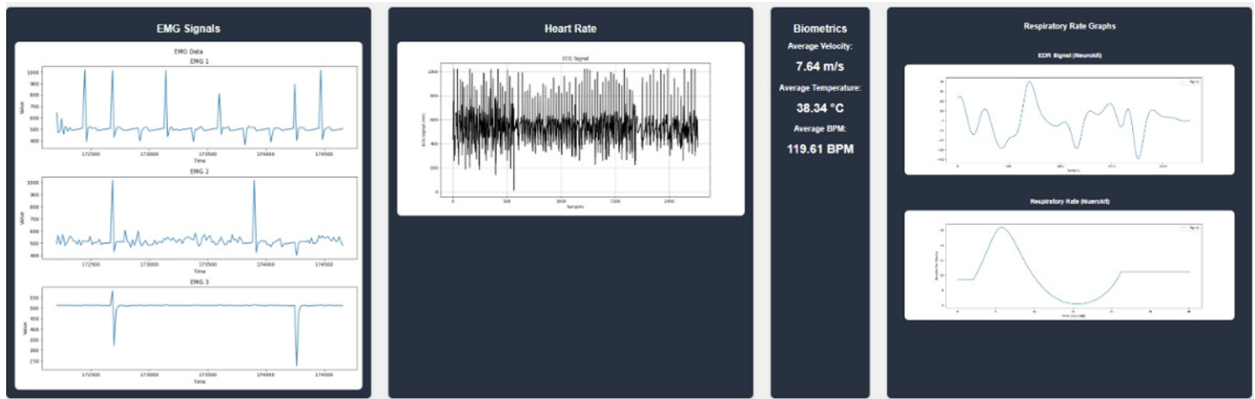


**Figure 4.16: Live Data Display Website Screenshot**

In the final product, additional analysis such as calculating the RMS and MDF of the EMG signals and generating the heat map off of GPS coordinates is done after the conclusion of the workout. This is also when the calculations for the fatigue index are conducted and other trends are displayed.

## **5.0 Testing and Procedures**

Before beginning testing procedures, participants are required to read and agree to a consent form that provides information on the tests being administered as well as allowing for usage of personal data in this project. A detailed briefing consisting of information from the consent form on how participant-provided information is collected and used is then conducted. This briefing contained but was not limited to setup procedures, testing methods and processes, data collection and analysis methods, publishing efforts, and more. Participants were sent a diagram of the human body with areas identified for the participants to shave themselves with a razor before beginning testing to properly clean the electrode placement sites for the ECG and bioimpedance sensors.

Participants were told to expect a total time commitment of up to 90 minutes. The time was broken into three segments of varying length. The first segment was 15 minutes long and in that time the participant read and signed the consent form, asked questions, and placed the electrodes, vest, and leg sleeve onto their body. The next segment was 60 minutes long and consisted of taking baseline biometric measurements, running soccer drills, and taking final biometric measurements. The final segment was 15 minutes long to allow the participant to cool down and remove electrodes.

After participant approval was obtained, logged, and certified, proper fitting of the vest, leg sleeve, and their sensors occurred. Participants properly sanitized the previously mentioned electrode placement sites that were shaved with alcohol wipes. Participants then applied electrodes to the previously mentioned sites with the possibility of doing so in a private environment. This required verification of proper placement by a group member after the

participant has applied the standard medical electrodes. Adjustments of these electrodes were done by either the participants themselves or a project group member based on consent.

The following steps were completed on one participant at a time as there was only one vest and leg sleeve for testing. The vest and leg sleeve were then placed and worn by the participant with the help of project members. All straps were correctly tightened so that the vest and leg sleeve are snug and sensors are properly contacting the skin of the participant. Precautions were taken to ensure the wearables were not uncomfortably tightened so that the participant is not caused any discomfort or pain. Sensors were then powered on and tested to check the accuracy of the readings as well as to measure baseline biometric data from the participants. Corrections were taken if sensor accuracy/data readings are erroneous.

The time to warm up and complete exercises of fatigue took about 90 minutes total. During this trial period, a total of 6 sensors measured data including 3 EMG sensors, an ECG sensor, 1 GPS, and 1 LM35 temperature sensor. The participants warmed up by jogging 20 yards, back peddling 20 yards, sprinting 20 yards, back peddling 20 yards, sprinting 20 yards, then back peddling 20 yards without stopping. This was to provide the team with a baseline of heart rate, temperature, and muscle activation. Participants next began the full trial to measure their fatigue during athletic performance, which occurred over a period of 60 minutes and consisted of constant exercise. The participant was asked to pass a soccer ball to their partner with a 20 yard distance, dribble and sprint with the soccer ball a distance of 50 yards forward and back, complete shuttle runs with intervals of 10 yards from 10 yards to 40 yards, and shoot the ball with a 10 yard run up. Activities remained contactless for both the participant and those exercising with the participant. Once exercising and data collection was completed, the data was saved to a database and contained within a folder for each participant. The folders for each

participant contained biometric data, health data, and performance metrics, but were labeled by the participant's number and did not contain the names of any participants or identifiable information.

After data was saved, the participants, if consent is given, were helped with removing the vest, leg sleeve, and any sensors or standard medical electrodes by a project group member.

## **6.0 Design Verification**

To verify the design on the smart wearable device, the team tested the device on six participants who ran soccer drills to simulate in-game activities. The tests included a warm up to determine a ‘non-fatigued’ baseline of data, passing and shooting drills to simulate higher impact exercises, a dribbling drill, and concluded with a shuttle run to collect ‘fatigued’ data.

The data from each sensor was analyzed separately according to the methods outlined previously. From this analysis individual biometric scores were calculated to help develop the scoring system. Unfortunately, during this stage it was seen that some of the sensors failed to collect adequate data during testing. The success of the sensors varied depending on the type of sensor, the individual testing the sensor, the type of exercise, and other factors. However, even if some types of data were imperfect depending on the trial, oftentimes the other data collected was workable.

Finally the data was segmented into the ‘fatigued’ and ‘non-fatigued’ categories to evaluate the validity of the Fatigue Index. A Fatigue Index score for non-fatigued and fatigued data was calculated. This was done as a proof of concept to determine if the index could be a numerical approximation of fatigue.

### **6.1 ECG Results**

The quality of ECG results varied depending on the participant, activity, and skin contact of the electrodes. Most of the degradation in results came from poorly secured wires that created electrical noise when moving. The wires were often well secured to the subject’s midsection at the beginning of the workout, but as the workout progressed the adhesive securing the wires

weakened. Despite the challenge that was present for the majority of subjects, measures were taken to secure the wires as much as possible and some data from the subjects was viable.

To analyze and evaluate the ECG data, it was run through a python script that segmented the data into six chunks. The BPM for each chunk was calculated, and then the HR Score was calculated by dividing it by that subject's maximum heart rate. Then each chunk was color coded as green, yellow, or red depending on the level of fatigue in the chunk. Red was used for HR scores over 77, yellow was used for scores between 64 and 77, and green was used for scores below 64. If the data had noise present and a heart rate could not be calculated then a reading of nan was displayed. According to equation 3, heart rate score was calculated for each subject and each data set. A higher heart rate score indicates that the subject was more fatigued.

For subject 1, heart rate data collection was successful as seen in the table of graphs below from the “Baseline” portion of the testing procedures. The third and fourth graph are color coded green because the heart rate scores are below 64. The first graph is color coded yellow because the heart rate score is between 64 and 77. Finally, the second, fifth, and sixth graphs are color coded red because the heart rate scores are about 77 (Figure 6.1). There is little to no noise seen in this data set since this was the first testing procedure completed with the wires still secured and adhesive recently adhered to the skin.

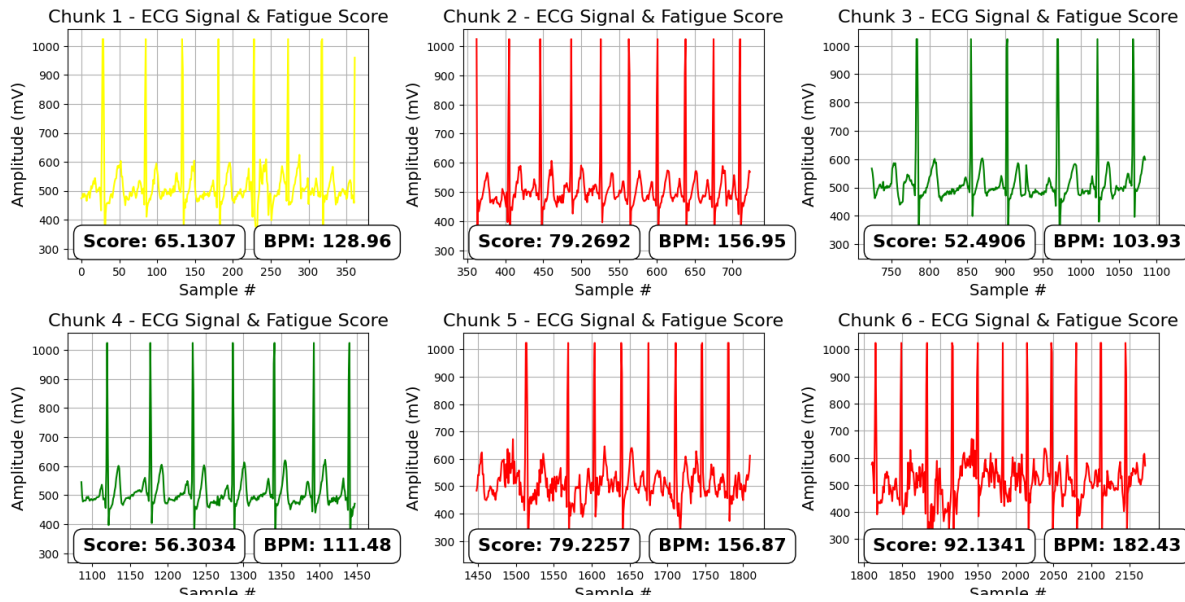


**Figure 6.1: Subject 1 heart rate for “Baseline” testing procedure**

For subject 1, heart rate data collection was also successful in the “Dribble” portion of the testing procedure as seen in the table of graphs below. The first, second, and fifth graphs are color coded green because the heart rate scores are below 64. The third graph is color coded yellow because the heart rate score is between 64 and 77. Finally, the fourth and sixth graphs are color coded red because the heart rate scores are above 77 (Figure 6.2). This data set contains little noise which could be due to the success of the adhesive throughout the testing procedures. There appears to be slight noise toward the end of the workout which could be caused by the movement of the wires as the adhesive loosened and the workout progressed.

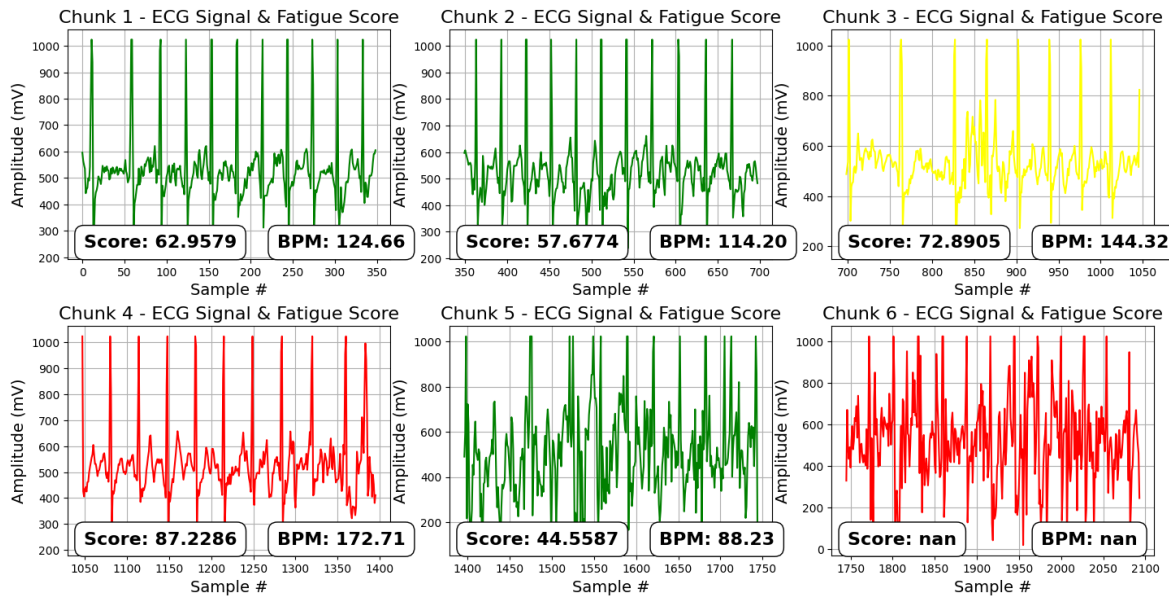


**Figure 6.2: Subject 1 heart rate for “Dribble” testing procedure**

According to equation 2, maximum heart rate for subject 1 is 199 BPM. According to equation 3, the heart rate score for each graph was calculated. The average heart rate score for subject 1’s “Baseline” is 70.759 and the average heart rate score for subject 1’s “Dribble” is 65.063. This data suggests that subject 1 could have been more fatigued in their “Baseline” than “Dribble” data set.

For subject 2, heart rate data collection was somewhat successful as seen in the table of graphs below from the “Baseline” portion of the testing procedures. The second graph is color coded green because the heart rate score is below 64. The first graph is color coded yellow because the heart rate score is between 64 and 77. The last four graphs are color coded red and no score was able to be calculated due to noise. The end of graph two displays noise which could indicate potential disconnection of the ECG, and would explain the noise displayed in the last four graphs.

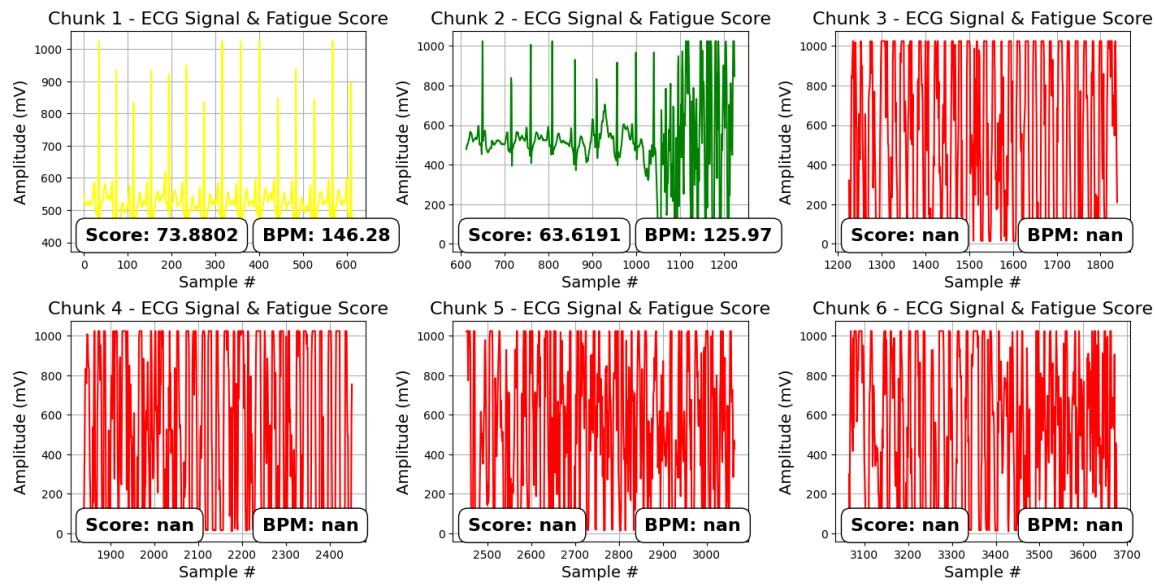


**Figure 6.3: Subject 2 heart rate for “Baseline” testing procedure**

For subject 2, heart rate data collection was successful as seen in the table of graphs below from the “Dribble” portion of the testing procedures. The first five graphs are color coded green because the heart rate score was below 64. The sixth graph is color coded red because the heart rate score is above 77. After the baseline, the team reconnected the ECG which may explain the reduction of noise in the “Dribble” data set as seen below (Figure 6.4).

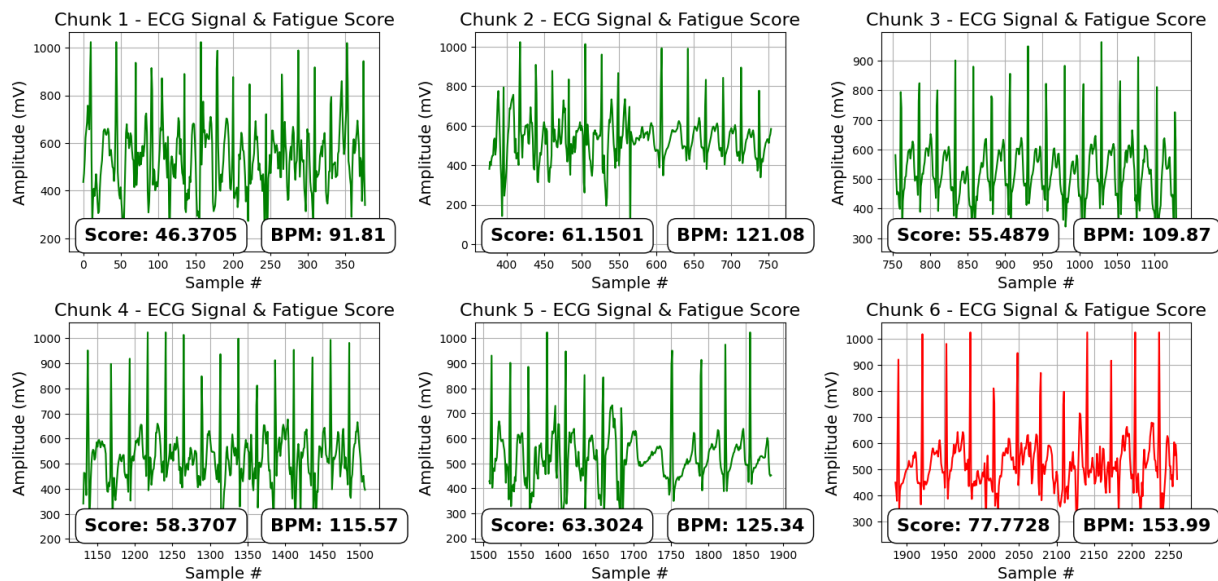


**Figure 6.4: Subject 2 heart rate for “Dribble” testing procedure**

According to equation 2, maximum heart rate for subject 2 is 198 BPM. According to equation 3, the heart rate score for each graph was calculated. The average heart rate score for subject 1’s “Baseline” is 68.749 and the average heart rate score for subject 2’s “Dribble” is 60.409. Due to the ECG disconnection and excess noise, the average heart rate score for “Baseline” may be inaccurate. This data suggests that subject 2 could have been more fatigued in their “Baseline” than “Dribble” data set, but no real conclusion can be made.

For subject 3, heart rate data collection was mostly successful as seen in the table of graphs below from the “Shuttle Runs” portion of the testing procedures. Slight noise can be identified in graphs four and six, but this could be due to wire movement. The sixth graph is color coded green because the heart rate score is below 64. The third and fifth graphs are color coded yellow because the heart rate scores are between 64 and 77. The first, second, and fourth graphs are color coded red because the heart rate scores are above 77.

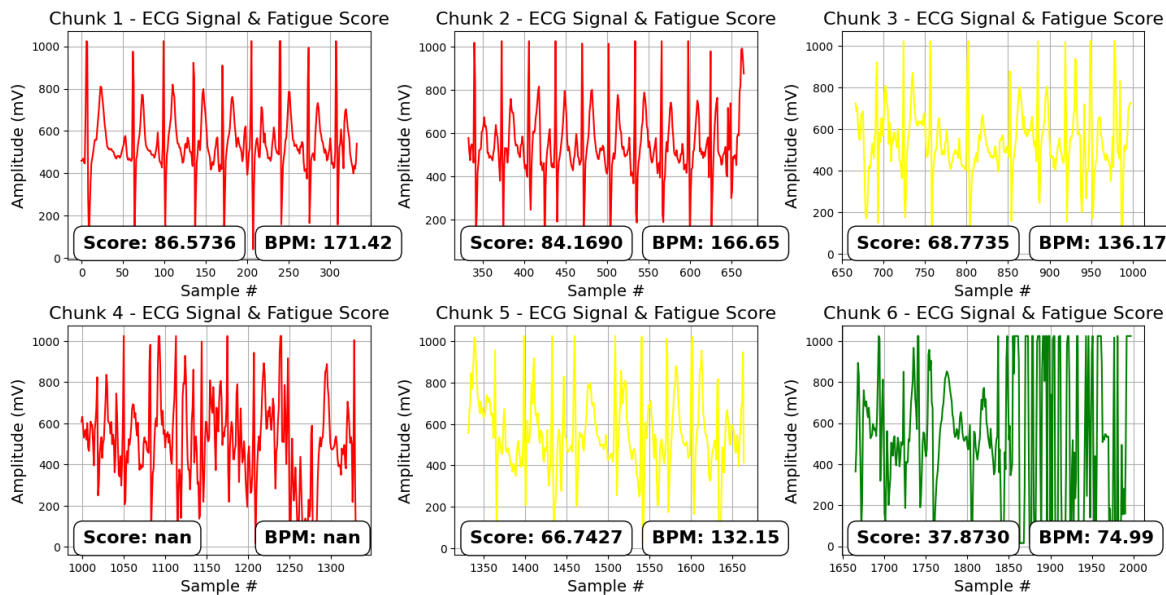


**Figure 6.5: Subject 3 heart rate for “Shuttle Run” testing procedure**

For subject 3, heart rate data collection was somewhat successful as seen in the table of graphs below from the “Dribble” portion of the testing procedures. The second and third graphs are color coded green because the heart rate score is below 64. The first graph is color coded yellow because the heart rate score is between 64 and 77. The last three graphs are color coded red because the heart rate scores are above 77. There is some noise displayed in the last three graphs which could be caused by bad ECG connection, wire movement or lack of strong adhesive gel.

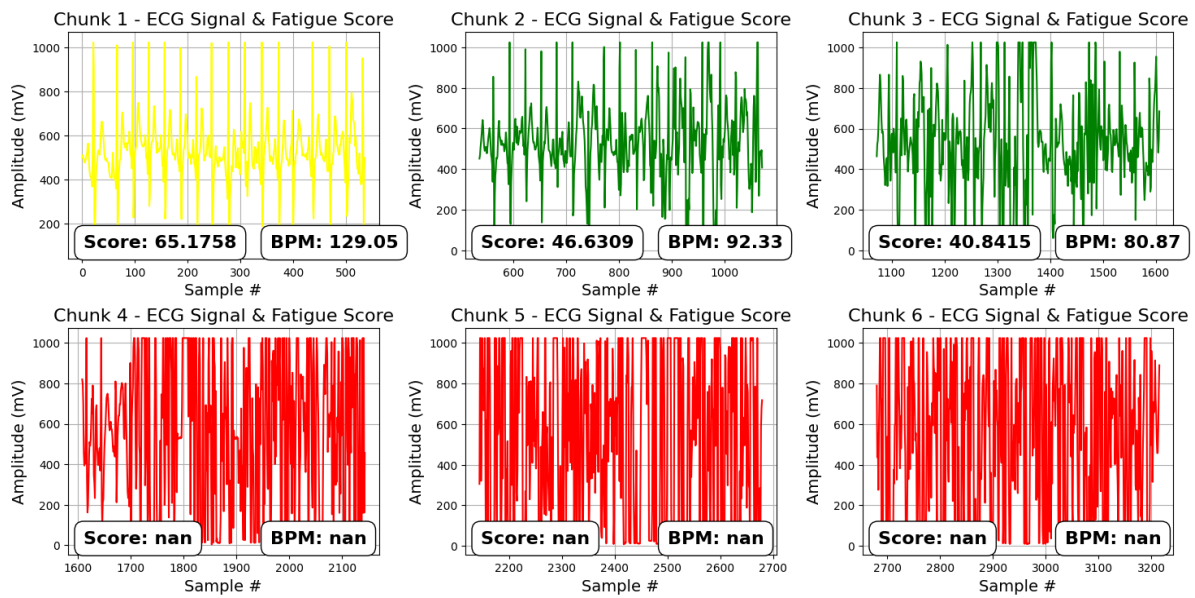


**Figure 6.6: Subject 3 heart rate for “Dribble” testing procedure**

According to equation 2, maximum heart rate for subject 3 is 199 BPM. According to equation 3, the heart rate score for each graph was calculated. The average heart rate score for subject 3’s “Shuttle Runs” is 74.468 and the average heart rate score for subject 3’s “Dribble” is 50.88. Due to potential poor ECG connection and excess noise, the average heart rate score for “Shuttle Runs” and “Dribble” may be inaccurate. The “Dribble” data set could not calculate BPM for the last three portions of the workout, so this average is skewed. This data suggests that

subject 3 could have been more fatigued in their “Shuttle Runs” than “Dribble” data set, but no real conclusion can be made.

For subject 4, heart rate data collection was somewhat successful as seen in the table of graphs below from the “Baseline” portion of the testing procedures (Figure 6.7). All six parts of the workout are color coded green because the heart rate scores are below 64. There is slight noise seen throughout the data set, most likely due to wire movement.

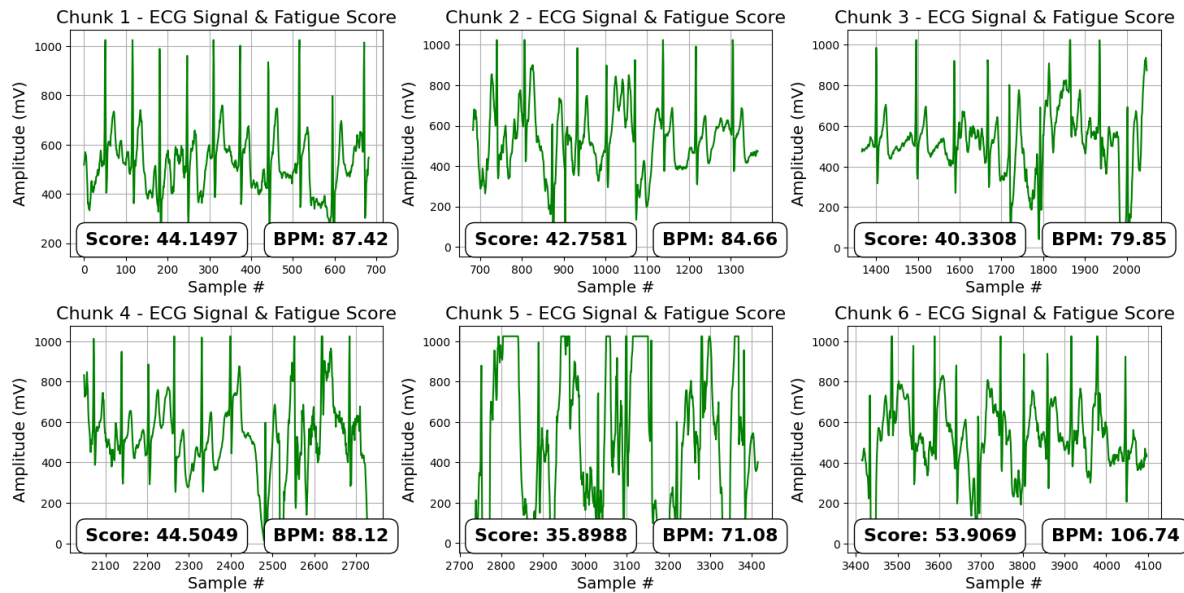


**Figure 6.7: Subject 4 heart rate for “Baseline” testing procedure**

For subject 4, heart rate data collection was somewhat successful as seen in the table of graphs below from the “Dribble” portion of the testing procedures (Figure 6.8). The last two graphs are color coded green because the heart rate scores are below 64. The first, second, and fourth graphs are color coded yellow because the heart rate scores are between 64 and 77. The third graph is color coded red because the heart rate score is above 77. There is slight noise seen throughout the data set, most likely due to wire movement.

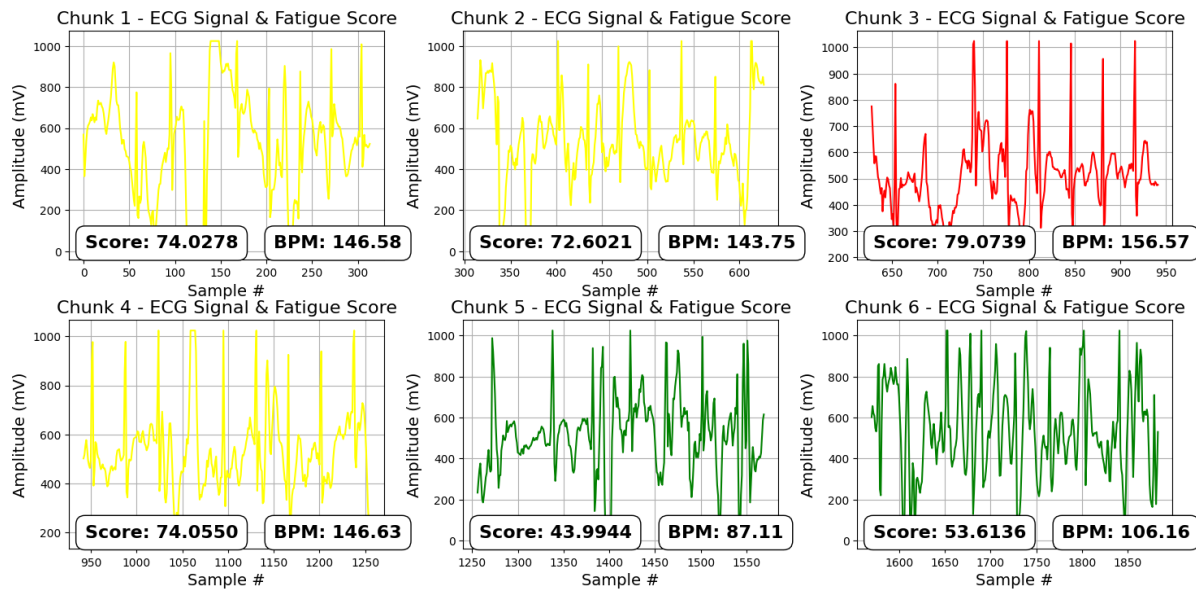


**Figure 6.8: Subject 4 heart rate for “Dribble” testing procedure**

According to equation 2, maximum heart rate for subject 4 is 198 BPM. According to equation 3, the heart rate score for each graph was calculated. The average heart rate score for subject 4’s “Baseline” is 43.592, and the average heart rate score for subject 4’s “Dribble” is 71.228. Since there was little noise with these sets of data, this analysis suggests that subject 4 may be more fatigued during their “Dribble” set than during “Baseline”.

For subject 5, heart rate data collection was somewhat successful as seen in the table of graphs below from the “Baseline” portion of the testing procedures (Figure 6.9). The fifth graph is color coded green because the heart rate score is below 64. The first two graphs are color coded yellow because the heart rate score is between 64 and 77. The third, fourth, and sixth graphs are color coded red because the heart rate scores are above 77. There is noise displayed in graphs 4-6 which can be caused by wire movement, lack of strong adhesive, or poor ECG connection.

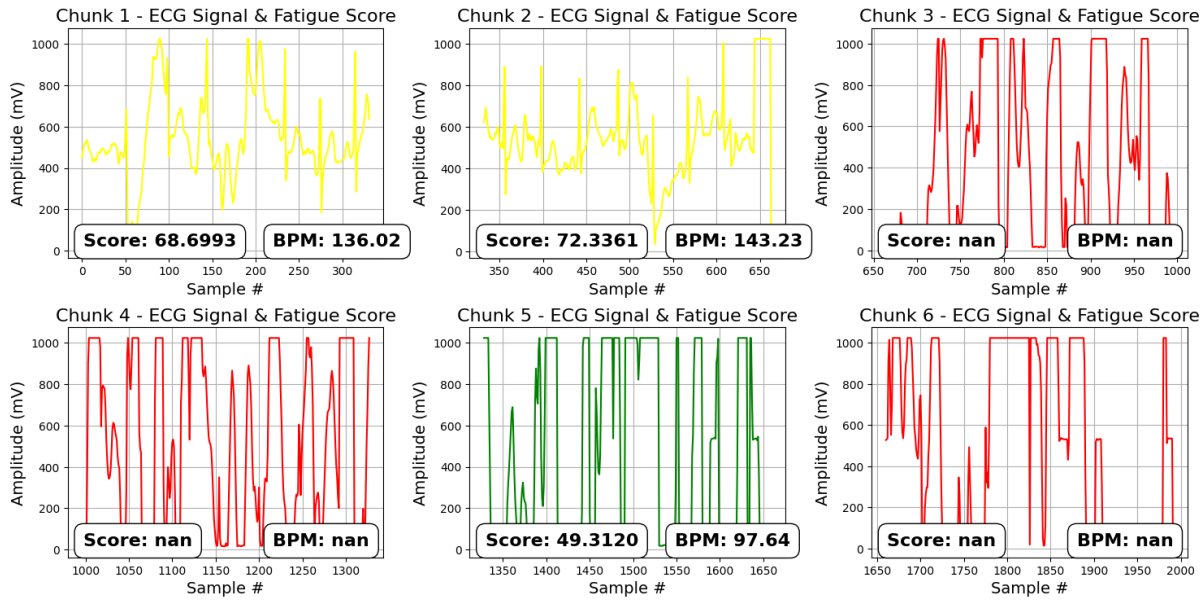


**Figure 6.9: Subject 5 heart rate for “Baseline” testing procedure**

For subject 5, heart rate data collection was somewhat successful as seen in the table of graphs below from the “Shuttle Runs” portion of the testing procedures (Figure 6.10). All six graphs are color codes green because the heart rate scores are below 64. Noise is present among almost all six graphs which can be caused by wire movement, lack of strong adhesive, or poor ECG connection.

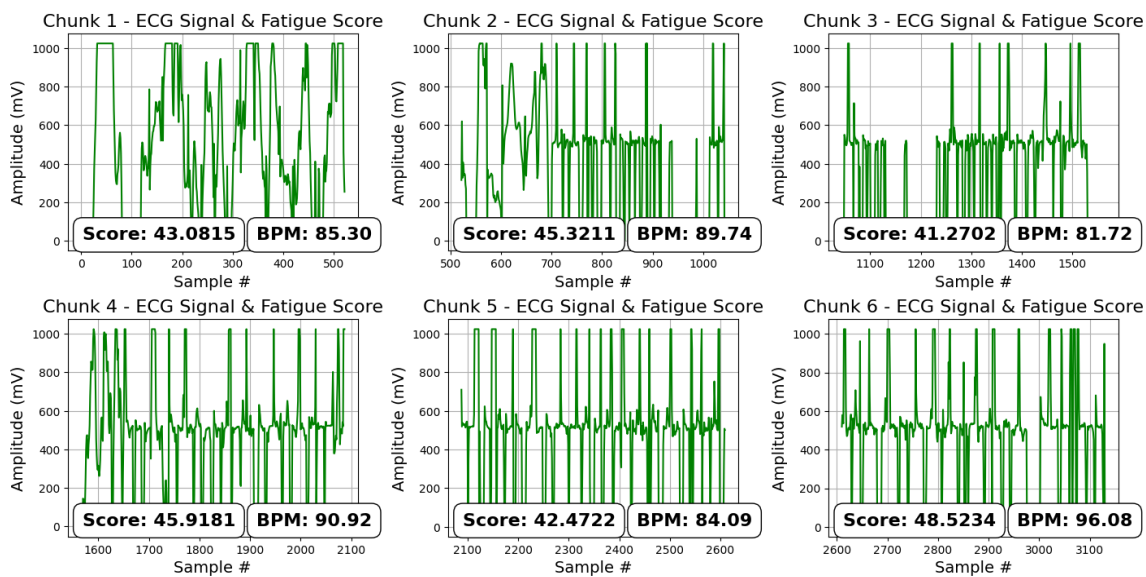


**Figure 6.10: Subject 5 heart rate for “Shuttle Runs” testing procedure**

According to equation 2, maximum heart rate for subject 5 is 199 BPM. According to equation 3, the heart rate score for each graph was calculated. The average heart rate score for subject 5’s “Baseline” is 63.449, and the average heart rate score for subject 5’s “Shuttle Runs” is 44.431. Due to potential poor ECG connection and excess noise, the average heart rate score for “Baseline” and “Shuttle Runs” may be inaccurate. The “Baseline” data set could not calculate BPM for three portions of the workout, so this average is skewed. This data suggests that subject 5 could have been more fatigued in their “Baseline” than “Shuttle Runs” data set, but no real conclusion can be made.

For subject 6, the team was only able to collect data for the “Baseline” workout due to the participants inability to attach the electrodes to the skin and excess hair on the body. According to the data collected, the average heart rate for “Baseline” is 50.903 (Figure 6.11). Since no data was collected for potentially “fatigue”, there can be no comparison or conclusion made. This emphasizes the importance of effectively shaving the skin and the effectiveness of the adhesive on the electrodes for optimizing data collection.

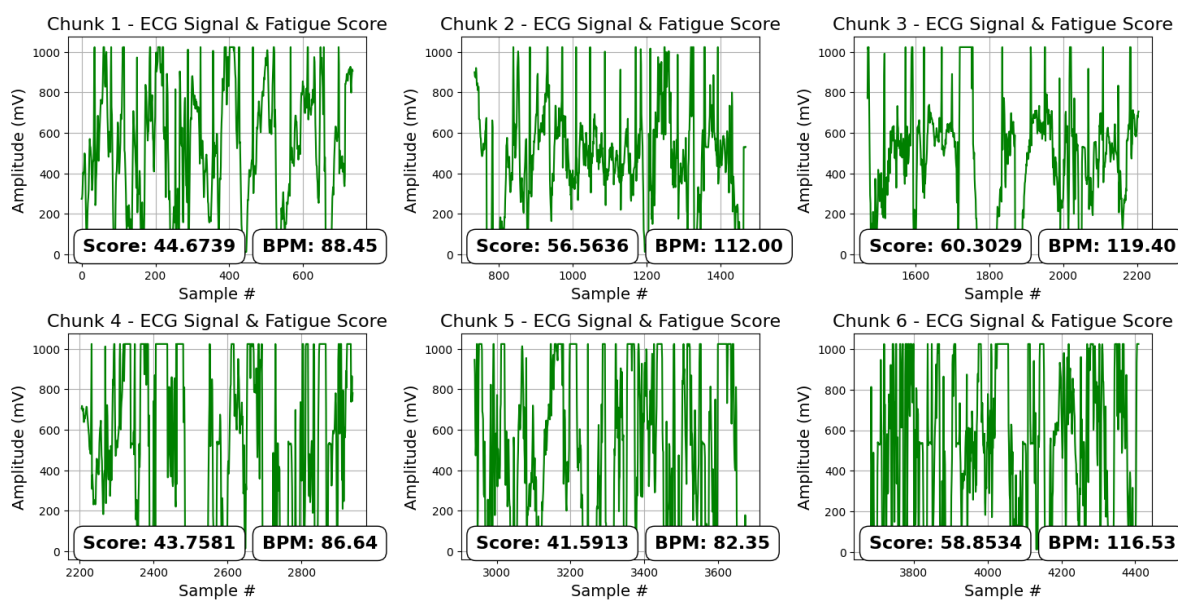


**Figure 6.11: Subject 6 heart rate for “Baseline” testing procedure**

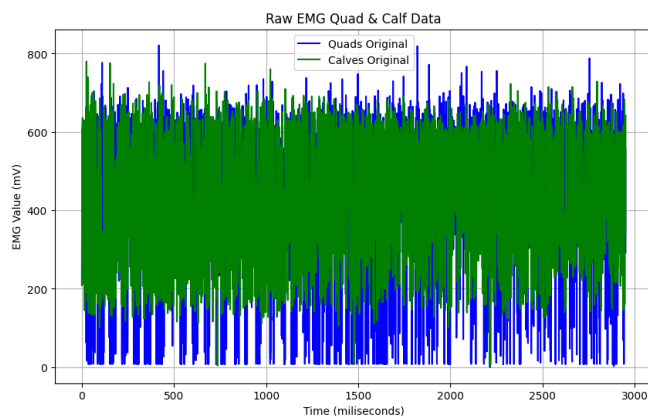
## 6.2 EMG Results

Unfortunately, achieving consistent EMG results across subjects, muscle groups, and exercises was a difficult task. Often one muscle group would fail to collect data, but other muscle groups would be successful. These issues would stem from skin contact problems, poor placement on the muscle group, and disconnections from the physical wires during movement. Additionally, the sampling rate of the EMG sensors had to be artificially lowered to enable communication between the Arduino Uno and ESP8266.

However, despite these challenges, some EMG data was able to be successfully collected and analyzed. The EMG data was broken up by subject and by workout they completed. The data was analyzed for the RMS and MDF and the line of fit was calculated to ascertain fatigue.

For subject 1, data collection was possible for most exercises on the calf and on the quadriceps. However, data for the passing exercise and the shuttle run was faulty due to issues with wires becoming unplugged. Additionally, data for hamstrings was poor due to bad placement along the hamstring muscle.

Below is the raw, analyzed, and best linear fit data for subject 1’s baseline ‘non-fatigued’ warm up workout for the quadricep and calf.



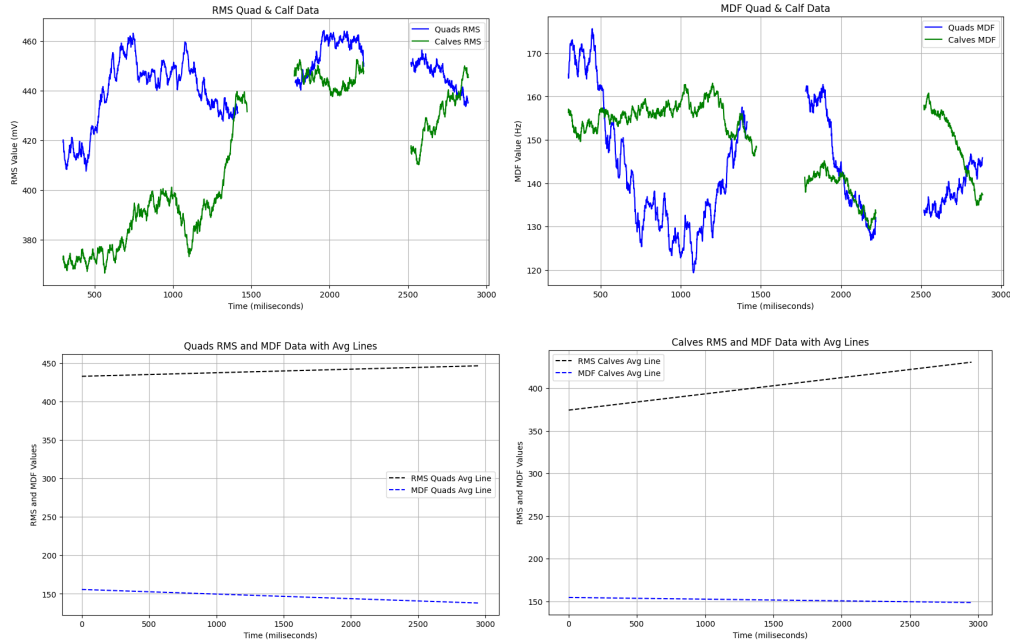


**Figure 6.12: Subject 1 “Baseline” raw, analyzed, and linear fit graphs**

The baseline data collected for subject 1 was of relatively high quality for the quadricep and calf. In total, 3000 data points were collected by each sensor and the raw data shows consistent activation across the entire time period. For the RMS features the quadriceps showed a slight increase throughout the trial. This corresponded to a decrease in the MDF for the quad data. Since the RMS trended upwards while the MDF trended downwards, that could indicate that subject 1 experienced some minor fatigue in the quadriceps during the warm up section of the workout. The calf experienced a similar trend, though with a more pronounced RMS positive trend and a less significant MDF downwards trend. This could also indicate that subject 1’s calves experienced fatigue during the warmup.

Shown below is the raw, analyzed, and best linear fit data for the quadricep and calf of subject 1’s dribble workout.

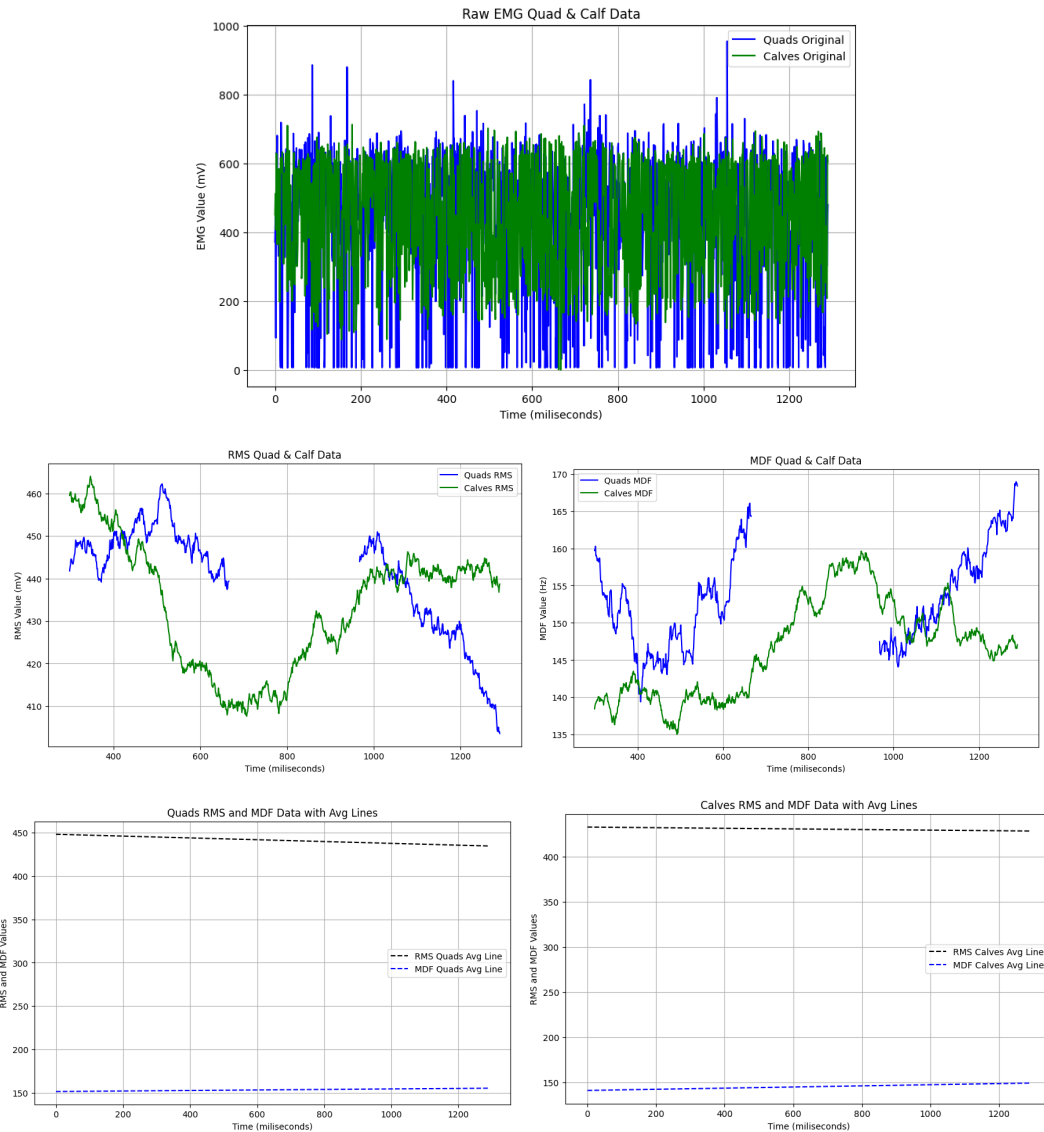


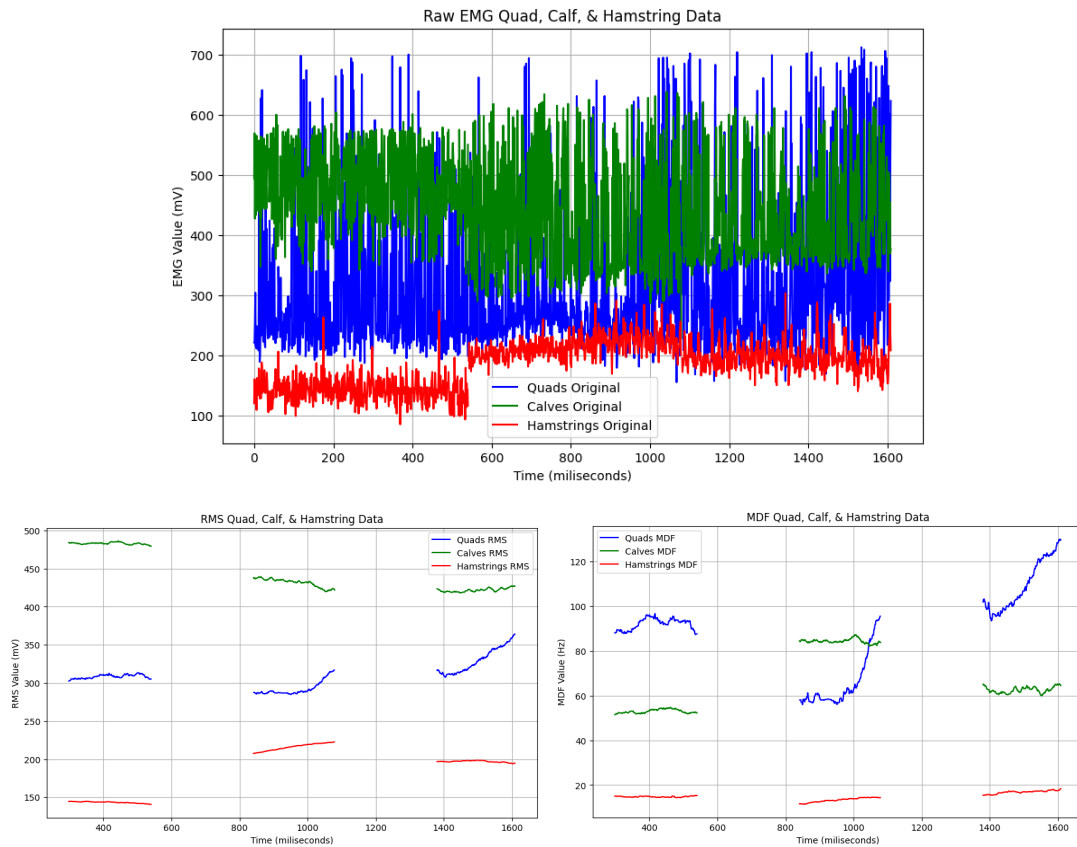
**Figure 6.13: Subject 1 “Dribble” raw, analyzed, and linear fit graphs**

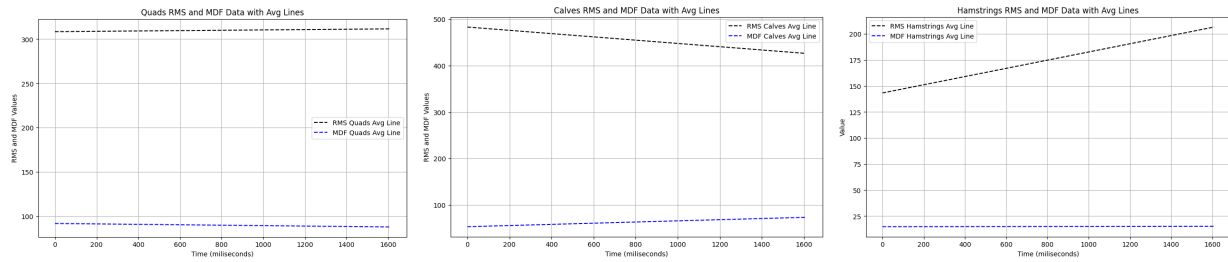
Subject 1’s raw dribble data was also of high quality for the quad and calf. This data also showed consistent activation across the 1200 samples collected for each muscle. The RMS of the quads on this dataset decreases throughout the workout while the MDF of the quads increases. This does not suggest indications of fatigue in the quad muscles for this subject. For the calves, the RMS slightly decreased while MDF increased slightly. This also does not suggest fatigue for subject 1. This could indicate that the dribble was less tiring for subject 1 than the warmup.

Unfortunately there was limited data available for the other workouts done by this subject. This was due to wired connection errors that caused the EMG sensors to be unplugged throughout the workout. However, the data collection was good for the other workouts.

For subject 2, the data was of medium quality across all three muscle groups, but some strange characteristics were observed. The middle of the EMG signal would wander throughout the workout. For example, for the final sprint portion of the workout the hamstring EMG signal hovered around the 150 mV mark before transitioning into a middle value of 200 mV. Similar variations and jumps were seen in the other sections of the workout as well. The wandering of the EMG signals has an unknown cause, and this issue was not replicated in the other five subjects. However, it was not believed to significantly affect the validity of the results.

The final sprint shuttle run raw, analyzed, and linear fit data of subject 2 is shown below:

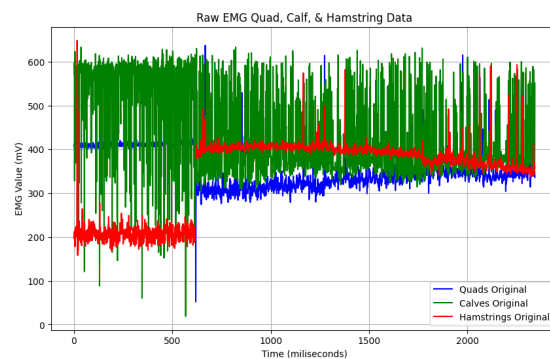




**Figure 6.14: Subject 2 “Shuttle Sprint” raw, analyzed, and linear fit graph**

This data is from the conclusion of the workout, and is of medium quality depending on the muscle being investigated. The quad data consists of a lot of noise, which can be seen by the extremely high peaks that reach values of 700 mV. The calf also contains some noise but it is not as pronounced as the quad. The hamstring has a reasonable amplitude but suffers from the jumping issue described previously. However this jump should not significantly affect results. None of the muscles in this exercise exhibited a decrease in MDF values, so it cannot be said if muscle fatigue was experienced from this data. This is because of the amount of noise and gaps in the software's ability to calculate the RMS and MDF of the signal.

Below the baseline raw, analyzed, and linear fit data for subject 2 is shown:



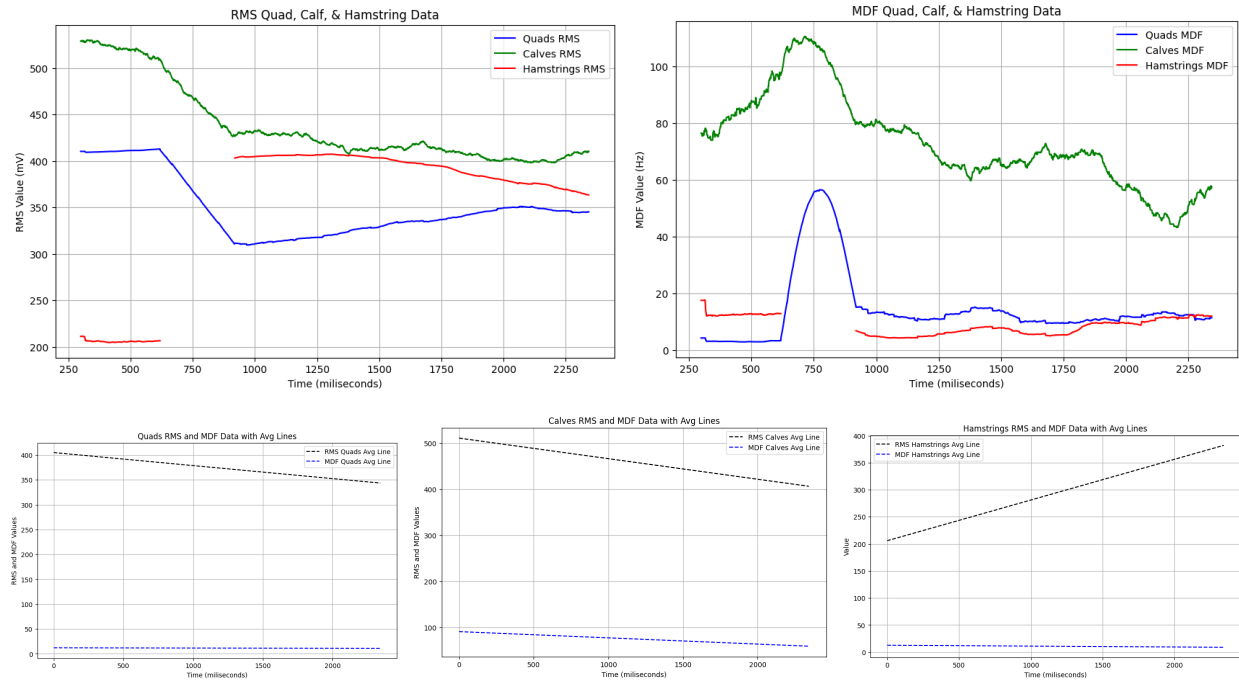


**Figure 6.15: Subject 2 “Baseline” sprint raw, analyzed, and linear fit graph**

The EMG data collected for subject 2’s warmup was also of medium quality. The calf data contains almost entirely noise, which could be due to poor placement along the muscle, bad skin contact, or other issues. The quad and the hamstring data both experienced that jumping issue that caused the baseline value to wander. Only the calves experienced a decline in the MDF value for this subject, but that was not accompanied by an increase in RMS value and the data included significant noise. Therefore it is not possible to determine if fatigue occurred in any of the muscles from this data.

Data for subject 2’s passing and dribble workout also contains significant noise and baseline jumping issues. No discernable fatigue was detected in those data sets and it was difficult to ascertain when contact with the ball was made due to significant noise.

EMG data collection for subject 3 was more successful. There were minor issues with EMG skin contact and disconnections during running, but overall the results were more

consistent across exercises. The baseline raw, analyzed, and linear fit data is shown below for subject 3:

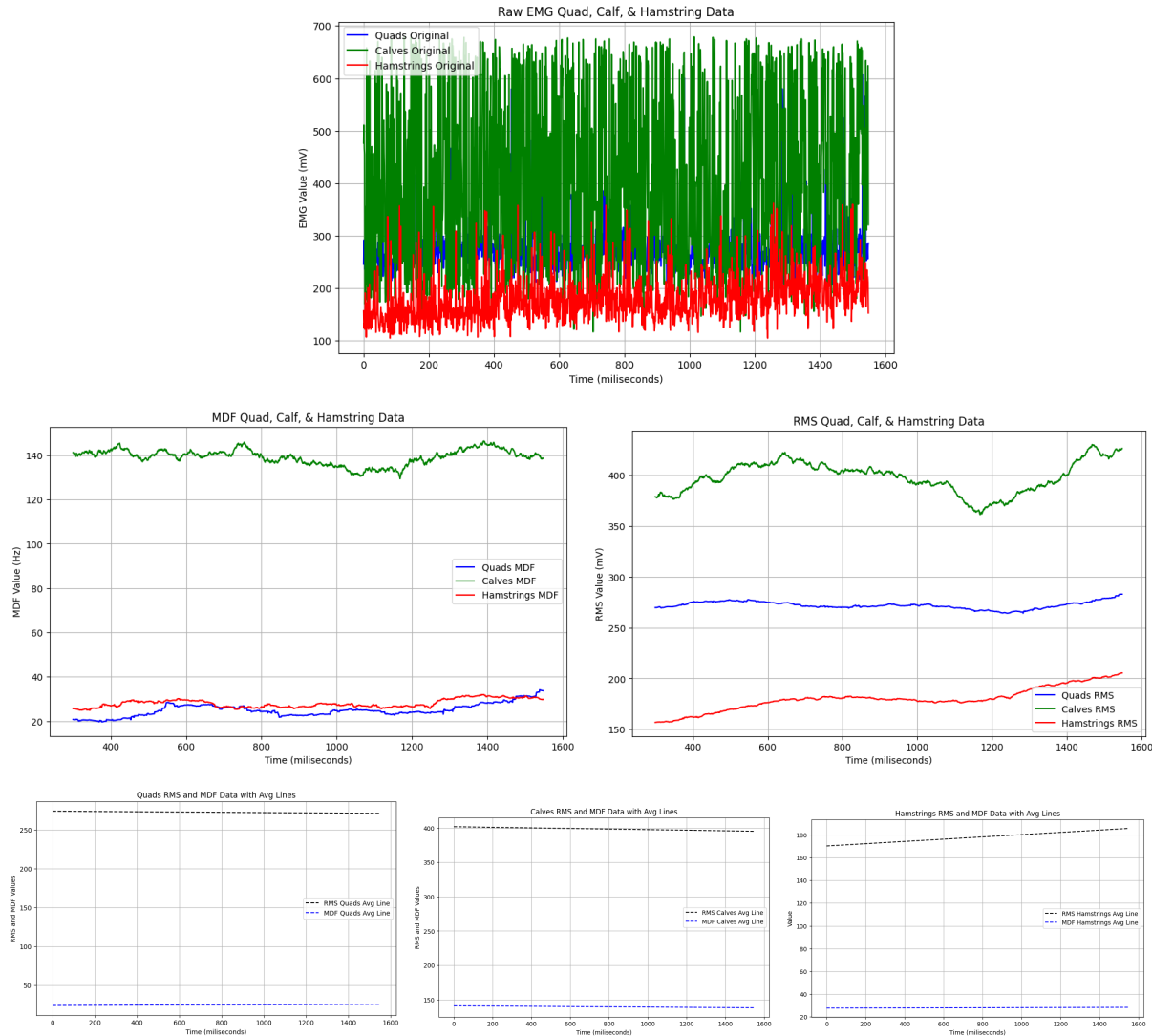


**Figure 6.16: Subject 3 “Baseline” data**

The baseline data for subject 3 was successful. While the calves had some noise present, the quad and hamstring data collection was successful. Additionally, the RMS and MDF was able to be calculated throughout the dataset of 1600 points. No fatigue was observed from this data set, but this is expected because it was less strenuous exercise. This makes this dataset ideal for creating a baseline expectation of what a non fatigued EMG signal looks like.

The non-fatigued signal can be compared to a fatigued signal at the conclusion of the workout. To make the analysis easier to complete and read, only one muscle group, the calves, was used for the comparison. Below is the raw signal, RMS, MDF, and linear fit for the calf muscle at the beginning and at the end of the workout.

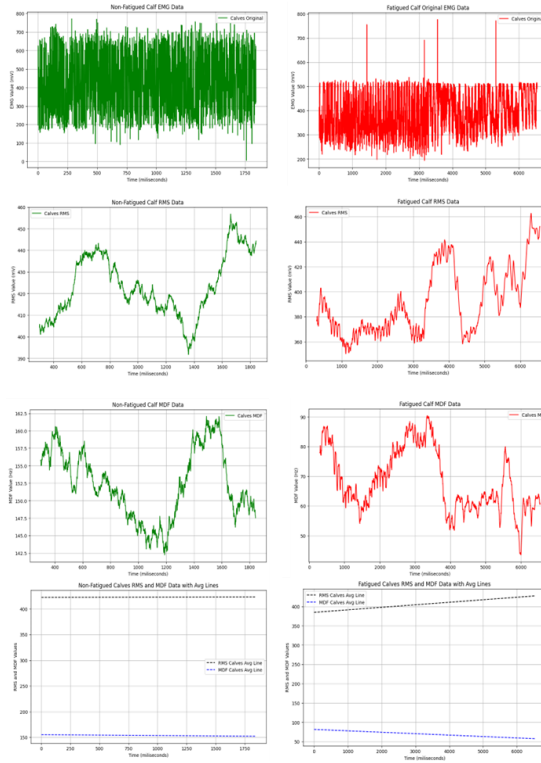


**Figure 6.17: Subject 3 fatigue (left) vs non fatigued (right) calf muscle**

Shown on the left and in green is the baseline non-fatigued data and on the right and in red is the fatigued calf data from the shuttle run. This figure is an ideal example of what muscle fatigue is expected to look like on an EMG signal. The fatigued graph shows an increment in the RMS and a decline in the trend of the MDF for the signal. This is in contrast to the baseline data, which showed a relatively constant trend in the RMS and the MDF. This indicates that subject 3 experienced fatigue in their calf muscle as their workout progressed.

Subject 4 has a variety of data quality depending on the muscles investigated and the exercise performed. The warm up baseline data collected was not ideal, as it contained a lot of noise from poor skin contact. However, this issue was addressed after the first workout, and muscle activation data was collected for the dribbling workout drill. This data is shown below:

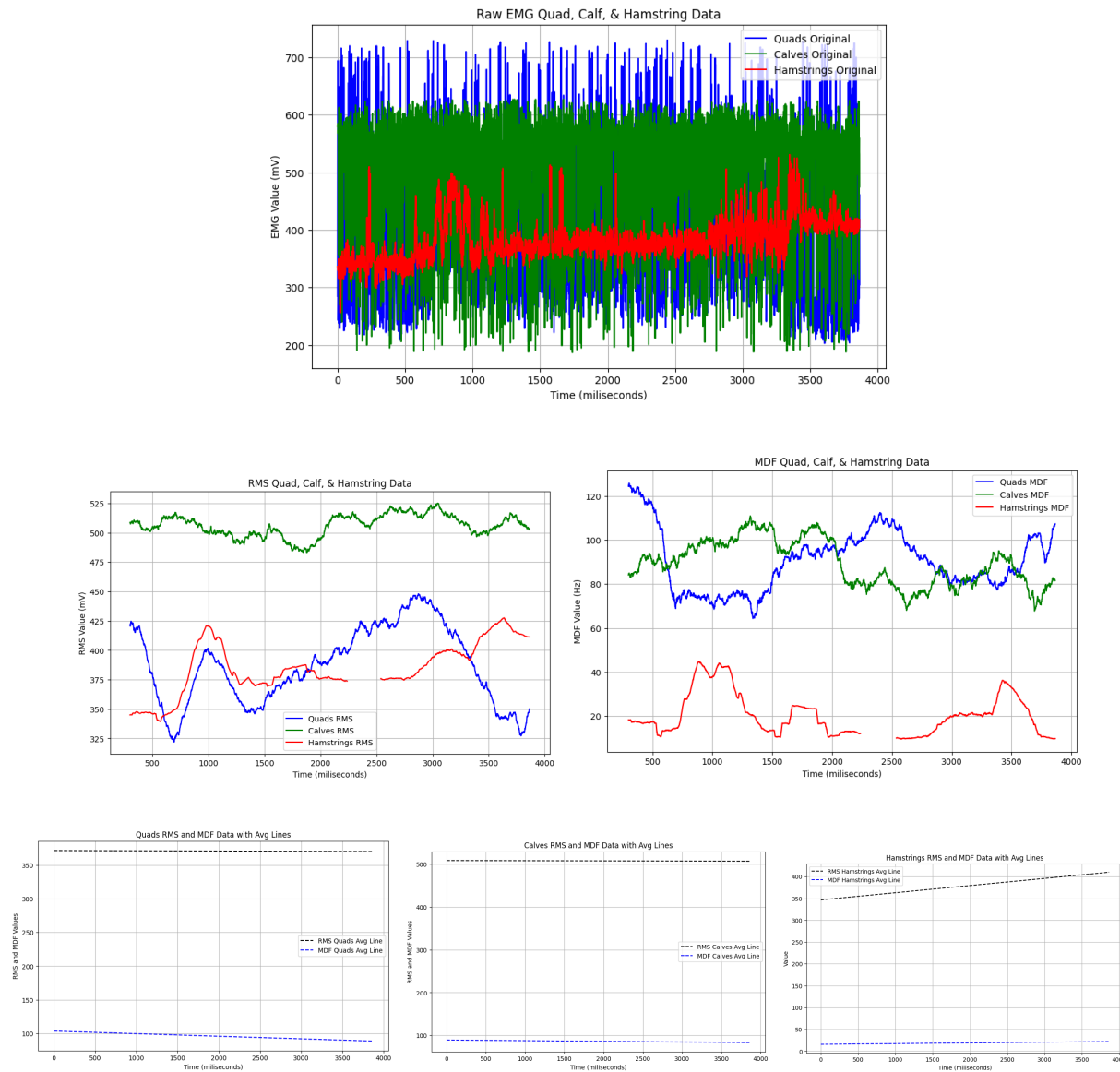


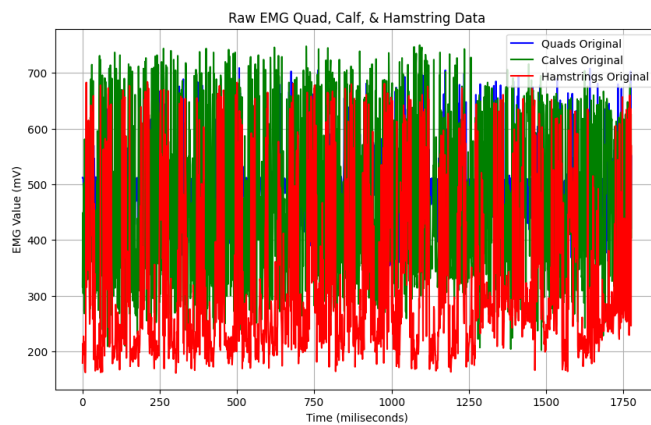
**Figure 6.18: Subject 4 “Dribbling” data**

Data collection was successful on all three muscles for subject 4’s dribbling drill. For the hamstring data in red there were two small areas of noise, but the remainder of the graph shows

activation. Additionally, the amplitude of the calves and quads were very large, which could indicate some level of constant noise throughout the test. Only the hamstring muscle experienced a positively sloping RMS trend line, while the calf experienced a relatively constant RMS line and the quad experienced a decline. However, the increase in RMS for the hamstring could be a byproduct of the noise present in the dataset. The MDF of the calf and hamstring muscle groups did not experience a significant decline. However the quad did experience a general decline in the MDF of a signal. Unfortunately this was not paired with an increase in the RMS value for the quad, so no conclusions can be drawn about the fatigue level of subject 4 from this data.

Data for the remaining workout was limited and poor quality for this subject due to connectivity issues, disconnected wires, and poor skin contact. The weather on the day of testing also likely played a role in the poor data quality and collection.

Subject 5 experienced similar issues with the EMG, and the amount and quality of data collected. The baseline data suffered from excessive noise that resulted in difficulties in calculating RMS and MDF across the entire dataset. The data is shown below:



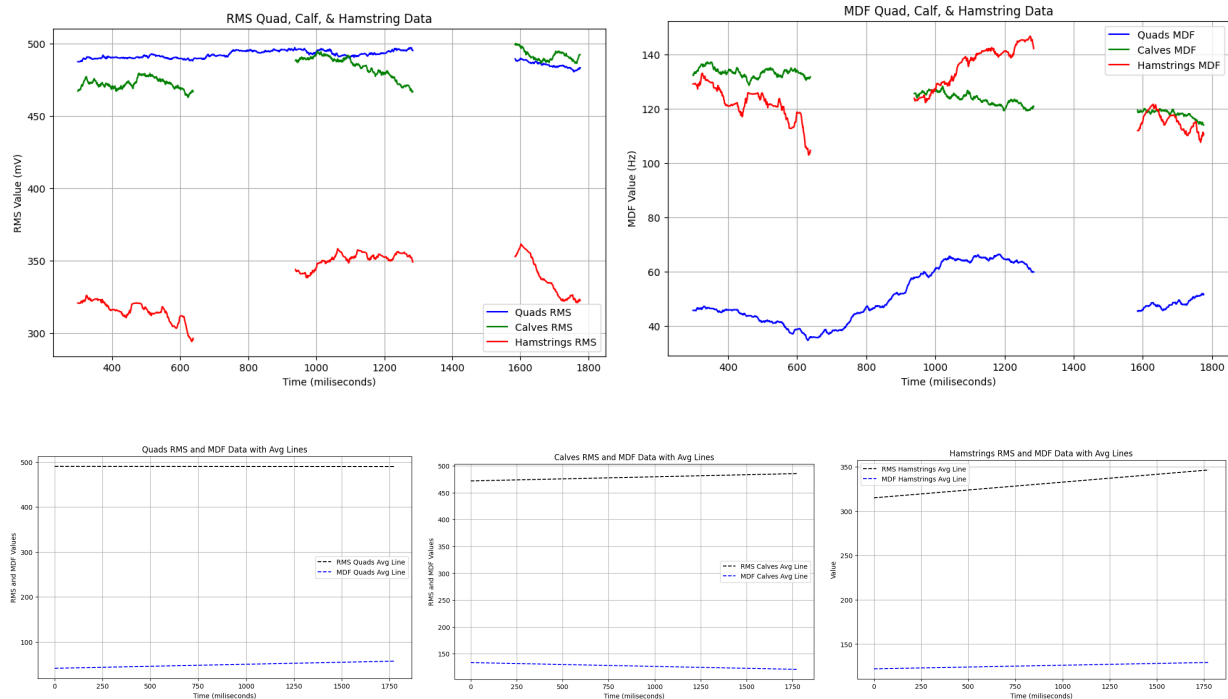


**Figure 6.19: Subject 5 “Baseline” data**

The data collected here was of poor quality. All three muscle groups experienced significant noise, which can be seen in the abnormally high peaks present in all three raw data sets. This also manifested in the RMS and MDF graphs, as there are large gaps where calculating these properties was not possible. However, even with limited data it appears that subject 3’s calf muscle experienced an increase in RMS accompanied by a decline in MDF. This could indicate fatigue in the subject’s calf, but the gaps in the RMS and MDF and the noise present in the raw signal make it difficult to determine. There are no notable trends in the RMS or MDF of the other two muscle groups.

The data for the shuttle run workout was similar in noise level to the baseline, although it was of slightly higher quality. The calf experienced significantly less noise and RMS and MDF could be calculated across the entire dataset. Additionally, the hamstring and quad had higher

quality data, though some small gaps were still present in the RMS and MDF. The data is shown below:

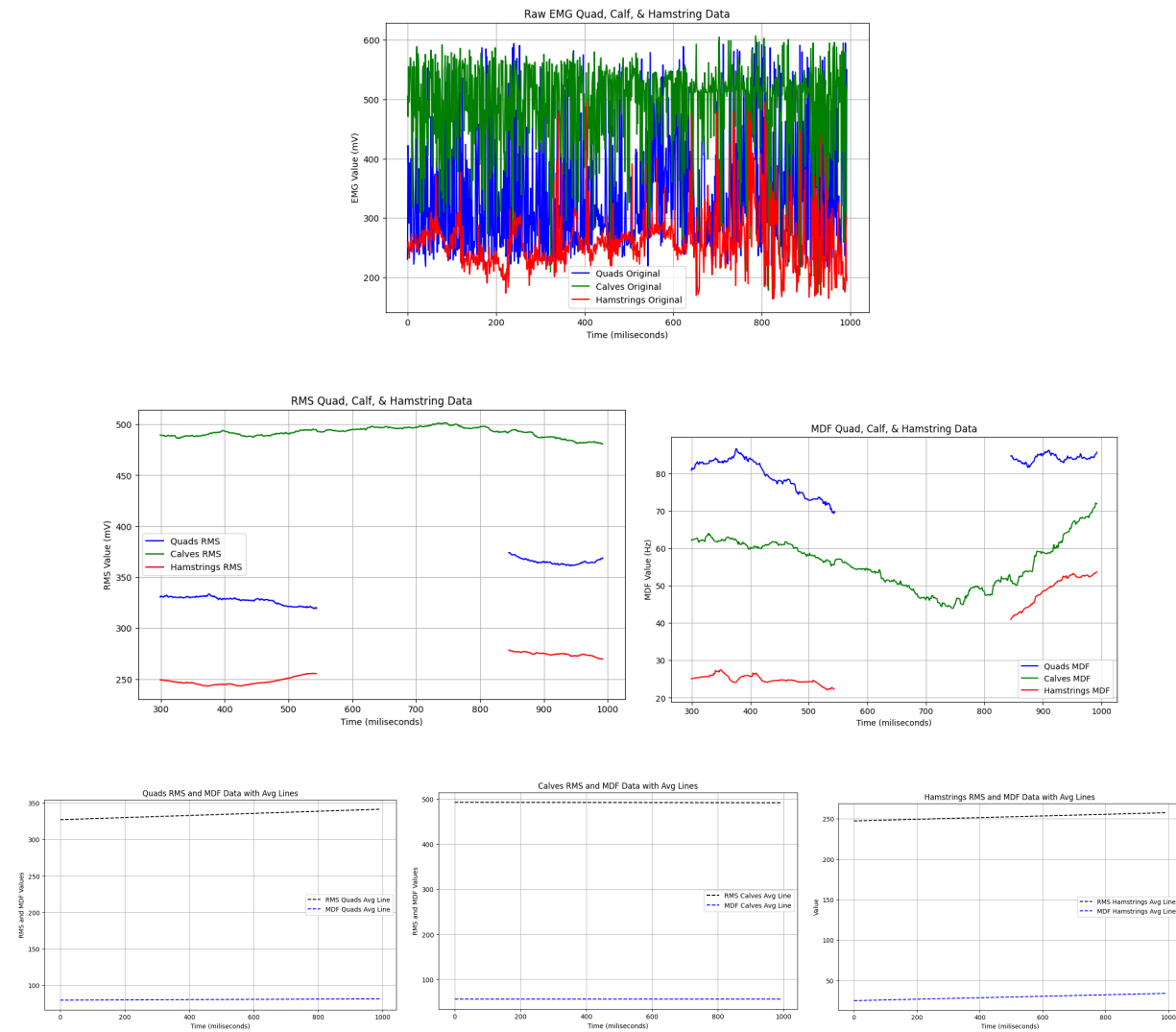


**Figure 6.20: Subject 5 “Shuttle Run” Data**

The RMS did not significantly change throughout the data set for any of the three muscle groups. Additionally, the MDF remained constant for the quad muscle, while increasing for the calf and the hamstring. This means that fatigue cannot be determined for this subject from the EMG data given.

Subject 6 had no viable EMG data. This was due to extremely poor skin contact on the electrodes that prevented the sensors from staying attached. The presence of hair on the electrode sites made it difficult to successfully attach the electrodes and caused the sensors to fall off. Unfortunately they could not be reattached and no data could be collected for this subject.

Overall the EMG data collected was less than ideal. There was a large amount of noise stemming from poor skin contact, wireless connection issues, and insecure wires. Additionally, subjects were of different proportions and identifying ideal electrode placement along the muscle fiber presented challenges. However, despite these challenges fatigue was observed in Subject 3 during the final shuttle run exercise. The expected trend of increased RMS and decreased MDF was observed. This demonstrates a proof of concept for the EMG set up and this method of fatigue evaluation.

### **6.3 Temperature Results**

It is noted that the optimal body temperature range for athletic performance is between 36.1°C to 37.2°C (97°F to 99°F) (Khandelwal, 2024). The LM35 temperature sensor was placed flush to the sleeve of each subject, close to the armpit. Given how the temperature reading is subject to electrical noise and various external factors (outdoor temperature, clothing layers, change of placement, etc.), data within 2°C of the recommended maximum range was considered, and the rest was filtered out. The data values considered were between 35.1°C and 39.2°C. Much of the data collected was considered noise and filtered out, with some values being overshot at over 68°C and under 4°C. These values are obviously incorrect, and were most likely due to short circuiting caused by unreliable subject movement. Sharp turns and pivots caused noticeable displacement of the sensor, which provides context to the abrupt switching of data between an optimal range, 68°C, and 4°C. It can also be noted that the temperature sensor

wasn't calibrated on a regular basis, which seemed to have caused a +2°C measurement. This is why the range of maximum usable data was altered from 37.2°C to 40.0°C.

	Subject 1	Subject 2	Subject 3	Subject 4	Subject 5	Subject 6
Baseline	2.25	0.97	1.29	2.77	3.42	4.06
20 Yard Pass	0	2.25	2.91	N/A	N/A	N/A
Dribble Run	0	0.32	2.58	N/A	N/A	N/A
Shuttle Run	0	0.65	2.90	N/A	N/A	N/A

**Figure 6.21: Maximum increase in recorded body temperature of subjects during different activities**

Subject 1 was seen to have a positive maximum increase in body temperature with no maximum increase in body temperature during other activities, which could be attributed to fatigue occurring during the baseline tests while the body properly cooled down during the following less-strenuous activities, creating zero maximum increase in body temperature. For subjects 2 and 3, an increase in maximum recorded body temperature occurred in the 20 yard pass from the baseline activity. This could be related to a continuous increase in body temperature after the baseline activity, with the recordings for each activity being too late and the body taking longer periods of time to efficiently and properly cool down. This can again be seen with the increase in maximum body temperature from the dribble run to the shuttle run, where an increase in recorded body temperature was seen to occur after a fatigue-inducing activity. The increase in temperature during the shuttle run also could be due to strain of the muscles throughout the body, resulting in a rise of body temperature throughout the activity.

Data for subjects 4 through 6 were found to be consistent with illegible and inaccurate data, not falling within the predicted range of theoretical body temperatures, sometimes being as low as 5.0°C for an entire activity. When accounting for different body temperatures, these

datasets were still observed to have incorrect data that would not be usable, with the maximum increase in body temperature recorded to be higher than 10.0°C. The errors that occurred with subject 4 can be attributed to the unsecure LM35 temperature sensor in addition to ambient temperatures as low as 20°C, as this subject was first to undergo full testing and was used as a basis for change in future trials.

Subject 5 was observed to have inaccurate temperatures recorded in the low 20s, which can possibly be attributed to incorrect placement of the sensor, with the temperature sensor repeatedly found to become unfastened from the arm band restraints. Subject 6 also was unable to complete full testing trials, resulting in shortened and incomplete temperature datasets with inaccurate readings due to sensor placement contrary to protocols from the best practices. Although a baseline maximum increase in body temperature was recorded, it can be assumed that this reading is inaccurate, and the baseline temperature value was found to be unusable as it could not be compared to the temperature values in other activities.

#### **6.4 GPS Results**

The NEO-6Mv2 is a compact, high-performance GPS module based on the u-blox 6 positioning engine. It provides precise geolocation data, which includes time, latitude, longitude, and velocity. The time is typically reported in Coordinated Universal Time (UTC), latitude and longitude are given in degrees, and velocity is measured in meters per second (m/s). The module can output this data in a comma-separated values (CSV) format, which is convenient for logging and analyzing movement over time. This made the NEO-6Mv2 an ideal choice for the username based workout system touched on in previous sections. All NEO-6MV2 data is stored in the csv file output of the website python file, similar to figure 6.22 below:

	gps_data_james_baseline.csv > data
1	31289,42.274364,-71.811409,0.222240
2	31320,42.274364,-71.811409,0.222240
3	31414,42.274364,-71.811409,0.222240
4	31462,42.274364,-71.811409,0.222240
5	31525,42.274364,-71.811409,0.222240
6	31603,42.274364,-71.811409,0.222240
7	31650,42.274364,-71.811409,0.222240
8	31712,42.274364,-71.811409,0.222240
9	32122,42.274357,-71.811348,0.611160
10	32170,42.274357,-71.811348,0.611160
11	32248,42.274357,-71.811348,0.611160
12	32295,42.274357,-71.811348,0.611160
13	32358,42.274357,-71.811348,0.611160
14	32437,42.274357,-71.811348,0.611160
15	32500,42.274357,-71.811348,0.611160
16	32546,42.274357,-71.811348,0.611160
17	33129,42.274364,-71.811241,1.555680
18	33160,42.274364,-71.811241,1.555680
19	33254,42.274364,-71.811241,1.555680
20	33302,42.274364,-71.811241,1.555680

**Figure 6.22: example GPS data from a workout**

After collecting data from the csv file outputs, the final step was to process the gps data by creating a frequency based location density heatmap, similar to Figure 6.23 below:

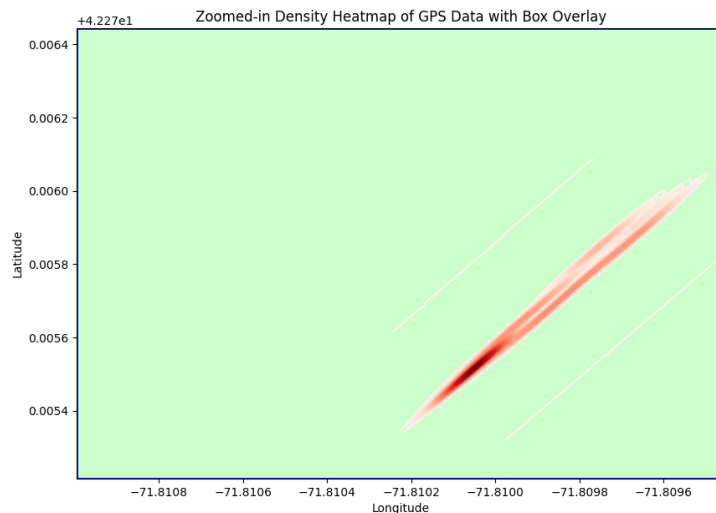


**Figure 6.23: Total workout heatmap over Rooftop Field**

It can be noted that since all Rooftop field workouts were only conducted in one section of the field, the data appears in one straight line. It can also be noted that more data points were collected than shown on the graph, as Subject 1 and 4 also ran tests in Alumni Field, the neighboring field. Additionally, data points were lost due to analog noise and disconnection of the sensor mid-workout. Average velocity information was also shown on the general companion website at a constant refresh rate of 2 seconds.

## **6.5 Fatigue Index**

After the subjects completed their workout and the individual biometrics were evaluated for fatigue, the Fatigue Index formula was evaluated for its accuracy and effectiveness. The data was segmented for each participant into categories of fatigued and non-fatigued data. Then a fatigue score was calculated for each segment of data in each category and the results were compared. This enabled the team to determine if the Fatigue Index formula was capable of quantifying an individual's level of fatigue.

Unfortunately, it was not possible to calculate Fatigue Index scores for all participants due to errors and inconsistencies with data collection. Some subjects' data suffered from excessive noise in ECG data, poor skin contact and muscle placement in EMG data, and external factors that affected temperature readings. The culmination of these noise factors meant that a valid score could not be calculated for all participants. The datasets of subjects 5 and 6 all suffered from these issues and a score cannot be calculated for them. However, some participants did have enough data to calculate a Fatigue Index score, and this data can be used to verify the proof of concept of a Fatigue Index. Subjects 1, 2, 3, and 4 had enough usable data to calculate a fatigue score.

For subject 1, the baseline warm up data and the dribble data were used. This selection was made based on the amount of available data that existed for those workouts. They had a baseline HR score of 70.59 and a dribble HR score of 65.063. Additionally, their EMG data suggests that they experienced fatigue in the quads and calves throughout their warm up but they did not experience fatigue during the dribble exercise. Finally, for subject 1's temperature, there was a slight increase during the warm up and no increase during dribble. From this data a Fatigue Index score can be calculated for each workout. For the warm up data, this subject had a fatigue score of 76.854. For the dribble data, subject 1 had a fatigue score of 39. This could indicate that the subject experienced fatigue during their warm up but not during dribbling. All of the individual biometrics pointed towards fatigue during the warm up while few of them indicated fatigue during dribbling. This is the opposite of what is expected, but this subject said they felt noticeably more fatigued after warming up than dribbling. This is likely because their dribbling distance was lower and their pace less intense than what they did during the warm up. Ideally a comparison would be made between the warm up and the shuttle run at the conclusion of the workout, but difficulties with data collection prevents that analysis.

For subject 2, the most viable data was found in their dribble workout dataset. While some limited data was obtained for their baseline, noise means that this data could be unrepresentative of the level of fatigue subject 2 actually experienced. The subject's HR score for dribbling was 60.409 and their baseline HR score was 68.749. Unfortunately EMG data for the dribble workout set suffered from significant noise issues and a conclusion could not be drawn from it. The baseline EMG score was slightly better, and the conclusion is that fatigue cannot be seen in the data collected. For temperature, this subject experienced a slight increase in temperature for both baseline and dribbling exercises. Due to a lack of viable EMG data for

dribbling, only the baseline Fatigue Index could be calculated for subject 2. The fatigue score for their baseline workout was 41.868. This is a relatively low level of fatigue and it lines up with expectations of a warm up and the participant's stated level of fatigue at the end of the exercise.

For subject 3, the most viable data collected was in the shuttle run at the conclusion of the workout. Their heart rate score during this exercise was 74.468. Additionally, their EMG signal demonstrated an increase in RMS and a decrease in MDF trend, so the muscles are said to be fatigued. Finally, their temperature score was unfortunately unviable for this exercise, but temperature has a low overall effect on the Fatigue Index, so this is negligible. The Fatigue Index score for this workout is 74.468. This is a large score and indicates that the subject was fatigued during this shuttle run. This was the most intense workout at the conclusion of the test, so this score would be expected.

For subject 4, their only viable data was from the dribble test. Other segments of the workout had too much noise, connection issues, or other problems that prevented collection. However, for some workouts data from some sensors was usable while other sensors had significant issues. For example during the warm up, the ECG sensor successfully collected data while the EMG sensors were unusable. This would account for 30% of the overall score, so calculating a fatigue index would not be accurate for the baseline. For dribbling, 90% of the data for the fatigue index was collected, so a Fatigue Index score can be calculated. The HR score during dribbling is 71.228, and the EMG sensors did not show any of the markers of fatigue. The temperature data was not usable for this subject;s workout. This gives a fatigue score of 43.176. This is expected, as dribbling has not been fatiguing for the other subjects and subject 4 indicated that they did not feel fatigued at the conclusion of the dribble exercise.

Subjects 5 and 6 did not have enough viable data for a fatigue score to be calculated from any of their workouts. This can be attributed to error in placing electrodes, poor skin contact due to hair, and poorly secured wires that introduced more noise into the system. These issues were addressed in the tests for other subjects, which is how they were able to collect usable data.

The hypothesized Fatigue Index appears to be a good approximation of the fatigue levels of the subjects. When the subjects reported feeling tired after a workout, their fatigue score was generally higher. When most of them were warming up or doing less intensive exercises such as dribbling they had lower fatigue scores. This could indicate that the formula developed is a good proof of concept that fatigue can be quantified by a combination of biometric sensors.

## **7.0 Final Design Validation**

### **7.1 Economics**

The purpose of this section is to estimate the potential economic value of the wearable biometric monitoring system as it is used for one soccer team over the course of five soccer seasons.

#### **7.1.1 Net Present Value**

The value of the wearable biometric monitoring system to its target market can be estimated as the difference between how much consumers would spend on it and how much consumers would save with it over time as it assists in reducing injuries. The net present value of the system at some future point in time can be calculated according to the following equation (Fernando, 2024):

$$NPV = \frac{R_t}{(1+i)^t} \quad (6)$$

Where the net present value (NPV) equals the net cash flow at time equals t,  $R_t$ , divided by the one plus the discount rate,  $i$ , to the power of  $t$ , the time of the cash flow rate. A cash flow diagram can be created to visually represent the income and expenses of this product over a certain period of time using the equation above.

#### **7.1.2 Estimated Costs**

The wearable biometric monitoring system incorporates a number of parts to properly function. The team was given \$850 for this MQP. The team used \$380 directly for the production

of the product. The team used an additional \$370 on other parts such as the initial EMG sensor, other GPS modules due to broken ones during testing, excess wires, and other miscellaneous parts in the original design. Below is a list of every part in the final product and their cost:

<b>Part name</b>	<b>Price</b>
Athletic vest	\$23
12 volt battery	\$25
Temperature sensor	\$10
GPS module	\$11
ECG sensor	\$20
Electrodes (disposable pack of 100)	\$24
ESP-8266	\$8
Multiplexer	\$8
Heat shrink	\$6
Wire	\$12
Arduino uno	\$27
EMG Myoware sensors (quantity: 3)	\$40 each
Myoware link shield (quantity: 3)	\$10 each
Arduino shield	\$12
Buck converter	\$14
Velcro	\$10
Waist bag	\$12
<b>Total</b>	<b>\$380</b>

**Figure 7.1: Part cost list for each component in the final prototype**

### 7.1.3 Economic Value

The potential economic value of the wearable biometric monitoring system was also estimated as if it is used for one team over the course of five soccer seasons. College soccer seasons span from August to December with an average of 15-20 games. Over this time, the average amount of injuries a team undergoes is about 10 injuries per season (Tinney, 2023). Under these statistical conditions and for the potential economic value of this product, these numbers are used. The average cost to visit the doctors in Massachusetts is \$140 (Sidecare Health, n.d.).

Therefore, if 10 players on one team visit the doctor for their injury once, it would accumulate to \$1400 for one season. Typically, sports injuries visit the doctors a second or third time or a check up which would double this price to \$2800 per team per season if each athlete visited twice. Assume these conditions occur for 5 years in a row.

On average a college soccer team consists of 25 players. So if a soccer team were to purchase this product for each of their players at \$400 each, it would cost \$10,000 as a fixed cost in year 1. If 10 players were to get a basic injury and visit the doctor twice per season, this would cost them \$14,000 over 5 years. Therefore, assuming that this product can eliminate injuries on the team, it would financially benefit the team by saving about \$4,000 or more over the course of 5 years.

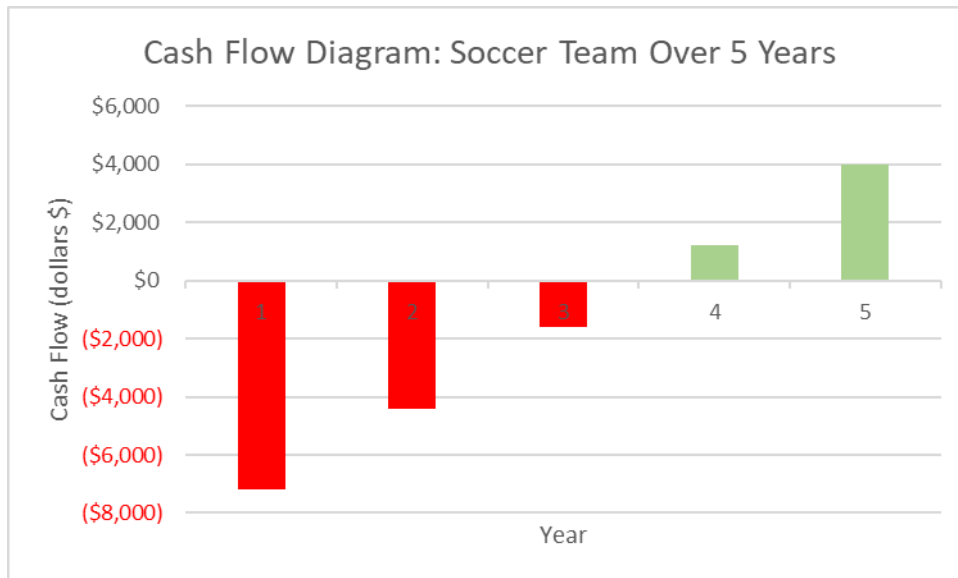


**Figure 7.2: Cash Flow of one soccer team over 5 years**

## 7.2 Environmental Impact and Sustainability

There are some parts of this system that are toxic to the environment and contribute to excess pollution. Lithium ion batteries contain metals such as cobalt, nickel, manganese, and lead which are toxic to the environment including water sources and landfills (Kang et al, 2013). Since these batteries are not easily recyclable, they end up in landfills which increases the likelihood of chemical leaks and fires. Furthermore, this project requires electrodes to collect ECG and EMG data. However, the team opted for disposable electrodes due to price and health and safety reasons per person. Disposable electrodes are made with nontoxic metals, conductive gel, and adhesive components (Moro et al., 2019). However, each electrode includes a plastic peelable piece covering the gel which is disposed of and contributing to excess plastic waste to the environment. Additionally, the rest of the electrode is contributing to electronic waste, or e-waste. This environmental phenomenon contaminates ecosystems and the air when toxic dust particles are released causing negative health for animals and the atmosphere.

### **7.3 Societal Influence**

The introduction of a non-invasive body sensor network for monitoring key biometrics in soccer athletes represents a significant advancement in the realm of sports performance and athlete health. Such technology has the potential to profoundly influence various aspects of collegiate soccer and the wider sporting community.

The incorporation of advanced sensors and data analysis techniques into athlete monitoring could revolutionize coaching methodologies. Coaches could have access to personalized data, allowing them to tailor training regimens more effectively to individual athletes. By identifying patterns in biometric data, coaches can adjust training intensity, volume, and recovery strategies to optimize performance and minimize the risk of overexertion or burnout. This approach to coaching has the potential to maximize the potential of each player while protecting their long-term health and well-being.

Furthermore, the availability of detailed biometric data could empower athletes to take a more proactive role in managing their own health and performance. By gaining insights into how their bodies respond to training and competition, athletes can make informed decisions about rest, recovery, and lifestyle choices. This increased self-awareness could lead to improved overall health and performance, as athletes learn to listen to their bodies and make adjustments accordingly.

From a broader societal perspective, the adoption of non-invasive body sensor networks in sports could have ripple effects beyond the realm of athletics. The technological advancements and insights gained from monitoring athletes could have applications in healthcare, rehabilitation, and workplace wellness programs. By demonstrating the efficacy of such technology in optimizing performance and reducing injury risk in athletes, there may be

increased interest and investment in utilizing similar systems to monitor and improve the health and well-being of the general population.

#### **7.4 Political Ramifications**

Introducing a non-invasive body sensor network for monitoring key biometrics may have significant political ramifications spanning sports governance, athlete rights, and public health policies. As technology increasingly permeates the realm of athletics, questions arise regarding regulatory oversight and fairness within collegiate sports organizations. Political debates may center on issues such as data ownership, consent, and the potential for technology for unfair advantages.

Moreover, concerns about athlete privacy and data protection emerge as biometric data collection becomes more widespread. Political pressure may mount for the implementation of stringent regulations to safeguard sensitive health information and ensure equitable access to monitoring technology. Additionally, policymakers may recognize the broader public health implications of wearable technology, prompting discussions about its potential applications beyond athletics. There could be calls for government funding to support research and innovation in sports technology, as well as initiatives to integrate such technology into educational curricula.

#### **7.5 Ethical Concerns**

The ASME Code of Ethics of Engineers was used as a precedent for the academic and ethic standard that was upheld for all aspects of this project. Through the analysis of the associated system hazards and of the organizations and companies used to support this system, the fundamental canons were followed in order to ensure that, as stated in the society policy, the team would “uphold and advance the integrity, honor and dignity of the engineering profession”

(American Society of Mechanical Engineers, 2021). The team used the Code of Ethics of Engineers to verify that the environmental impact was considered and minimized, acted in the best interest of Worcester Polytechnic Institute by representing themselves as a professional team of engineers supported by the school, and only acted and represented themselves in a form that authentically conveyed their expertise (American Society of Mechanical Engineers, 2021).

With a congregation of personal data being centralized into one location, there is a concern with the possible release of this Personal Identifiable Information (PII) in data breaches or malicious acts from third party adversaries. Steps should be taken to reduce the potential for spillage of data, including increased access controls such as password and authentication security measures, encrypted files, and/or consistent monitoring of the database system. Training and certification for users of the system also can help prevent any phishing or social engineering attacks from occurring with the intention to steal administrative credentials for the database.

There also exists an ethical concern with the testing of a medical device without the full knowledge of possible outcomes and/or complete health risks associated with the medical system (Citron, 2012). The proper development of a system using lifecycle modeling would be able to mitigate the potential hazards that may be present with a medical system, but without the proper laboratory equipment, review boards, and documentation/tracking softwares available, limited precautions could be taken that will not have the ability to identify all possible consequences of such a device. During the concept stage of this project, precautions were taken to identify all possible hazardous effects that would result from the creation, usage, and retirement of such a system in order to limit the severity and probability of any mishap that may occur.

## **7.6 Health and Safety Issues**

Over-reliance on the system can result in injury if the data analysis methods produce inaccurate readings, which could lead to improperly informed users overexerting themselves. An error of this magnitude could increase the probability of muscle injuries, overfatigue, and hyperthermia. Some components used in this system can pose a threat to the user's health due to the hazardous materials that are used. Medical grade electrodes can potentially cause its users to experience skin irritation or develop rashes after extended periods of use, but requires no treatment. Gels and adhesives can potentially contain allergenic materials, resulting in the previously mentioned symptoms and containing the previously mentioned recovery ("Risks of Electrocardiogram", n.d.).

Lithium material used in the battery can be subject to thermal runaway in the event of overheating due to increased ambient temperatures or as a result of the lack of battery management system precautions to monitor cell conditions during overcharging. A lithium battery that undergoes this hazardous event can result in outgassing of toxic fumes, combustion of gasses, and fragmentation of the battery components ("Lithium-Ion Battery Safety", 2023). This presents a multitude of hazards, potentially causing tissue burns, lacerations or deep penetrating wounds, and debilitating or fatal injuries. Constant exposure to improperly-contained lithium components can also experience allergenic and carcinogenic effects as a result of the increased content of lead, cobalt, chromium, and thallium (Kang et al, 2013).

## **7.7 Manufacturability**

The usage of Commercial-Off-The-Shelf (COTS) components for sensors, microcontrollers, clothing, and wiring enables easy repeatability of the design. The only

modification required for the majority of hardware pieces was soldering to increase the security of the connections. Additionally, some detachable connection pins were used on the GPS sensor and to connect the Arduino Uno and ESP8266 to increase the wearability of the vest. Other than those modifications the sensors required little hardware modifications and only had to be assembled in the correct order.

The most complex portion of assembly is the wiring of the ESP8266 to the other sensors and microcontroller. The ESP8266 is the hub of the entire design, and all sensor data passes through it to be transmitted. Care must be taken to ensure that the multiplexor is correctly wired to the ESP and that data from the ECG and LM35 sensors can be correctly read from it. If the design were to move to mass manufacturing, protoboards could be used as a base to wire all of the sensors off of. This process could be automated, as the wiring would be identical on all models.

Manufacturing the Arduino Uno portion of the project is simpler to manufacture. The Myoware power and link shields snap onto the Arduino Uno and the EMG sensors connect to the power shield using auxiliary cables. None of those connections require soldering and they can be done quickly. However, to connect the Arduino Uno to the ESP8266 some soldering is required. The Rx, Tx, and ground pins on top of the Myoware power shield. This can be a frustrating process due to the small size of the connections on the top of the power shield. However the process could still likely be automated.

Next the battery is affixed to the ESP circuit using hot melt adhesive, and various power solutions such as a buck converter are also affixed. This turns the entire circuit into a self contained unit with the battery attached.

The last step in manufacturing the product is to place the completed ESP and Arduino Uno circuits in the appropriate location on the wearable portion of the project. The vest requires some stitching to reinforce its mesh backing so the circuit and battery do not fall out. For the Arduino Uno, it can be placed in the waist bag securely. Overall, the use of COTS makes the product easy to manufacture and reproduce, with only minor soldering, sewing, and placement needed to create the final design.

## **8.0 Discussion and Recommendations**

Reviewing the results from the 6 participants, the vest sensor network was able to record and identify fatigue markers across multiple biometrics. The vest design and circuit proved to be durable, holding up in a variety of environmental conditions and after being exposed to movement from testing. The wires and circuit remained functional throughout all testing of the vest across all 6 participants. Additionally, battery life was not a limiting factor during testing and the device had enough charge to exceed the 90 minute duration of the tests conducted.

In terms of sensors, they were all tested individually and preliminary data was collected. All sensors were verified in isolation and in a controlled environment, and they were successful in collecting viable biometric data. The preliminary data collected suggested that the sensors were capable of recording accurate biometric data. Unfortunately, on the integrated vest the sensors were not as reliable, as a variety of issues including electrode skin contact, connectivity issues, and variations in participant anatomy. These issues prevented a Fatigue Index score from being calculated for two of the participants and noise issues were present in many of the workouts of the remaining participants. However enough viable data was collected from some of the participant's workouts to provide a proof of concept of the Fatigue Index.

The Fatigue Index results from participants 1, 2, 3, and 4 indicate that it is possible for a smart wearable device to quantify fatigue. All participants were asked about their level of fatigue after the individual workouts and their responses broadly agreed with the Fatigue Index score. The participants had low fatigue scores for the “Dribbling” exercise, and also reported not feeling tired after completing it. Additionally, participant 3’s “Shuttle Run” data demonstrated the level of fatigue they felt when completing that exercise, which was designed to be the most exhausting.

Ideally, more viable data from the 6 participants combined with a greater number of participants would have enabled further verification. Despite limited data, the Fatigue Index was capable of combining information from three different biometrics into a comprehensive fatigue evaluation. While more data would have allowed the team to modify the weights of each biometric and improve the accuracy of the formula, the formula presented here appears to give a reasonable approximation of fatigue levels.

Another major success of this project is the creation of a visual application that can display biometric data live from the vest and software that can perform post workout analysis on the raw signals to identify signs of fatigue. Data from all sensors on the vest was able to be wirelessly sent across a WiFi network, where it could be displayed and analyzed as needed. For all four sensors no degradation in data quality was attributed to wireless transmission, demonstrating the effectiveness of using an ESP 8266 to transmit data. Additionally, analysis on the data such as BPM calculations, ECG derived respiratory rate, RMS and MDF of EMG signals, and data averages were able to be performed. This can enable athlete's and their coaches access to critical raw data that can enable them to make informed decisions about their health and training.

This project also did suffer from some key limitations that affected the quality of data collected. For the ECG sensor, noise caused by the movement of lead wires was a frequent issue. While this was attempted to be addressed through the use of adhesive, this was a temporary and imperfect solution. This resulted in a great deal of noise in the final data. Additionally, while an ECG derived respiration rate was able to be calculated from the raw ECG signal, there was no control respiratory rate measurement to compare it to. That meant the team could not verify the

results provided by the ECG derived respiration rate and this excluded the measurement from inclusion in the Fatigue Index.

Other key limitations stemmed from the EMG sensors used in the project. These sensors had limited documentation, making troubleshooting and set up difficult. The sensors chosen also required that electrodes be placed very close to one another, which required modification of the electrode size and shape. Also, variations in participant anatomy made finding a consistent sensor placement along muscle fibers difficult and electrodes suffered from poor skin contact if hair was present. One of the largest limitations with the EMG sensors was the method of wired data transmission between the two microcontrollers. Data passed through the Rx/Tx connections had a maximum sample rate, and if that rate was exceeded the data would not be read properly. This artificially lowered the EMG sampling rate to 15 Hz, far less than the 1000 Hz industry standard.

The LM35 temperature measurements also had key limitations stemming from the inaccuracies of axillary temperature measurement, inconsistent source voltage from the ESP 8266, insecure placement on the participant's arm and low ambient temperature causing erroneous readings. Additionally, a limitation of GPS results is that testing was not performed at the same location for all 6 participants. This made it difficult to generate heat maps and compare data across trials.

Future considerations in order to improve this complex system include the addition of a variety of metrics, not limited to but including respiratory rate, blood pressure, distance traveled, and calories burned. Moreover, advancement in the current biometric sensors would further improve the quality, accuracy, and amount of data collected, allowing for better quantification of fatigue. EMG sensor improvements in regards to live and post processing of data, the

implementation of a granular system for the observation of multiple muscles, and increased EMG data transmission rate would allow for a holistic approach for the quantification of fatigue. The usage of a new wireless strategy that uses a customized Printed Circuit Board (PCB) design tailored to the specific requirements and functionalities of the vest system can potentially simplify and reduce the complexity of the system, increasing the sampling rate, dataset size, and overall cost of the project. In addition to a PCB, the creation of custom biometric and performance sensors for the body sensor network instead of hobby-grade sensors would improve the results in accuracy, range, and size. While a PCB was not used for the microcontroller unit in this project, the application of this component would allow for a more permanent solution for the securement of the final prototype when compared to the breadboard and hot melting adhesive solution used.

In addition to the changes mentioned above in relation to the design of the final prototype, changes in the testing with the final prototype would heavily benefit future work in the quantification of fatigue. The usage of more test subjects would not only allow for more data collection to form a more accurate fatigue index equation, but could better validate the fatigue index score by having multiple datasets run through the equation in order to compare the score with the actual fatigue levels of the subjects. In order to better suit the increased amount of subjects, with assumption that a variety of physical anatomies will be tested upon, the adoption of a new prototype that would allow for separate top and bottom subsystems, consisting of the vest and waist bag respectively, would allow increased patient comfort, accessibility, and ease of usage to sufficiently create a universal fatigue measuring system.

## **9.0 Conclusion**

This project developed a wearable body sensor network capable of measuring key biometrics and evaluating them for markers of fatigue. Data was viewable on a live website that displayed raw data, provided live basic analysis, and more in depth post processing and analysis. While key features of fatigue were observed in the datasets, limitations were present in the design. Factors such as external noise, cost limitations, sensor documentation, and data transmission limitations impacted the accuracy of measurements. Additionally, a sample size of six provided limited data, and ideally the results would be verified with a larger sample size. Despite these limitations, this project demonstrates that fatigue can be quantifiably measured using a wearable sensor network. This project also identifies key biometrics that a sensor network should contain and suggests a method to combine their data into a comprehensive Fatigue Index.

## References

- Adidas. (2022, July 1). *Adidas Reveals The First FIFA World CupTM Official Match Ball Featuring Connected Ball Technology*. Adidas News Site.  
<https://news.adidas.com/football/adidas-reveals-the-first-fifa-world-cup--official-match-ball-featuring-connected-ball-technology/s/cccb7187-a67c-4166-b57d-2b28f1d36fa0>
- American Academy of Orthopaedic Surgeons. (2021). *Emergency Care and Transportation of the Sick and Injured Essentials Package* (12th ed.). Jones & Bartlett Pub Incorporated.
- American Society of Mechanical Engineers. (2021). *Code of Ethics* (P-15.7). ASME.  
<https://www.asme.org/about-asme/governance/ethics-in-engineering>
- Apple. (2023). *Watch*. Apple. <https://www.apple.com/watch/>.
- Archevapanich, T., Sithiyopasakul, J., Sithiyopasakul, J., Sithiyopasakul, P., Anuwongpinit, T., & Purahong, B.. (2021). Athletes Movement Tracking device for Soccer players, *IEEE*.  
<https://doi.org/10.1109/ecti-con51831.2021.9454802>
- Arun Faisal, I., Waluyo Purboyo, T., & Siswo Raharjo Ansori, A. (2019). A Review of Accelerometer Sensor and Gyroscope Sensor in IMU Sensors on Motion Capture. *Journal of Engineering and Applied Sciences*, 15(3), 826–829.  
<https://doi.org/10.36478/jeasci.2020.826.829>
- CDC. (2020, September 17). *Target Heart Rate and Estimated Maximum Heart Rate*.  
<https://www.cdc.gov/physicalactivity/basics/measuring/heartrate.htm#:~:text=You%20can%20estimate%20your%20maximum>

- Chu, M., Nguyen, T., Pandey, V., Zhou, Y., Pham, H., Bar-Yoseph, R., Radom-Aizik, S., Jain, R., Cooper, D., & Khine, M. (2019). Respiration rate and volume measurements using wearable strain sensors. *npj Digital Medicine*. Springer Nature. 0.1038/s41746-019-0083-3
- Citron, P. (2012). Ethics Considerations for Medical Device R&D. *Progress in Cardiovascular Diseases*, 55(3), 307–315. <https://doi.org/10.1016/j.pcad.2012.08.004>
- Damatto, R. L., Cezar, M. D. M., & Santos, P. P. dos. (2019). Control of Body Temperature during Physical Exercise. *Arquivos Brasileiros de Cardiologia*. <https://doi.org/10.5935/abc.20190081>
- Exercise-Related Heat Exhaustion*. (2021, August 8). [Www.hopkinsmedicine.org](https://www.hopkinsmedicine.org); John Hopkins. <https://www.hopkinsmedicine.org/health/conditions-and-diseases/exerciserelated-heat-exhaustion#:~:text=What%20are%20the%20symptoms%20of>
- Falzon, A., Grech, V., Caruana, B., Magro, A., & Attard-Montalto, S. (2003). How reliable is axillary temperature measurement? *Acta Paediatrica (Oslo, Norway: 1992)*, 92(3), 309–313. <https://doi.org/10.1080/08035250310009220>
- Fernando, J. (2024, March 7). Net Present Value (NPV): What it Means and Steps to Calculate It. Investopedia. <https://www.investopedia.com/terms/n/npv.asp>
- Galgani, J., & Ravussin, E. (2008, Dec). Energy metabolism, fuel selection and body weight regulation. *Int J Obes (Lond)*, 32(7), S109-119. National Library of Medicine. 10.1038/ijo.2008.246
- Galli, A., Montree, R., Que, S., Peri, E., & Vullings, R. (2022, May). An Overview of the Sensors for Heart Rate Monitoring Used in Extramural Applications. *Sensors (Basel)*, 22(11). National Library of Medicine. 10.3390/s22114035

- González-Alonso, J., Teller, C., Andersen, S. L., Jensen, F. B., Hyldig, T., & Nielsen, B. (1999). Influence of body temperature on the development of fatigue during prolonged exercise in the heat. *Journal of Applied Physiology*, 86(3), 1032–1039.  
<https://doi.org/10.1152/jappl.1999.86.3.1032>
- Gravina, R., Alinia, P., Ghasemzadeh, H., & Fortino, G. (2017, May). Multi-sensor fusion in body sensor networks: State-of-the-art and research challenges. *Information Fusion*, 35, 68-80. <https://doi.org/10.1016/j.inffus.2016.09.005>
- Gray, A. J., Jenkins, D., Andrews, M. H., Taaffe, D. R., & Glover, M. L. (2010). Validity and reliability of GPS for measuring distance travelled in field-based team sports. *Journal of Sports Sciences*, 28(12), 1319–1325. <https://doi.org/10.1080/02640414.2010.504783>
- Hakimi, N., Jodeiri, A., Mirbagheri, M., & Kamaledin Setarehdan, S. (2020). Proposing a convolutional neural network for stress assessment by means of derived heart rate from functional near infrared spectroscopy. *Computers in Biology and Medicine*, 121, 103810–103810. <https://doi.org/10.1016/j.combiomed.2020.103810>
- Hexoskin. (2023). Hexoskin Smart Shirts - Cardiac, Respiratory, Sleep & Activity Metrics. Retrieved October 12, 2023, from <https://www.hexoskin.com/>
- Hoppe, M., Baumgart, C., Polglaze, T., & Freiwald, J. (2018, February). Validity and reliability of GPS and LPS for measuring distances covered and sprint mechanical properties in team sports. *PLOS ONE*, 13(2). PLOS ONE Journals.  
<https://doi.org/10.1371/journal.pone.0192708>
- How to Determine Your Level of Soccer Fitness.* (2017, September 17). Sport Fitness Advisor.  
<https://www.sport-fitness-advisor.com/soccer-fitness.html>.

- International Association Football Federation. (2023). *Laws of the Game*.  
<https://www.theifab.com/laws-of-the-game-documents/?language=all&year=2023%2F24>
- International Organization for Standardization. (2024). *Medical electrical equipment* (IEC/CD 80601-2-86.2). ISO. <https://www.iso.org/home.html>
- International Organization for Standardization. (2017). *Medical electrical equipment* (ISO 80601-2-56:2017). ISO. <https://www.iso.org/home.html>
- Jiang, Y., Spies, C., Magin, J., Bhosai, S. J., Snyder, L., & Dunn, J. (2023, July). Investigating the accuracy of blood oxygen saturation measurements in common consumer smartwatches. *PLOS Digit Health*. 10.1371/journal.pdig.0000296
- Kang, D. H., Chen, M., & Ogunseitan, O. A. (2013). Potential Environmental and human health impacts of rechargeable lithium batteries in electronic waste. *Environmental Science & Technology*, 47(10), 5495–5503. <https://doi.org/10.1021/es400614y>
- Khandelwal, S. (2024). 14.2.2 Body Temperature Range. Tutorchase.com.  
<https://www.tutorchase.com/notes/ib/sehs/14-2-2-body-temperature-range>
- Koshy, A., Sajeev, J., Nerlekar, N., Brown, A., Rajakariar, K., Zureik, M., Wong, M., Roberts, L., Street, M., Cooke, J., & Teh, A. (2018, May). Utility of photoplethysmography for heart rate estimation among inpatients. *Internal Medicine Journal*, 48(5), 587-591. Wiley Online Library. 10.1111/imj.13777
- Li, H., Zhao, G., Zhou, Y., Chen, X., Ji, Z., & Wang, L. (2014). Relationship of EMG/SMG features and muscle strength level: an exploratory study on tibialis anterior muscles during plantar-flexion among hemiplegia patients. *BioMedical Engineering OnLine*, 13(5), 5. <https://doi.org/10.1186/1475-925X-13-5>

*Lithium-Ion Battery Safety.* (2023). Nfpa.org.

<https://www.nfpa.org/education-and-research/home-fire-safety/lithium-ion-batteries>

Mackey, E. (2023, July 27). *How Long Is A Soccer Game? Regulation, Extra Time And Penalties Explained.* The Athletic. <https://theathletic.com/3952500/2022/11/30/how-long-is-a-soccer-game-regulation-extra-time-and-penalties-explained/>

Makarov, D. (n.d.). *Effortlessly Convert Joules to Calories with Our Calculator.* Asutpp.

<https://www.asutpp.com/joules-to-calories.html>

Mannheimer,, P. (2007, December). The Light–Tissue Interaction of Pulse Oximetry. *Anesthesia & Analgesia, 105*(6), S10-S17. 10.1213/01.ane.0000269522.84942.54

Massaroni, C., Nicolò, A., Lo Presit, D., Sacchetti, M., & Silvestri, S. (2019). Contact-Based Methods for Measuring Respiratory Rate. *Sensors (Basel, Switzerland), 19*(4). National Library of Medicine. 10.3390/s19040908

MedlinePlus. (2018). *Temperature measurement: MedlinePlus Medical Encyclopedia.* Medlineplus.gov. <https://medlineplus.gov/ency/article/003400.htm>

Moro, G., Bottari, F., Van Loon, J., Du Bois, E., De Wael, K., & Moretto, L. M. (2019). Disposable electrodes from waste materials and renewable sources for (bio)electroanalytical applications. *Biosensors and Bioelectronics, 146*, 111758.  
<https://doi.org/10.1016/j.bios.2019.111758>

Nicolò, A., Massaroni, C., Sacchetti, E., & Sacchetti, M. (2020). The Importance of Respiratory Rate Monitoring: From Healthcare to Sport and Exercise. *Sensors (Basel), 20*(21). Sensors (Basel). 10.3390/s20216396

- Non-contact Temperature Measurement FAQs.* (n.d.). Omega Engineering.  
<https://www.omega.com/en-us/resources/body-temperature-screening-faq#:~:text=Obstructions%20will%20lead%20to%20inaccurate>
- Owen, A. L., Forsyth, J. J., Wong, D. P., Dellal, A., Connelly, S. P., & Chamari, K. (2015). Heart Rate-Based Training Intensity and Its Impact on Injury Incidence Among Elite-Level Professional Soccer Players. *Journal of Strength and Conditioning Research*, 29(6), 1705–1712. <https://doi.org/10.1519/jsc.00000000000000810>
- P. Välisuo. (2015). Optical methods for assessing skin flap survival. *Elsevier EBooks*, 331–346. <https://doi.org/10.1016/b978-0-85709-662-3.00012-9>
- Rahnama, N., Reilly, T., Lees, A., & Graham-Smith, P. (2003). Muscle fatigue induced by exercise simulating the work rate of competitive soccer. *Journal of Sports Sciences*, 21(11), 933–942. <https://doi.org/10.1080/0264041031000140428>
- RestWise: What We Do -The Process.* (2017). Restwise.com; RestWise. Retrieved April 9, 2024, from <http://restwise.com/whatwedo/theprocess/>
- Rhode Island University. (n.d.). *Work, Power, and Energy*. Work, Power, & Energy.  
[http://faculty.ric.edu/psci103/work\\_energy/Work%20911.pdf](http://faculty.ric.edu/psci103/work_energy/Work%20911.pdf)
- Rice University. (n.d.). *Exercise Physiology Laboratory #5*. laboratory#5.  
<https://www.ruf.rice.edu/~kines/laboratory5.htm>
- Risks of Electrocardiogram (EKG).* (n.d.). Stanfordhealthcare.org.  
<https://stanfordhealthcare.org/medical-tests/e/ekg/risks.html#:~:text>You%20may%20develop%20a%20mild>

Russell, S., Jenkins, D., Rynne, S., Halson, S. L., & Kelly, V. (2019, May). What is mental fatigue in elite sport? Perceptions from athletes and staff. *Eur J Sport Sci.* 10.1080/17461391.2019.1618397

Shelley, K., & Alian, A. (2014). Photoplethysmography. *Best Practice & Research Clinical Anaesthesiology*, 28(4), 395-406. ScienceDirect. 10.1016/j.bpa.2014.08.006

Sidecar Health. (n.d.). *Cost of doctor visit by state*. Cost.sidecarhealth.com.  
<https://cost.sidecarhealth.com/c/doctor-visit-cost>

Singh, P., Esposito, M., Barrons, Z., Clermont, C., Wannop, J., & Stefanyshyn, D. (2021, April). Measuring Gait Velocity and Stride Length with an Ultrawide Bandwidth Local Positioning System and an Inertial Measurement Unit. *Sensors (Basel)*, 21(9). National Library of Medicine. 10.3390/s21092896

*Smart Fitness Market Size, Share Global Analysis Report, 2023-2030*. (2023, August). Facts and Factors. <https://www.fnfresearch.com/smart-fitness-market>

Steinach, M., & Gunga, H.-C. (2020). Chapter 3 - Exercise Physiology. In *Human Physiology in Extreme Environments* (2nd ed., pp. 77-116). Elsevier Science.  
10.1016/B978-0-12-386947-0.00003-4

Subasi, A. (n.d.). Chapter 2 - Biomedical Signals. In *Practical Guide for Biomedical Signals Analysis Using Machine Learning Techniques* (pp. 27–87). 2019.  
<https://doi.org/10.1016/B978-0-12-817444-9.00002-7>

Taylor, K.-L., Chapman, D., Cronin, J., Newton, M., & Gill, N. (2012, March). Fatigue Monitoring in High Performance Sport: A Survey of Current Trends. *Journal of Australian Strength and Conditioning*, 20.

[https://www.researchgate.net/publication/270905024\\_Fatigue\\_Monitoring\\_in\\_High\\_Performance\\_Sport\\_A\\_Survey\\_of\\_Current\\_Trends](https://www.researchgate.net/publication/270905024_Fatigue_Monitoring_in_High_Performance_Sport_A_Survey_of_Current_Trends)

Tinney, S. (2023, October 26). *When is College Soccer Season? Fall and Spring Rules*. Ball at Your Feet. <https://ballatyourfeet.com/when-is-college-soccer-season-fall-spring-rules/>

Toreno-Aguilera, J. F., Jimenez-Morcillo, J., Rubio-Zarapuz, A., & Clemente-Suarez, V. (2022, April 22). Central and Peripheral Fatigue in Physical Exercise Explained: A Narrative Review. *Int J Environ Res Public Health*. National Library for Medicine. 10.3390/ijerph19073909

Wang, C. (2022, May 13). Sports-Induced Fatigue Recovery of Competitive Aerobics Athletes Based on Health Monitoring. *Comput Intell Neurosci*. 10.1155/2022/9542397  
*Waste & its negative effects on the environment*. E. (n.d.).

<https://elytus.com/blog/e-waste-and-its-negative-effects-on-the-environment.html#:~:text=Electronic%20waste%2C%20also%20known%20as,no%20longer%20wanted%20or%20needed.>

Weavil, J. C., & Amann, M. (2019, August). Neuromuscular fatigue during whole body exercise. *Curr Opin Physiol*. National Library of Medicine. 10.1016/j.cophys.2019.05.008

Vinzio Maggio, A. C., Paula, M., Laciari, E., & David, P. (2012). Quantification of Ventricular Repolarization Dispersion Using Digital Processing of the Surface ECG. *Advances in Electrocardiograms - Methods and Analysis*. <https://doi.org/10.5772/23050>

# **Appendices**

## **Appendix A**

### **A.1 Generalized Soccer Athlete Health**

Healthy collegiate soccer athletes rely on a combination of physical fitness, tactical understanding, and various tests to analyze health. Achieving peak performance is important to the player and the sport but requires a versatile approach to conditioning and training. Physical fitness is multifaceted and includes cardiovascular endurance, strength, speed, agility, and flexibility and each is measured through varying assessments. These assessments play a crucial role in understanding overexertion and how that may impact athletes' health, fitness, and risk of injuries.

#### **A.1.1: What makes a healthy soccer athlete?**

On average, collegiate soccer athletes on the outfield cover 12 kilometers (km) per game with most players reaching speeds of 9 meters per second throughout the 90-minute game. According to Medical News Today, the average person walks 2.4 km to 3.2 km per day (Medical News Today, 2021) with most people not reaching above a speed of 1.3 meters per second in a day (Fletcher et al., 2022). The distance covered and speeds reached by soccer players are significantly higher than the average person indicating that these athletes must meet certain physical standards to be able to perform this way. To train for these rigorous distances and speeds, they undergo stop and go endurance drills as a form of a high intensity workout so that their body gets used to constantly walking, jogging, and running.

A common test of athlete health includes sprinting 30 yards from a standing point and taking the average of the time it takes for the person to complete this over 5 trials. Age, height,

body fat percentage and other personal factors can determine one's sprint time, but on average, a healthy soccer athlete should run at or below 5 seconds (Sport Fitness Advisor, 2017). However, this is just a healthy average and sprint test scores for competitive athletes would likely fall beneath 4 seconds (Davis, 2005, Figure A.1).

30 meter Sprint Rating	Male	Female
Excellent	<4.0	<4.5
Above Average	4.2 - 4.0	4.6 - 4.5
Average	4.4 - 4.3	4.8 - 4.7
Below Average	4.6 - 4.5	5.0 - 4.9
Poor	>4.6	>5.0

Reference: Davis B. et al; Physical Education and the Study of Sport; 2000

**Figure A.1: National sprint test scores for 16 to 19 year olds (Davis, 2005)**

In relation to distance and speed, oxygen consumption rate is measured to determine the healthy range for soccer athletes. This is measured with a VO<sub>2</sub> max score which measures the amount of oxygen consumed in milliliters (ml) per kilogram of body mass per second. The average VO<sub>2</sub> maximum for an average man is 35-40 ml and 60-70 ml for a soccer player (Sport Fitness Advisor, 2017). These numbers reflect the athlete's aerobic fitness and health. A common test to measure aerobic fitness for college athletes includes the "Beep Test" or "Shuttle Run Test" which is conducted on a flat field spanning 20 meters long. The athlete must run back and forth between the 20 meters with the speed of the run increasing each time. A beep sound is presented by the instructor and the player must reach the end of the 20 meters before the beep; otherwise, they fail the level. The number of "levels" the player can pass indicates their score, so a healthy soccer athlete typically makes it to level 11 or higher (Figure A.2). However, this score can be influenced by varying factors and is just an average. The beep test is a standardized test, so it is used to evaluate and compare players and help gauge fitness and health (SoccerWire, 2023).

Level	No.of Shuttles	Time Per Shuttle	Cumulative Shuttles	Total Distance Covered	Cumulative Time
1	7	9.00	7	140	1:03
2	8	8.00	15	300	2:07
3	8	7.58	23	460	3:08
4	9	7.20	32	640	4:12
5	9	6.86	41	820	5:14
6	10	6.55	51	1020	6:20
7	10	6.26	61	1220	7:22
8	11	6.00	72	1440	8:28
9	11	5.76	83	1660	9:31
10	11	5.54	94	1880	10:32
11	12	5.33	106	2120	11:36
12	12	5.14	118	2360	12:38

**Figure A.2: Beep test levels and associating measurements (SoccerWire, 2023)**

### A.1.2: Risks of overexertion

Overexertion is the physical strain an athlete places on their body during practice, a game, or other physical activity that exceeds their physical capacity. On average, soccer athletes get two injuries per season for a variety of reasons spanning from overexertion to incorrect form (Jaspers, A. et al., 2018). Some examples of overexertion in soccer include excessive running, lack of recovery, playing in extreme weather, playing through fatigue, overtraining, and inadequate nutrition. There are two types of loads, external and internal load, that can contribute to overexertion. External load is a quantifiable and measurable metric referring to the physical demand on the body during physical activity such as distance covered, acceleration, deceleration, or speed. Internal load refers to the body's reaction to external loads including how they perceive psychophysiological stress such as heart rate, motivation, and injury risk (STATSports, 2020).

Therefore, measuring exertion is complex, but can be crucial for preventing player injuries and improving performance. Various studies have tested that there is a positive correlation between overexertion and higher risk of injury with one study stating that 42% of

injuries in athletes results from muscle overuse and overexertion (Franco, 2021). Furthermore, there are additional risks associated with overexertion including muscle fatigue, musculoskeletal injuries, heat exhaustion, dehydration, mental fatigue, and decreased immune function.

Muscle fatigue is a temporary reduction in the ability of a muscle to develop force which results in performance decline. Belgian University players covered about 444 meters more in the first half of the game than in the second half, a reduction they attributed to muscle fatigue in the players (Rahnama et al., 2003). A study by Rahnama simulated the work force of a soccer game and found that the workrate of the quadriceps and hamstrings decreased after exercising by measuring the angular velocity (rad/s) and peak torque (Nxm). The fatigued muscles resulted in less accuracy and less strength which can lead to higher risk of strain and injury for the player (Rahnama et al., 2003).

## Appendix B

**Table X. Complete FR-DP Decomposition**

Number	Functional Requirements	Number	DP Description
<b>FR 0</b>	Monitor biometrics in collegiate soccer athletes to indicate athlete readiness from sensors mounted on an athletic shirt and leg strap	<b>DP 0</b>	System to monitor biometrics in collegiate soccer athletes to indicate athlete readiness from sensors mounted on an athletic shirt and leg strap
<b>FR 1</b>	Measure biometrics on the athlete	<b>DP 1</b>	Method with appropriate sensor to measure biometrics on athlete
<b>FR 1.1</b>	Provide power to system(s)	<b>DP 1.1</b>	Appropriate sized and volt battery connected to sensors and shirt
<b>FR 1.1.1</b>	Understand how to measure heart rate	<b>DP 1.1.1</b>	Education and research on how to measure heart rate
<b>FR 1.1.1.1</b>	Identify heart rate baseline	<b>DP 1.1.1.1</b>	Create a scoring system to measure heart rate baseline
<b>FR 1.2.1</b>	Understand how to measure blood pressure	<b>DP 1.2.1</b>	Education and research on how to measure blood pressure
<b>FR 1.2.1.1</b>	Identify blood pressure baseline	<b>DP 1.2.1.1</b>	Create a scoring system to measure blood pressure baseline
<b>FR 1.3.1</b>	Understand how to measure respiratory rate	<b>DP 1.3.1</b>	Education and research on how to measure respiratory rate
<b>FR 1.3.1.1</b>	Identify respiratory rate baseline	<b>DP 1.3.1.1</b>	Create a scoring system to measure respiratory rate baseline
<b>FR 1.4.1</b>	Understand how to measure body temperature	<b>DP 1.4.1</b>	Education and research on how to measure body temperature
<b>FR 1.4.1.1</b>	Identify body temperature baseline	<b>DP 1.4.1.1</b>	Create a scoring system to measure body temperature baseline
<b>FR 1.5.1</b>	Understand how to use EMG to measure muscle activity	<b>DP 1.5.1</b>	Education and research on how to measure muscle activity
<b>FR 1.5.1.1</b>	Identify muscle activity baseline	<b>DP 1.5.1.1</b>	Create a scoring system to

			measure muscle activity baseline
<b>FR 2</b>	Determine whether the biometrics are over or under the baseline for healthy state	<b>DP 2</b>	Create and analyze an exhaustive scoring system to measure all biometrics
<b>FR 2.1</b>	Compare heart rate baseline to active data	<b>DP 2.1</b>	Analyze heart rate score with created scoring system
<b>FR 2.2</b>	Compare blood pressure baseline to active data	<b>DP 2.2</b>	Analyze blood pressure score with created scoring system
<b>FR 2.3</b>	Compare respiratory rate baseline to active data	<b>DP 2.3</b>	Analyze respiratory rate score with created scoring system
<b>FR 2.4</b>	Compare body temperature to active data	<b>DP 2.4</b>	Analyze body temperature score with created scoring system
<b>FR 2.5</b>	Compare muscle activity to active data	<b>DP 2.5</b>	Analyze muscle activity score with created scoring system
<b>FR 3</b>	Issue warning(s) to coach(es) via website or mobile device when athlete's biometrics are at unsafe level	<b>DP 3</b>	Interactive visualization on website or mobile device
<b>FR 3.1</b>	Identity which biometric(s) and performance metric(s) need attention	<b>DP 3.1</b>	Interactive visualization on website or mobile device that relays specific information regarding biometric(s) and performance metric(s) that need attention

## Appendix C

### Top Level FR-DP Matrix

	<b>DP 1:</b> Method with appropriate sensor to measure biometrics on athlete	<b>DP 2:</b> Create and analyze an exhaustive scoring system to measure all biometrics	<b>DP 3:</b> Interactive visualization on website or mobile device
<b>FR 1:</b> Measure biometrics on the athlete	X	O	O
<b>FR2:</b> Determine whether the biometrics are over or under the baseline for healthy state	X	X	O
<b>FR 3:</b> Issue warning(s) to coach(es) via website or mobile device when athlete's biometrics are at unsafe level	X	X	X

## **Appendix D**

### **GitHub Repository Link**

**MQP Smart Wearable GitHub Repository:**

**<https://github.com/krishpatel1077/MQP-WEBSITE-C24>**

## Appendix E

### Collection of Datasheets

Component	Datasheet
Analog Multiplexor (CD4051B)	<a href="#">CD405xB CMOS Single 8-Channel Analog Multiplexer or DemultiplexerWith Logic-Level Conversion datasheet (Rev. L)</a>
12V Battery	<a href="#">YB1203000   12V Lithium ion battery   12V Lithium ion battery - Talentcell Technology Co.,Ltd</a>
ESP8266	<a href="#">0a-esp8266ex_datasheet_en (espressif.com)</a>
Arduino Uno	<a href="#">A000066-datasheet.pdf (arduino.cc)</a>
Buck Converter	<a href="#">Amazon.com: UCTRONICS DC 9V 12V 24V to DC 5V 5A Buck Converter Module, 9-36V Step Down to USB 5V Transformer Dual Output Voltage Regulator Board [2 Pack] : Electronics</a>
SEN-0213 Heat Rate Sensor	<a href="#">Heart Rate Monitor Sensor SKU SEN021 3-DFRobot</a>
Myoware EMG Sensor Module	<a href="#">MYO004_AdvancedGuide_v12 (myoware.com)</a>
LM35 Temperature Sensor	<a href="#">LM35 Precision Centigrade Temperature Sensors datasheet (Rev. H)</a>
NEO6MV2 GPS Module	<a href="#">NEO-6_DataSheet_(GPS.G6-HW-09005).pdf (u-blox.com)</a>